THE ZORA EQUATION

VRIJE UNIVERSITEIT

THE ZORA EQUATION

ACADEMISCH PROEFSCHRIFT

ter verkrijging van de graad van doctor aan
de Vrije Universiteit te Amsterdam,
op gezag van de rector magnificus
prof.dr E. Boeker,
in het openbaar te verdedigen
ten overstaan van de promotiecommissie
van de faculteit der scheikunde
op donderdag 18 januari 1996 te 15.45 uur
in het hoofdgebouw van de universiteit, De Boelelaan 1105

door

Erik van Lenthe

geboren te Zwolle

Promotoren:	prof.dr E.J. Baerends
	prof.dr J.G. Snijders
Referent:	prof.dr W.C. Nieuwpoort

Contents

Chapter 1

Introduction and general overview

1.1 Introduction

At present the standard description of the electromagnetic field and the motion of electrons is Quantum Electrodynamics (QED). Highly accurate QED calculations on small systems, like the hydrogen and helium atom, are in very good agreement with highly accurate experiments. For larger systems accurate QED calculations are in general too expensive from a computational point of view. It is therefore convenient to approximate QED. Such an approximation is the Dirac equation [1, 2]. This four-component equation can be solved exactly for a hydrogen-like atom with a point charge [3, 4]. In many cases this equation is further approximated, because it is still quite expensive to calculate. The standard expansion gives in zeroth order the non-relativistic or Schrödinger equation. This expansion is defective for Coulomb-like potentials. In this thesis a regular expansion is used, which remains valid even for a Coulomb-like potential. This potential-dependent expansion, earlier derived by Chang et al. [5] and Heully et al. [6], gives in zeroth order a regular approximated (ZORA) equation, which accounts for most of the relativistic effects. The ZORA equation will be the main subject of this thesis.
Since the nuclei have much larger masses than the electrons, we will use the Born-Oppenheimer approximation. In this approximation the electronic problem is solved in the external potential coming from fixed nuclei. Besides the kinematics, in many-electron systems we also have to consider the electron-electron repulsion, which is often approximated by the instantaneous Coulomb interaction $1/r_{ij}$, where r_{ij} is the distance between the electrons. Sometimes relativistic correction terms to the electron-electron repulsion are used, like the Breit [7] or Gaunt [8] term. In so called *ab initio* calculations one often starts by solving the (Dirac-)Hartree-Fock equation. Afterwards one can use standard techniques to take correlation effects into account. A different standard method is density functional theory. In this thesis the Kohn-Sham approach to this theory is used (see next section). For practical use one needs to have a good approximation for the density functional of the exchange-correlation energy. Successful approximations have been applied in non-relativistic calculations. In this thesis we will use the same approximations for the exchange-correlation energy in relativistic calculations.
Valence electrons are for a large part responsible for most of the chemical properties. Core orbitals of an atom do not change much from one molecule to another. This is used in the frozen core approximation, also used in this thesis, which can make the calculations cheaper,

without much loss of accuracy. A more severe approximation is the use of effective core potentials (ECP). In this approximation valence electrons feel a parametrised effective core potential, which for example also can take relativistic effects effectively into account.
Quantum chemistry is full of approximations. In this introduction I have only mentioned a few of them. Time will tell which approximations remain fruitful.

1.2 Relativistic density functional theory

In non-relativistic theory Hohenberg and Kohn [9] proved that in principal ground state properties, like the total energy, only depend on the ground state electron density of the interacting many-electron system. The explicit dependence is generally not known and in practice approximations are made. If one assumes that a minimum property of the energy similar to the non-relativistic case is also valid in the relativistic case, one can also proof the Hohenberg-Kohn theorem in the relativistic case [10, 11, 12]. However, this minimum property of the energy is not proven rigorously [13]. In this section we will look more closely at the minimum property of the energy used in this proof, without considering QED effects. The Dirac equation has besides positive total energy solutions, also negative energy solutions. The Dirac Hamiltonian H_D for one electron moving in an external electrostatic potential V can be written as:

$$H_D = H^{sys} + V \tag{1.1}$$

where H^{sys} is the relativistic kinetic energy operator of the electron. In the one-electron case the standard procedure is that the solution with the lowest possible positive energy is the ground-state. In this case one can surround the Hamiltonian H_D with projection operators Λ_V^+ [14, 15], which are the projection operators onto the positive energy states, to obtain the Hamiltonian H_D^+, which only has positive energy solutions:

$$H_D^+ = \Lambda_V^+ H_D \Lambda_V^+ = \Lambda_V^+ (H^{sys} + V) \Lambda_V^+ \tag{1.2}$$

The eigenstates of H_D with positive energy are not altered due to the projection operators in H_D^+, only the negative energy-states are removed. We now have a minimum principle for the energy, which says that for any trial wavefunction Ψ^T, with $\Lambda_V^+ \Psi^T \neq 0$:

$$\frac{\langle \Psi^T | H_D^+ | \Psi^T \rangle}{\langle \Psi^T | \Lambda_V^+ | \Psi^T \rangle} = \frac{\langle \Psi^T | \Lambda_V^+ (H^{sys} + V) \Lambda_V^+ | \Psi^T \rangle}{\langle \Psi^T | \Lambda_V^+ | \Psi^T \rangle} \geq E_0 \tag{1.3}$$

where E_0 is the energy of the ground state of H_D^+. The projection operator Λ_V^+ depends on the external potential V, which is clearly shown in an example of Hardekopf and Sucher [16]. They solved the hydrogen-like system in the space of positive energy solutions of the free particle. They found that the energy is lower than the exact $1s$ ground state energy of the hydrogen-like system. Heully et al. [15] have explained this by noting that the projection operator on the postive energy solutions of the Dirac equation for a given external potential will introduce negative energy states in the case of another external potential (see also the standard textbook of Sakurai [17], §3.7). A related dependence on the external potential can also be found in the Foldy-Wouthuysen transformation [18], which decouples the four-component Dirac equation in two two-component equations, one of which has only positive energy eigenvalues and the other only negative ones. In the standard expansion in α^2

($\alpha \approx 1/137$) of the Foldy-Wouthuysen transformed Dirac equation, non-trivial dependence on the external potential starts to appear in first order, in the Darwin and spin-orbit term (see chapter 2).

In the first step of the Hohenberg-Kohn theorem one can prove a one-to-one correspondence between the external potential and the ground state wave function. We suppose a non-degenerate ground state, such that for a given external potential we only have one ground state. The proof, that there is only one external potential (apart from an arbitrary constant) for a given ground state, is done by contradiction. Suppose we have the same ground state $|\Psi\rangle$ for two different external potentials V_1 and V_2, which differ more than a constant, noting that the ground state of H_D^+ is also an eigenfunction of H_D, thus:

$$H_D^+(V_1)|\Psi\rangle = H_D(V_1)|\Psi\rangle = (H^{sys} + V_1)|\Psi\rangle = E_1|\Psi\rangle \tag{1.4}$$

$$H_D^+(V_2)|\Psi\rangle = H_D(V_2)|\Psi\rangle = (H^{sys} + V_2)|\Psi\rangle = E_2|\Psi\rangle \tag{1.5}$$

In these equations we have used that the ground state of H_D^+ is also an eigenfunction of H_D. Subtraction of these equations leads to:

$$(V_1 - V_2)|\Psi\rangle = (E_1 - E_2)|\Psi\rangle \tag{1.6}$$

Since V_1 and V_2 are multiplicative operators, we must have $V_1 - V_2 = E_1 - E_2$, which means that V_1 and V_2 only differ by a constant. This contradicts our assumption and the proof of the one-to-one correspondence between the external potential and the ground state wave function is complete.
Suppose we have $|\Psi_g^1\rangle$, the ground state of $H_D^+(V_1)$, and $|\Psi_g^2\rangle$, the ground state of $H_D^+(V_2)$, where V_1 and V_2 are arbitrary potentials, which differ more than a constant. In the second step of the Hohenberg-Kohn theorem one wants to prove that these two different normalised ground state wave functions yield different ground state densities. In the standard proof one uses that the following minumum property of the energy is valid:

$$E_1 = \langle\Psi_g^1|H_D(V_1)|\Psi_g^1\rangle < \langle\Psi_g^2|H_D(V_1)|\Psi_g^2\rangle \tag{1.7}$$

For the non-relativistic Hamiltonian this is provided by the variational principle, for the Dirac Hamiltonian this is not proven rigorously. On the other hand, we did not find a counter-example, which invalidates this inequality for the Dirac Hamiltonian. Problems will definitely arise if one is not restricted to ground state wave functions, as we have seen in the example of Hardekopf and Sucher [16]. According to the inequality 1.3 one *can* prove:

$$\langle\Psi_g^1|H_D(V_1)|\Psi_g^1\rangle = \langle\Psi_g^1|H_D^+(V_1)|\Psi_g^1\rangle \leq \frac{\langle\Psi_g^2|H_D^+(V_1)|\Psi_g^2\rangle}{\langle\Psi_g^2|\Lambda_{V_1}^+|\Psi_g^2\rangle} = \frac{\langle\Psi_g^2|\Lambda_{V_1}^+(H^{sys} + V_1)\Lambda_{V_1}^+|\Psi_g^2\rangle}{\langle\Psi_g^2|\Lambda_{V_1}^+|\Psi_g^2\rangle} \tag{1.8}$$

If we assume inequality 1.7 is true the standard proof of the second step of the Hohenberg-Kohn theorem is again by contradiction. Suppose $|\Psi_g^1\rangle$ and $|\Psi_g^2\rangle$ yield the same ground state density ρ. We then have:

$$E_1 < \langle\Psi_g^2|H_D(V_1)|\Psi_g^2\rangle = \langle\Psi_g^2|H_D(V_2) + V_1 - V_2|\Psi_g^2\rangle = E_2 + \int d^3x \;\; \rho(V_1 - V_2) \tag{1.9}$$

Changing the role of V_1 and V_2 and adding the inequalities one obtains the contradiction:

$$E_1 + E_2 < E_1 + E_2 \tag{1.10}$$

Thus our assumption was wrong and $|\Psi_g^1\rangle$ and $|\Psi_g^2\rangle$ should yield different densities, which finishes the proof of the one-to-one correspondence between ground state wave function and density. As said before this proof is only valid if inequality 1.7 is true. Essential in the proof is that in the expectation values of the Hamiltonian in inequality 1.7, the terms containing the external potential explicitly seperate out and only need the electron density. Due to the complicated dependence on the external potential V_1 this is not true for the term after the inequality in equation 1.8. It is possible that one can only derive rigorously minimal properties for the energy in the relativistic case which have a non-trivial dependence on the external potential like in this inequality. Then it will be very hard to prove the Hohenberg-Kohn theorem for the Dirac equation, if it exists at all.

The many particle Dirac equation suffers from the Brown-Ravenhall disease [19]. For example a system with two bound electrons is degenerate with a system, where one electron is in the negative energy continuum and one is in the very high positive energy continuum (continuum dissolution). In the non-interacting many-particle system the same one-particle projection operator Λ_V^+ can be used as in the one-electron case, to avoid these problems. However, it will become more complicated for interacting electrons, where H^{sys} also contains the electron-electron repulsion. In that case the projection operator Λ_V^+ is more difficult to obtain [20, 21]. In this case one often expands the wavefunction in terms of single-particle functions. To avoid continuum dissolution, one can use the positive energy solutions of the single-particle orbitals only, coming from for example a Dirac-Fock calculation. In either case the separation of the space of positive energy solutions and the space of negative energy solutions depends on the external potential. The question of the validity of the Hohenberg-Kohn theorem is not simplified.
In the Kohn-Sham approach [22] of density functional theory one replaces the complicated interacting many-electron system with an effective non-interacting many-electron system, such that the non-interacting system has the same ground state electron density. In order to solve the resulting Kohn-Sham equations one needs to know the effective (Kohn-Sham) potential. In non-relativistic theory it is proven that there is a one-to-one correspondence between this effective potential and the exact ground-state density. One can then also show using inequality 1.7 that the exchange-correlation part of the Kohn-Sham potential is the functional derivative of the exchange-correlation energy. In relativistic theory this can not be proven rigorously. Of course, in the one-electron case for the Dirac equation, one Kohn-Sham potential is trivial, but the question concerning its uniqueness remains.
In this thesis we will nevertheless use relativistic Kohn-Sham equations, with the same approximate density functionals for the exchange-correlation energy as were used in non-relativistic theory. These density functionals depend on the local density (LDA) or also on density-gradients (GGC).

1.3 Overview of this thesis

In this thesis regular approximated relativistic equations are used in atomic and molecular calculations. In chapter 2 this regular expansion is obtained, using an expansion in $E/(2c^2 - V)$ of the relativistic equation, which remains regular even for a Coulomb-like potential. In that case the standard expansion in $(E - V)/2c^2$ is defective. This potential-

dependent expansion, earlier derived by Chang et al. [5] and Heully et al. [6], is used in relativistic classical mechanics as well as in relativistic quantum mechanics. The zeroth order regular approximated (ZORA) equation obtained already accounts for most of the relativistic effects.
In the chapters 3 to 7 this ZORA Hamiltonian is further investigated. In chapter 3 it is shown that this Hamiltonian is bounded from below. There it is also shown that the ZORA equation is not gauge invariant, but that the scaled ZORA method almost completely solves this problem. This method again can be approximated using the so called electrostatic shift approximation (ESA), which is an easy and accurate way to obtain energy differences. In chapter 4 the exact solutions of the ZORA equation are given in the case of a hydrogen-like atom. This is done by scaling of coordinates in the Dirac equation. The same scaling arguments are used to obtain exact relations for one and two electron systems in more general systems. For the discrete part of the spectrum of the hydrogen-like atom it is shown there that the scaled ZORA energies are exactly equal to the Dirac energies. Numerical atomic calculations are done in chapter 5, showing the high accuracy of the ZORA method for valence orbitals. The implementation of this method in molecular and in band structure calculations is given in chapter 6. The results of molecular calculations on a number of diatomics is given in chapter 7, with an explicit treatment of the spinorbit operator. In this chapter a method is proposed for the calculation of the total energy of open shell systems using density functionals if spinorbit is present.
Chapter 8 and 9 show methods for solving the Dirac equation, using basis sets for the large components only. In chapter 8 this is done using the standard method of eliminating the small component and requires a diagonalisation of a Hamiltonian for every occupied orbital. In chapter 9 the Dirac equation is solved by a new method. In the iterative procedure used, it requires the evaluation of matrix elements of the Hamiltonian between the large component solutions of the previous cycle. In this chapter also a method was given for construction of the exact Foldy-Wouthuysen transformation, once one has the (large component) solution to the Dirac equation.

This thesis is based on the following articles:

E. van Lenthe, E.J. Baerends, and J.G. Snijders.
J. Chem. Phys., **99**:4597, 1993.
Relativistic regular two-component Hamiltonians.

R. van Leeuwen, E. van Lenthe, E.J. Baerends, and J.G. Snijders.
J. Chem. Phys., **101**:1272, 1994.
Exact solutions of regular approximate relativistic wave equations for hydrogen-like atoms.

E. van Lenthe, E.J. Baerends, and J.G. Snijders.
J. Chem. Phys., **101**:9783, 1994.
Relativistic total energy using regular approximations.

A.J. Sadlej, J.G. Snijders, E. van Lenthe, and E.J. Baerends.
J. Chem. Phys., **102**:1758, 1995.
Four component regular relativistic Hamiltonians and the perturbational treatment of Dirac's equation.

E. van Lenthe, E.J. Baerends, and J.G. Snijders.
(to be submitted).
Spinorbit energy using regular approximations.

E. van Lenthe, R. van Leeuwen, E.J. Baerends, and J.G. Snijders.
in New Challenges in Computational Chemistry, Proceedings of the Symposium in honour of W.C. Nieuwpoort (eds.) R. Broer, P.J.C. Aerts, and P.S. Bagus, Groningen U. P., Groningen, page 93, 1994.
Int. J. Quantum Chem.:accepted
Relativistic regular two-component Hamiltonians.

E. van Lenthe, E.J. Baerends, and J.G. Snijders.
Chem. Phys. Lett., **236**:235, 1995.
Solving the Dirac equation, using the large component only, in a Dirac-type Slater orbital basis set.

E. van Lenthe, E.J. Baerends, and J.G. Snijders.
(submitted).
Construction of the Foldy-Wouthuysen transformation and solution of the Dirac equation using large components only.

Chapter 2

Regular Expansions in Relativistic Mechanics

In this chapter potential-dependent transformations are used to transform the four-component Dirac Hamiltonian to effective two-component regular Hamiltonians. To zeroth order the expansions give second order differential equations (just like the Schrödinger equation), which already contain the most important relativistic effects, including spin-orbit coupling. This potential-dependent expansion is based on earlier work by Chang, Pélissier and Durand [5] and of Heully et al. [6].

2.1 Classical Relativistic Mechanics and the Coulomb potential

In this section the classical expression for the relativistic energy of a particle in a potential is expanded in several ways, to prepare for similar expansions in relativistic quantum mechanics. We will see that if one expands the energy expression in c^{-1}, as is usually done, this will give rise to some problems if the momentum of the particle is too large. For Coulomb-like potentials there are always regions where this is the case. A potential dependent expansion can be found, which is well behaved even if the momentum of the particle is large. This expansion will be considered after we have explained the shortcomings of the c^{-1}-expansion. Consider a particle that is moving in a potential V. In the special theory of relativity the expression for the total energy W of the particle is:

$$W = \sqrt{m_0^2c^4 + p^2c^2} + V \tag{2.1}$$

In this equation m_0 is the rest-mass of the particle, p its momentum and c the velocity of light. It is convenient to define the energy of a particle as:

$$E = W - m_0c^2 \tag{2.2}$$

Equation 2.1 can be rewritten as:

$$E = m_0c^2\left(\sqrt{1+\frac{p^2}{m_0^2c^2}} - 1\right) + V \tag{2.3}$$

This equation can be expanded in $p/(m_0c)$, giving:

$$E = V + \frac{p^2}{2m_0} - \frac{p^4}{8m_0^3c^2} + \cdots \tag{2.4}$$

where in second order the so called mass-velocity term $p^4/(8m_0^3c^2)$ appears. The use of this expansion is not justified if $p/(m_0c) > 1$, i.e. if the momentum of the particle is too large, as has been stressed by Farazdel and Smith [23]. If the potential is Coulomb-like ($V \sim -1/r$), then there is always a region where the potential is so negative that the momentum of the particle p is larger than m_0c, even if the energy E is small. However, another expansion can be found, which is valid for Coulomb-like potentials over all space, even if the momentum of the particle is at times larger than m_0c. The only restriction is that the energy (a constant of the motion) is not too large, $|E| < (2m_0c^2 - V)$, which in chemical applications is always the case. At energies for which this inequality would not apply other effects should be taken into account, like pair-creation. The expansion can be found by first rewriting equation 2.3:

$$\begin{aligned}
E &= \sqrt{m_0^2c^4 + p^2c^2} - m_0c^2 + V \\
&= \frac{p^2c^2}{m_0c^2 + \sqrt{m_0^2c^4 + p^2c^2}} + V \\
&= \frac{p^2c^2}{2m_0c^2 + E - V} + V = \frac{p^2}{2m_0(1 + \frac{E-V}{2m_0c^2})} + V \\
&= \frac{p^2c^2}{(2m_0c^2 - V)(1 + \frac{E}{2m_0c^2 - V})} + V
\end{aligned} \tag{2.5}$$

The last two terms have been written down in order to exhibit more clearly which expansions one can make. The price to be paid to get rid of the root is that the equation is now quadratic in the energy. The equation has therefore an extraneous negative total energy solution. By choosing a particular expansion the spurious solution will be thrown away. Expanding in $(E-V)/(2m_0c^2)$ will give in zeroth order the non-relativistic (NR) energy and in first order something we shall call the Pauli energy:

$$E_{NR} = V + \frac{p^2}{2m_0} \tag{2.6}$$

$$E_{Pauli} = E_{NR} - \left(\frac{E_{NR}-V}{2m_0c^2}\right)\frac{p^2}{2m_0}$$

$$= V + \frac{p^2}{2m_0} - \frac{p^4}{8m_0^3c^2} \tag{2.7}$$

Up to first order this gives the same expansion as equation 2.4. It is obvious that this expansion is not valid for $r \to 0$, where $E - V > 2m_0c^2$. A correct expansion can be found (for energies smaller than $2m_0c^2$) by expanding in $E/(2m_0c^2-V)$. In zeroth order this expansion gives, what we shall call the zeroth order regular approximated (ZORA) energy:

$$E^{zora} = \frac{p^2c^2}{2m_0c^2 - V} + V \tag{2.8}$$

The $E/(2m_0c^2-V)$-expansion is valid for Coulomb-like potentials everywhere, whereas this is not true for the $(E-V)/(2m_0c^2)$-expansion. Up to first order the expansion in $E/(m_0c^2-V)$ gives (first order regular approximation (FORA)):

$$E^{fora} = E^{zora}\left(1 - \frac{p^2c^2}{(2m_0c^2-V)^2}\right)$$

$$= V + \frac{(2m_0c^2-2V)}{(2m_0c^2-V)^2}p^2c^2 - \frac{p^4c^4}{(2m_0c^2-V)^3} \tag{2.9}$$

We can make an even better approximation than this first order expansion using a slightly different form, such that certain higher order terms are included. We will call this the scaled ZORA energy:

$$E^{scaled} = \frac{E^{zora}}{1 + \frac{p^2c^2}{(2m_0c^2-V)^2}} \tag{2.10}$$

After expansion of the numerator one can indeed see that the first order result is obtained and that higher order terms appear. This scaled ZORA energy turns out to be sufficiently accurate in most cases and has certain desirable properties in the case of a one electron ion in relativistic quantum mechanics. Even if the energy is high, the scaled energy is a better approximation than the Pauli one. This can be seen for example in the case of a free particle. In this case one can see in figure 2.1 how the energy of the particle varies with momentum p for the various approximations. The results are given in atomic units ($m_0 = 1$ and $c \approx 137$). For a free particle ZORA is equal to NR and FORA is equal to Pauli. Due to the mass-velocity term the Pauli approximation (and FORA) gives negative energies for high momenta. We can do the same thing for a particle in a potential. In figure 2.2 we can see this for a potential equal to -5000 a.u. The relativistic, nonrelativistic and Pauli energy shift with the value of the potential. The ZORA, FORA and scaled energy do not have this uniform shift. The potential-dependent approximations are therefore not gauge invariant. On the other hand, the graphs of this regular expansion are closer to the relativistic one than the graphs of the standard expansion, especially if we look at relativistic energies close to zero. In figure 2.3 we have enlarged this part of figure 2.2. This figure clearly demonstrates that the regular approximated energies are in much closer agreement to the relativistic ones than the standard expanded energies in this region where the energies are small. This is of special interest for chemical applications, because the valence electrons, which are responsible for most chemical properties, have small energies compared to the rest mass energy (m_0c^2) of the electron. In fact the figure has not enough resolution to show the difference between the FORA, scaled ZORA and relativistic energies.

2.2 Expansions in Relativistic Quantum Mechanics

From now on atomic units are used. In this section we will demonstrate that the traditional approaches in relativistic quantum mechanics for generating effective two-component Hamiltonians rely on the expansion in $(E-V)/2c^2$ which is defective for Coulomb potentials. The result of application of the regular expansion in $E/(2c^2-V)$ is also derived.

2.2.1 Elimination of the small component

In the relativistic quantum theory, the Dirac equation can be used as a starting point for relativistic calculations. In this section the transformation of the four-component Dirac-equation into an effective two-component form using the method of eliminating

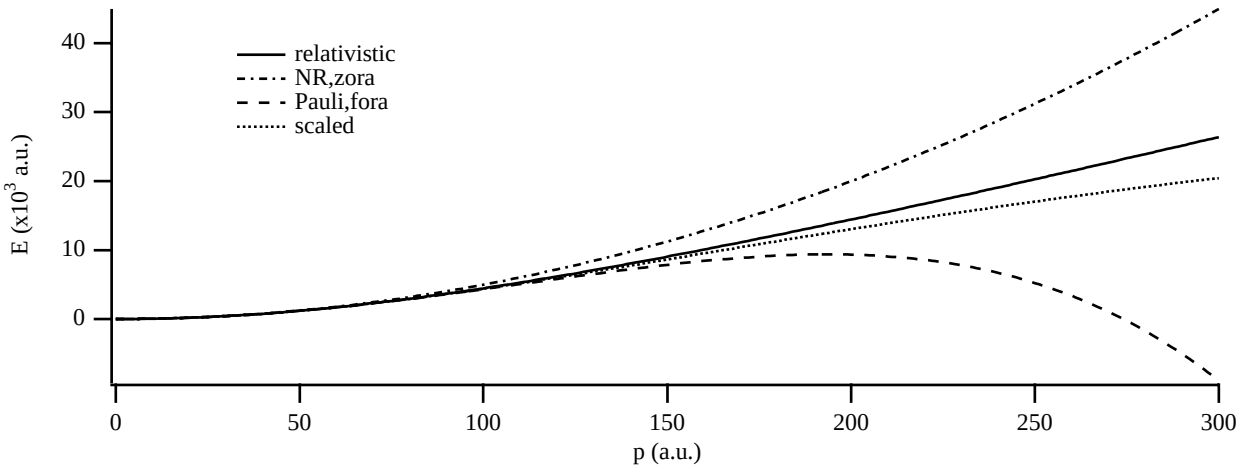

Figure 2.1: Energy E of a free particle with momentum p.

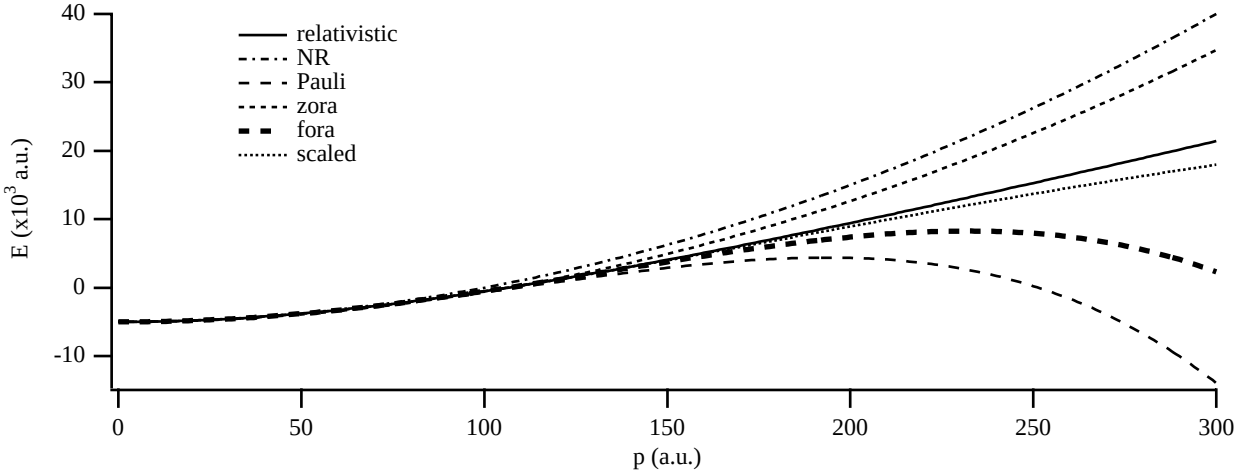

Figure 2.2: Energy E of a particle with momentum p in a potential $V = -5000$ a.u.

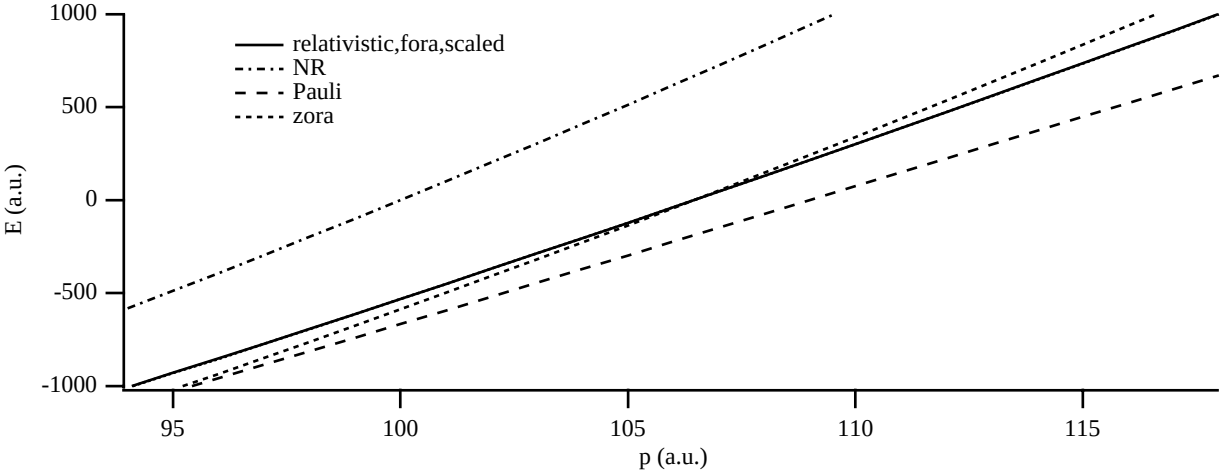

Figure 2.3: Part of figure 2.2 with relativistic energy $|E| < 1000$ a.u.

the small component (esc) is considered.
The Dirac Hamiltonian works on a four-component wave function Ψ:

$$\Psi = \begin{pmatrix} \phi \\ \chi \end{pmatrix} \tag{2.11}$$

where ϕ is called the large component and χ the small component. These are both two-component wave functions. The Dirac equation is:

$$\begin{aligned} V\phi + c\vec{\sigma}\cdot\vec{p}\chi &= E\phi \\ c\vec{\sigma}\cdot\vec{p}\phi + (V-2c^2)\chi &= E\chi \end{aligned} \tag{2.12}$$

Eliminating the small component gives:

$$\begin{aligned} \chi &= \frac{1}{2c^2+E-V} c\vec{\sigma}\cdot\vec{p}\phi \\ &= \frac{1}{2c}\left(1+\frac{E-V}{2c^2}\right)^{-1}\vec{\sigma}\cdot\vec{p}\phi \equiv \bar{X}\phi \end{aligned} \tag{2.13}$$

$$\begin{aligned} H^{esc}\phi &\equiv V\phi + c\vec{\sigma}\cdot\vec{p}\bar{X}\phi \\ &\equiv V\phi + \frac{1}{2}\vec{\sigma}\cdot\vec{p}\left(1+\frac{E-V}{2c^2}\right)^{-1}\vec{\sigma}\cdot\vec{p}\phi = E\phi \end{aligned} \tag{2.14}$$

The Hamiltonian H^{esc} is energy dependent and works solely on the large component ϕ, which is not normalised, whereas Ψ is. In the standard approach a normalised two-component wave-function $\Phi = O\phi$ is generated by a normalisation operator O (which in fact effects a picture change):

$$\begin{aligned} &\int \Phi^\dagger\Phi d^3r = \int \phi^\dagger O^\dagger O\phi d^3r = \int \Psi^\dagger\Psi d^3r = \\ &\int \left(\phi^\dagger\phi + \chi^\dagger\chi\right) d^3r = 1 \end{aligned} \tag{2.15}$$

Elimination of the small component gives:

$$\int \left(\phi^\dagger\phi + \chi^\dagger\chi\right) d^3r = \int \phi^\dagger\left(1+\bar{X}^\dagger\bar{X}\right)\phi d^3r \tag{2.16}$$

Note that there is still considerable freedom in the choice of O. One of the possible solutions for O is:

$$O = \sqrt{1+\bar{X}^\dagger\bar{X}} \tag{2.17}$$

The Hamiltonian for Φ will now become:

$$\begin{aligned} H &= OH^{esc}O^{-1} \\ &= \sqrt{1+\bar{X}^\dagger\bar{X}}[V + c\vec{\sigma}\cdot\vec{p}\bar{X}]\frac{1}{\sqrt{1+\bar{X}^\dagger\bar{X}}} \end{aligned} \tag{2.18}$$

The standard textbook approach (cf. Berestetskiĭ,Lifshitz and Pitaevskiĭ [24], McWeeny [25], Sakurai [17]) now proceeds with an expansion in $(E-V)/(2c^2)$ of the factor $\left(1+(E-V)/2c^2\right)^{-1}$ in $\bar{X}$, in both H^{esc} (eq. 2.14) and O (eq. 2.17). In addition the square root in eq. 2.17 is expanded

$$O = \sqrt{1+p^2/4c^2+\cdots} \approx 1 + p^2/8c^2 \tag{2.19}$$

which is only justified if $p^2 < 4c^2$ [classically equivalent to $(E-V)/2c^2 < 1$]. In quantum mechanics there is an extra problem if one wants to expand this operator in p^2/c^2 any further, because already the p^4-term is not a well-defined operator on the appropriate Hilbert space (it can produce non square integrable functions). If one nevertheless expands in this way one obtains in zeroth order the non-relativistic Hamiltonian and, after some manipulation, in first order the Pauli Hamiltonian:

$$H^{Pauli} = V + \frac{p^2}{2} - \frac{p^4}{8c^2} + \frac{\Delta V}{8c^2} + \frac{1}{4c^2}\vec{\sigma}\cdot(\vec{\nabla}V\times\vec{p}) \tag{2.20}$$

As pointed out before, the expansions used would only be valid for regular potentials where the classical velocity of the particles is everywhere small compared to the velocity of light. As a matter of fact, for a Coulomb potential where these conditions are not satisfied the Pauli Hamiltonian obtained in this way has well-known problematic features. The Darwin term $(\Delta V)/(8c^2)$ has a δ-function singularity at the origin, while the Dirac Hamiltonian does not pose this problem. In a Coulomb field the nonrelativistic eigenstates have components of high momentum, for which the use of the mass-velocity term as a first order perturbation is questionable, cf. Farazdel and Smith [23]. This is particularly troublesome since it has been demonstrated that relativistic effects almost entirely originate from the region close to the nucleus where classically the momentum would be too large [26]. Finally, the relativistic effects are so large in heavy element compounds that a perturbation theoretical treatment is insufficient. As demonstrated in refs. [27] and [28] a self-consistent treatment of relativistic effects is desirable, but the mass-velocity and spin-orbit operators cause problems if one wants to solve the eigenvalue equation $H^{Pauli}\Phi = E\Phi$. For one thing, due to the mass-velocity operator this is a fourth order differential equation that does not lead to quantisation of the energy under the usual boundary conditions. The spin-orbit operator $[\vec{\sigma}\cdot(\vec{\nabla}V\times\vec{p})]/(4c^2)$ also causes difficulties since close to the nucleus it behaves as an attractive $-1/r^3$ potential that leads to arbitrarily

large negative energies and not to a discrete eigenvalue spectrum. To solve most of the problems noticed above one can, as in the classical relativistic case, expand H^{esc} in $1/(2c^2 - V)$ [or $E/(2c^2 - V)$, which is equivalent as long as E is in the order of unity]. For a Coulomb potential the expansion in $1/(2c^2 - V)$ is justified even near the singularity of the potential at the nucleus, in which region it is very important to have a good expansion in view of the results of Schwarz et al. [26]. We obtain for H^{esc}:

$$V + \vec{\sigma}\cdot\vec{p}\frac{c^2}{2c^2 - V}\left(1 + \frac{E}{2c^2 - V}\right)^{-1}\vec{\sigma}\cdot\vec{p}$$

$$\approx V + \vec{\sigma}\cdot\vec{p}\frac{c^2}{2c^2 - V}\vec{\sigma}\cdot\vec{p}$$

$$-\vec{\sigma}\cdot\vec{p}\left(\frac{c^2}{2c^2 - V}\right)\frac{E}{2c^2 - V}\vec{\sigma}\cdot\vec{p} + \cdots \quad (2.21)$$

Since the expansion of O will have no effect in lowest order (see below), we observe that the first two terms constitute the zeroth order regular approximated (ZORA) hamiltonian (cf. eq. 2.8)

$$H^{zora} = V + \vec{\sigma}\cdot\vec{p}\frac{c^2}{2c^2 - V}\vec{\sigma}\cdot\vec{p} \quad (2.22)$$

So our zeroth order hamiltonian is not the nonrelativistic hamiltonian. In fact, it is expected to incorporate relativistic effects that traditionally are only introduced at the level of the Pauli hamiltonian. The great advantage of our H^{zora} is that it can be used variationally and that it does not suffer from the singularities for $r \to 0$ that plague the Pauli hamiltonian. In order to obtain the contributions to first order in $E/(2c^2 - V)$ one needs, apart from the last term in eq. 2.21, contributions from the transformation with O. The square root in the operator O will be expanded as:

$$O = 1 + \frac{1}{2}\bar{X}^\dagger\bar{X} + \cdots$$

$$= 1 + \frac{1}{2}\vec{\sigma}\cdot\vec{p}\frac{c^2}{(2c^2 - V)^2}\left(1 + \frac{E}{2c^2 - V}\right)^{-2}\vec{\sigma}\cdot\vec{p}$$

$$+ \cdots \quad (2.23)$$

In classical relativistic mechanics it would be allowed to expand O in this way, because the classical analogue of $\bar{X}^\dagger\bar{X}$ is smaller than one:

$$\frac{p^2c^2}{(2c^2 + E - V)^2} = \frac{E - V}{2c^2 + E - V} < 1 \quad (2.24)$$

In quantum mechanics the situation is slightly more complicated, a point to which we shall return below. Expansion of the factor $\left(1 + E/(2c^2 - V)\right)^{-2}$ in eq. 2.23 yields

$$O = 1 + \frac{1}{2}\vec{\sigma}\cdot\vec{p}\left(\frac{c^2}{2c^2 - V}\right)\frac{1}{2c^2 - V}\vec{\sigma}\cdot\vec{p}$$

$$-\vec{\sigma}\cdot\vec{p}\left(\frac{c^2}{2c^2 - V}\right)\frac{1}{2c^2 - V}\frac{E}{2c^2 - V}\vec{\sigma}\cdot\vec{p} + \cdots \quad (2.25)$$

In zeroth order of the expansion in $1/(2c^2 - V)$ O is just the unit operator. The second term in the above expression for O is of first order in this expansion. We already used this result to obtain H^{zora} of eq. 2.22. Using eq. 2.21 for H^{esc} and the first two terms of eq. 2.25 for O the first order regular approximated Hamiltonian H^{fora}, will now be:

$$H^{fora} = H^{zora} - \frac{1}{2}\vec{\sigma}\cdot\vec{p}\frac{c^2}{(2c^2 - V)^2}\vec{\sigma}\cdot\vec{p}H^{zora}$$

$$-\frac{1}{2}H^{zora}\vec{\sigma}\cdot\vec{p}\frac{c^2}{(2c^2 - V)^2}\vec{\sigma}\cdot\vec{p} \quad (2.26)$$

This Hamiltonian can be compared with equation 2.9. H^{fora} cannot be used in variational calculations without extra assumptions. It posesses fourth order derivatives and has no lower bound for the expectation value of the energy, just like the Pauli Hamiltonian.

The zeroth and first order Hamiltonians obtained here are identical to hamiltonians of these orders derived by Chang Pélissier and Durand [5] using the theory of effective Hamiltonians. Chang et al. obtain these hamiltonians when imposing the condition of hermiticity following des Cloizeaux [29]. Our approach here is energy-dependent and is not convenient to use for higher orders, but it gives direct physical insight in the origin of the trouble with the Pauli hamiltonian and its cure [expansion in $E/(2c^2 - V)$ instead of $(E - V)/(2c^2)$]. We finally return to the expansion of the square root in the operator O, see eq. 2.23. In practice we will be looking for solutions in a finite model space of two-component functions in which at least the bound states of H^{zora}, or equivalently the large components of the bound states of the Dirac hamiltonian, can be well represented. The expansion of O would be justified if for any normalized vector f in the model space the norm of the image vector $\bar{X}^\dagger\bar{X}f$ would be smaller than one. Some justification for this assumption may be given. Taking for f the large component ϕ of some eigenstate and

using $\chi = \bar{X}\phi$ the norm of $\bar{X}^\dagger \bar{X}\phi$ is seen to be just the norm of $\bar{X}^\dagger\chi$. Since

$$\bar{X}^\dagger = c\vec{\sigma}\cdot\vec{p}\frac{1}{2c^2+E-V} = \frac{1}{2c^2+E-V}c\vec{\sigma}\cdot\vec{p}$$

$$-i\frac{(c\vec{\sigma}\cdot\vec{\nabla}V)}{(2c^2+E-V)^2} \tag{2.27}$$

we have, using eq. 2.14

$$\bar{X}^\dagger\chi = \frac{E-V}{2c^2+E-V}\phi - i\frac{(c\vec{\sigma}\cdot\vec{\nabla}V)}{(2c^2+E-V)^2}\chi \tag{2.28}$$

Since the factors in front of ϕ and χ are much smaller than 1 everywhere except possibly very close to the nucleus, the norm of $\bar{X}^\dagger\chi$ is expected to be small.
It is interesting to note that the quantum mechanical effects, arising from the noncommuting of $\vec{p}$ and V and leading to the second term in eq. 2.27, are actually quite small.

2.2.2 The Foldy-Wouthuysen transformation

The most straightforward way to generate an effective two-component Hamiltonian would consist of finding a unitary transformation:

$$U = \begin{pmatrix} \frac{1}{\sqrt{1+X^\dagger X}} & \frac{1}{\sqrt{1+X^\dagger X}}X^\dagger \\ -\frac{1}{\sqrt{1+XX^\dagger}}X & \frac{1}{\sqrt{1+XX^\dagger}} \end{pmatrix} \tag{2.29}$$

$$U^{-1} = U^\dagger$$

$$= \begin{pmatrix} \frac{1}{\sqrt{1+X^\dagger X}} & -X^\dagger\frac{1}{\sqrt{1+XX^\dagger}} \\ X\frac{1}{\sqrt{1+X^\dagger X}} & \frac{1}{\sqrt{1+XX^\dagger}} \end{pmatrix} \tag{2.30}$$

that brings the Dirac Hamiltonian H_D:

$$H_D = \begin{pmatrix} V & c\vec{\sigma}\cdot\vec{p} \\ c\vec{\sigma}\cdot\vec{p} & V-2c^2 \end{pmatrix} \tag{2.31}$$

to block diagonal form. Foldy and Wouthuysen [18] introduced a systematic procedure for decoupling the large and small components to succesively higher orders of c^{-2}. In this section we closely follow the approach and notation of Kutzelnigg [30]. The transformed Hamiltonian:

$$H = UH_DU^{-1} \tag{2.32}$$

is block-diagonal if:

$$-XV - Xc\vec{\sigma}\cdot\vec{p}X + c\vec{\sigma}\cdot\vec{p} + (V-2c^2)X = 0 \tag{2.33}$$

The upper-left part of the transformed Hamiltonian is the Foldy-Wouthuysen Hamiltonian H^{FW}:

$$H^{FW} = \frac{1}{\sqrt{1+X^\dagger X}}\times$$

$$(c\vec{\sigma}\cdot\vec{p}X + X^\dagger c\vec{\sigma}\cdot\vec{p} - 2c^2X^\dagger X + V + X^\dagger VX)\times$$

$$\frac{1}{\sqrt{1+X^\dagger X}} \tag{2.34}$$

The same one-electron energies E_i as obtained from the Dirac equation (only the positive part of the spectrum) result from the Foldy-Wouthuysen transformed Dirac equation:

$$H^{FW}\Phi_i^{FW} = E_i\Phi_i^{FW} \tag{2.35}$$

We now make the regular approximation for X:

$$(2c^2-V)X \approx c\vec{\sigma}\cdot\vec{p} \tag{2.36}$$

The transformed Dirac Hamiltonian will not be block diagonal, but we will neglect this residual coupling. The Foldy-Wouthuysen Hamiltonian is in this approximation:

$$\frac{1}{\sqrt{1+\vec{\sigma}\cdot\vec{p}\frac{c^2}{(2c^2-V)^2}\vec{\sigma}\cdot\vec{p}}}(\vec{\sigma}\cdot\vec{p}\frac{c^2}{2c^2-V}\vec{\sigma}\cdot\vec{p}+V)\times$$

$$\frac{1}{\sqrt{1+\vec{\sigma}\cdot\vec{p}\frac{c^2}{(2c^2-V)^2}\vec{\sigma}\cdot\vec{p}}} \tag{2.37}$$

In this form this is not a practical approximation, because of the $1/\sqrt{1+X^\dagger X}$ operator. In zeroth order we will approximate it as the identity operator. The Foldy-Wouthuysen Hamiltonian using this approximation will give the ZORA Hamiltonian, exactly the same as in the previous section:

$$H^{zora} = \vec{\sigma}\cdot\vec{p}\frac{c^2}{2c^2-V}\vec{\sigma}\cdot\vec{p} + V \tag{2.38}$$

and we have the one-electron ZORA equation:

$$H^{zora}\Phi_i^{zora} = E_i^{zora}\Phi_i^{zora} \tag{2.39}$$

If we would approximate the $1/\sqrt{1+X^\dagger X}$ operator as $1-\frac{1}{2}X^\dagger X$ we will get the FORA Hamiltonian, like in the previous section:

$$H^{fora} = H^{zora} - \frac{1}{2}\vec{\sigma}\cdot\vec{p}\frac{c^2}{(2c^2-V)^2}\vec{\sigma}\cdot\vec{p}H^{zora}$$

$$-\frac{1}{2}H^{zora}\vec{\sigma}\cdot\vec{p}\frac{c^2}{(2c^2-V)^2}\vec{\sigma}\cdot\vec{p} \tag{2.40}$$

The energy E_i^{zora} will in general not be equal to the Dirac energy. To improve this energy we will continue

as in first order perturbation theory, where the zeroth order solution is put in the energy expression for the first order. This will give for the FORA energy:

$$E_i^{fora} = E_i^{zora} \times$$

$$(1 - \langle \Phi_i^{zora} | \vec{\sigma} \cdot \vec{p} \frac{c^2}{(2c^2 - V)^2} \vec{\sigma} \cdot \vec{p} | \Phi_i^{zora} \rangle) \qquad (2.41)$$

We can proceed in a slightly different way if we introduce the following approximations:

$$\frac{1}{\sqrt{1 + X^\dagger X}} \Phi_i \approx \frac{1}{\sqrt{1 + \langle \Phi_i | X^\dagger X | \Phi_i \rangle}} \Phi_i$$

$$(X\Phi_i)^\dagger (X\Phi_i) \approx \langle \Phi_i | X^\dagger X | \Phi_i \rangle \Phi_i^\dagger \Phi_i \qquad (2.42)$$

The difference is the way we approximate the $1/\sqrt{1 + X^\dagger X}$ operator. This has the advantage that $1/\sqrt{1 + X^\dagger X}\Phi_i$ is correct to first order rather than zeroth order. The norm of $X\Phi_i$ will be exact in the approximation above. The improved energy, which follows from these approximations, we will call the scaled ZORA energy (see the resemblance with equation 2.10):

$$E_i^{scaled} = \frac{E_i^{zora}}{1 + \langle \Phi_i^{zora} | \vec{\sigma} \cdot \vec{p} \frac{c^2}{(2c^2 - V)^2} \vec{\sigma} \cdot \vec{p} | \Phi_i^{zora} \rangle} \qquad (2.43)$$

If $\langle \Phi_i^{zora} | X^\dagger X | \Phi_i^{zora} \rangle << 1$, which is true for valence orbitals, the scaled ZORA energies are very close to the FORA energies, which are seen to represent the first term in the expansion of $(1 + \langle \Phi_i^{zora} | \vec{\sigma} \cdot \vec{p} \frac{c^2}{(2c^2 - V)^2} \vec{\sigma} \cdot \vec{p} | \Phi_i^{zora} \rangle)^{-1}$. The scaling procedure sums certain higher order contributions to infinite order.

Kutzelnigg [30] has stressed the problems connected with the traditional procedure to obtain the Foldy-Wouthuysen transformation, which are already apparent from the lowest order (c^{-2}) approximate Hamiltonian (the Pauli Hamiltonian) obtained in the FW method. We pause briefly to demonstrate that part of the trouble is again caused by the neglect of $E - V$ with respect to $2c^2$ rather than E with respect to $2c^2 - V$. Suppose the transformation U (equation 2.29) generates the desired two-component FW wavefunction

$$\begin{pmatrix} \Phi \\ 0 \end{pmatrix} = U \begin{pmatrix} \phi \\ \chi \end{pmatrix} \qquad (2.44)$$

so that

$$\Phi = \frac{1}{\sqrt{1 + X^\dagger X}} \phi + \frac{1}{\sqrt{1 + X^\dagger X}} X^\dagger \chi$$

$$0 = -\frac{1}{\sqrt{1 + XX^\dagger}} X\phi + \frac{1}{\sqrt{1 + XX^\dagger}} \chi \qquad (2.45)$$

The last line is an identity if X satisfies $\chi = X\phi$. If we approximate X by expanding the energy dependent $\bar{X}$ for which $\chi = \bar{X}\phi = (2c^2 + E - V)^{-1} c\vec{\sigma} \cdot \vec{p}\phi$ in $(E - V)/2c^2$, we obtain in lowest order $X \approx (1/2c^2) c\vec{\sigma} \cdot \vec{p}$ and U becomes to order c^{-2}:

$$U = \begin{pmatrix} 1 - \frac{p^2}{8c^2} & \frac{c\vec{\sigma} \cdot \vec{p}}{2c^2} \\ -\frac{c\vec{\sigma} \cdot \vec{p}}{2c^2} & 1 - \frac{p^2}{8c^2} \end{pmatrix} \qquad (2.46)$$

This is precisely the traditional FW transformation to order c^{-2} that leads to the much criticized Pauli Hamiltonian. It is interesting to see what happens if we follow, in order to arrive at an improved effective Hamiltonian, the same strategy as before and avoid the erroneous expansion of $(2c^2 + E - V)^{-1}$ by expanding in $E/(2c^2 - V)$. This leads to inserting $X \approx (2c^2 - V)^{-1} c\vec{\sigma} \cdot \vec{p}$ in the expression for U. We also have to expand the square root operator $\sqrt{1 + X^\dagger X}$, just like in the esc method. Following exactly the same procedure of ordering the terms according to the number of $(2c^2 - V)$ factors in the denominator, the transformation matrix U will now be:

$$U = \qquad (2.47)$$

$$\begin{pmatrix} 1 - \frac{1}{2}\vec{\sigma} \cdot \vec{p} \frac{c^2}{(2c^2 - V)^2} \vec{\sigma} \cdot \vec{p} & \vec{\sigma} \cdot \vec{p} \frac{c}{2c^2 - V} \\ -\frac{c}{2c^2 - V} \vec{\sigma} \cdot \vec{p} & 1 - \frac{1}{2} \frac{c}{2c^2 - V} p^2 \frac{c}{2c^2 - V} \end{pmatrix}$$

This transformation will give in zeroth and first order exactly the same zero and first order (ZORA and FORA) Hamiltonians as obtained before.

The density as well as other properties can be written in terms of the Foldy-Wouthuysen transformed wave functions, but one then needs the unitary matrix 2.29. Denoting the components of the Dirac one-electron spinor Ψ by $\Psi_i, i = 1..4$, those of the transformed wavefunction $\Phi = U\Psi$ by $\Phi_i, i = 1..4$, (Φ_3 and Φ_4 are therefore zero), and the eigenstates of the $\vec{r}$ operator in the direct product space of spatial and spinor coordinates by $|\vec{r}, i\rangle$, we have

$$\rho^D(\vec{r}) = \sum_i |\langle \vec{r}, i | \Psi \rangle|^2$$

$$\neq \sum_i |\langle \vec{r}, i | \Phi \rangle|^2 = \rho^{FW}(\vec{r}) \qquad (2.48)$$

The components of the transformed wavefunction $\Phi = U\Psi$ along the $|\vec{r}, i\rangle$ are not identical to those of Ψ, but only the components of Φ along the *transformed* basis states $U|\vec{r}, i\rangle$ are: $\langle \vec{r}, i | U^\dagger | \Phi \rangle = \langle \vec{r}, i | \Psi \rangle$. This simply reflects the well known fact that a picture change effected by U requires that not only the

wavefunction is transformed but also the observables, in this case $\vec{r}$ to $U\vec{r}U^\dagger \equiv \vec{q}$, in order that the physics remains unaltered. The inverse transformation of the operator $\vec{r}$, $U^\dagger\vec{r}U$, is called $\vec{R}$. It is the operator that describes, in the Dirac picture, the famous average position or mass position r_{mass} of the electron, see Foldy and Wouthuysen [18] and Moss [31]. A clear example of the difference we introduce by using $\Phi(\vec{r})$ instead of $\Phi(\vec{q})$ is provided by the nodes that are present in the solutions Φ_0 to eq. 3.2 and therefore in the (orbital) density $\rho^{zora}(\vec{r})$. Such nodes do not occur in $\rho^D(\vec{r})$ since the nodes of the large component ϕ do not coincide with those of the small component χ. The effect of (neglect of) the picture change is probably small, but such effects are visible for core states, as extensively discussed by Baerends et al. [32]. Although the Dirac density is not $|\Phi(\vec{r})|^2$ it could in principle be calculated from $\Phi(\vec{r})$, for instance by using

$$\begin{pmatrix} \phi \\ \chi \end{pmatrix} = \begin{pmatrix} \frac{1}{\sqrt{1+X^\dagger X}} & -X^\dagger \frac{1}{\sqrt{1+XX^\dagger}} \\ X\frac{1}{\sqrt{1+X^\dagger X}} & \frac{1}{\sqrt{1+XX^\dagger}} \end{pmatrix} \begin{pmatrix} \Phi \\ 0 \end{pmatrix} \tag{2.49}$$

and writing the Dirac electron density as,

$$\begin{aligned} &\rho(\vec{r}) = \phi^\dagger(\vec{r})\phi(\vec{r}) + \chi^\dagger(\vec{r})\chi(\vec{r}) = \\ &= (\frac{1}{\sqrt{1+X^\dagger X}}\Phi(\vec{r}))^\dagger(\frac{1}{\sqrt{1+X^\dagger X}}\Phi(\vec{r}))+ \\ &(X\frac{1}{\sqrt{1+X^\dagger X}}\Phi(\vec{r}))^\dagger(X\frac{1}{\sqrt{1+X^\dagger X}}\Phi(\vec{r})) \end{aligned} \tag{2.50}$$

Note that one can not use the turn-over rule here. We will however approximate the electron density by:

$$\rho^{zora}(\vec{r}) = \Phi^{zora\dagger}(\vec{r})\Phi^{zora}(\vec{r}) \tag{2.51}$$

which follows from the approximations of equation 2.42 that lead to the scaled energy. Here Φ^{zora} are the solutions of equation 3.2. So, apart from using the approximate hamiltonian H^{zora} of eq. 3.2 we also make two presumably small errors for the density. In the first place the effect of the picture change is ignored, meaning we use $\Phi^\dagger(\vec{r})\Phi(\vec{r})$ instead of equation 2.50. In the second place we neglect - consistent with the order in which we work - the fact that the transformation U that we effectively use is only correct to order $E/(2c^2 - V)$, so the small components are not completely annihilated by U, as they are assumed to be in equations 2.49 and 2.50. Maybe this approximation is also most serious when the small component is relatively large. Note that the second approximation, neglect of residual small components, would disappear when more accurate transformations U would be used, but the first approximation, exemplified by the problem of the nodes, would not improve in that case. It can only be remedied by making the correct picture change for the position variable.

2.2.3 Direct Perturbation Theory

In this section we follow the approach of Sadlej and Snijders et al. [33, 34], who have used regular expansions in the direct perturbation theory (DPT) approach proposed by Rutkowski [35] and Kutzelnigg [36]. The approach starts by defining a 4-component wave function Ψ, which has the same large component ϕ as the Dirac wave function, but has a small component ψ which is c times the small component χ of the Dirac equation. To account for this one has to modify the metric. The Dirac equation in this approach is then written as:

$$\begin{aligned} H_D^{DPT}\Psi &= \begin{pmatrix} V & \vec{\sigma}\cdot\vec{p} \\ \vec{\sigma}\cdot\vec{p} & \alpha^2 V - 2 \end{pmatrix} \begin{pmatrix} \phi \\ \psi \end{pmatrix} \\ &= E \begin{pmatrix} 1 & 0 \\ 0 & \lambda^2 \end{pmatrix} \begin{pmatrix} \phi \\ \psi \end{pmatrix} \end{aligned} \tag{2.52}$$

with $\lambda = \alpha = 1/c$. The normalisation of the 4-component wave function Ψ in the modified metric is:

$$\langle\phi|\phi\rangle + \lambda^2\langle\psi|\psi\rangle = 1 \tag{2.53}$$

The standard way of DPT is that all terms that involve λ and α (with $\lambda = \alpha$) are treated as a perturbation. In the regular approximation one only treats terms that involve λ as a perurbation. In zeroth order this will give:

$$\begin{pmatrix} V & \vec{\sigma}\cdot\vec{p} \\ \vec{\sigma}\cdot\vec{p} & \alpha^2 V - 2 \end{pmatrix} \begin{pmatrix} \phi^0 \\ \psi^0 \end{pmatrix} = E^0 \begin{pmatrix} \phi^0 \\ 0 \end{pmatrix} \tag{2.54}$$

Elimination of the small component ψ^0:

$$\psi^0 = \frac{1}{2 - \alpha^2 V}\vec{\sigma}\cdot\vec{p}\phi^0 \tag{2.55}$$

gives:

$$(\vec{\sigma}\cdot\vec{p}\frac{1}{2-\alpha^2 V}\vec{\sigma}\cdot\vec{p} + V)\phi^0 = E^0\phi^0 \tag{2.56}$$

which is the ZORA equation, where the large component ϕ^0 is equal to the ZORA wave function of the previous section. This large component ϕ^0 is normalised to one, as in the previous section. The 4-component wave function obtained we shall call

Ψ^0. It is also possible to consider the approximate 4-component wave function as an approximation to the Dirac wave function without approximating the λ dependent metric. This means that we still solve the ZORA equation, but that the wave function, we will call Ψ_4^{zora} is normalised as:

$$\langle\phi_4^{zora}|\phi_4^{zora}\rangle + c^{-2}\langle\psi_4^{zora}|\psi_4^{zora}\rangle = 1 \tag{2.57}$$

There is just a simple normalisation factor between the functions Ψ^0 and Ψ_4^{zora}:

$$\Psi_4^{zora} = \frac{1}{\sqrt{1 + c^{-2}\langle\psi^0|\psi^0\rangle}}\Psi^0 =$$

$$\frac{1}{\sqrt{1 + c^{-2}\langle\phi^0|\vec{\sigma}\cdot\vec{p}\frac{1}{(2-c^{-2}V)^2}\vec{\sigma}\cdot\vec{p}|\phi^0\rangle}}\Psi^0 \tag{2.58}$$

For the expectation value of an operator A we will also use the new metric:

$$\langle A\rangle =$$

$$\langle\Psi_4^{zora}|\begin{pmatrix} 1 & 0 \\ 0 & c^{-1} \end{pmatrix} A \begin{pmatrix} 1 & 0 \\ 0 & c^{-1} \end{pmatrix}|\Psi_4^{zora}\rangle \tag{2.59}$$

If we apply this to the Dirac Hamiltonian H_D itself, remembering that:

$$H_D^{DPT} = \begin{pmatrix} 1 & 0 \\ 0 & c^{-1} \end{pmatrix} H_D \begin{pmatrix} 1 & 0 \\ 0 & c^{-1} \end{pmatrix} \tag{2.60}$$

we find for the improved energy:

$$E_{scaled}^{zora-4} = \langle\Psi_4^{zora}|H_D^{DPT}|\Psi_4^{zora}\rangle$$

$$= \frac{\langle\Psi^0|H_D^{DPT}|\Psi^0\rangle}{1 + c^{-2}\langle\psi^0|\psi^0\rangle}$$

$$= \frac{E^0}{1 + c^{-2}\langle\phi^0|\vec{\sigma}\cdot\vec{p}\frac{1}{(2-c^{-2}V)^2}\vec{\sigma}\cdot\vec{p}|\phi^0\rangle} \tag{2.61}$$

which is just the scaled ZORA energy of the previous section if the potential is an external potential. This rederivation of the scaled ZORA energy can be found in the article of Sadlej and Snijders et al. [34]. The electron density in this ZORA-4 approach is in view of equation 2.57:

$$\rho_4^{zora}(\vec{r})$$

$$= \phi_4^{zora\dagger}(\vec{r})\phi_4^{zora}(\vec{r}) + \chi_4^{zora\dagger}(\vec{r})\chi_4^{zora}(\vec{r}) \tag{2.62}$$

where:

$$\chi_4^{zora} = c\psi_4^{zora} = \frac{c}{2c^2 - V}\vec{\sigma}\cdot\vec{p}\phi_4^{zora} \tag{2.63}$$

If the potential depends on the density, like in SCF calculations, the ZORA-4 approach differs with respect to the ZORA approach of the last section.

2.2.4 The Douglas-Kroll transformation

In this section we briefly say some words about another successful method for approximating the Foldy-Wouthuysen transformation, the so called Douglas-Kroll transformation [37]. The starting point is the free particle transformation, which can be obtained exactly. If we make the approximation that the potential V commutes with the operator X ($VX = XV$), equation 2.33 will give for X:

$$X \approx \frac{c\vec{\sigma}\cdot\vec{p}}{c^2 + \sqrt{c^4 + p^2c^2}} \tag{2.64}$$

Using this approximation in the Foldy-Wouthuysen Hamiltonian (see equation 2.34), again using that V commutes with X, we get:

$$H^{FW} = \sqrt{c^4 + p^2c^2} - c^2 + V \tag{2.65}$$

which is the classical relativistic form of the energy of a particle in a potential (see section 2.1). If the potential is a constant (free particle case), this is the exact Foldy-Wouthuysen transformation, because in this case V and X commute. In general V and X will not commute. Using an expansion method one can take these effects to a certain order into account [37]. This expansion remains regular even for a Coulomb-like potential. For atomic and molecular calculations this method has been further developed by Hess [38]. In ordinary basis set programs one needs to evaluate integrals in momentum space in order to calculate rather complicated looking matrix elements. Practical implementations have been provided by Hess and co-workers in ab-initio schemes [38, 39] and by Knappe and Rösch [40] in a density-functional implementation. This method is now widely used in atomic and molecular calculations.

Chapter 3

The ZORA Hamiltonian

3.1 Basic equations

In chapter 2 we have derived a regularized two-component Hamiltonian by simply modifying the traditional esc, FW and DPT approaches so as to take care of the radius of convergence of the employed expansions. The present simple approach becomes more complicated for higher orders. It has been presented in some detail in order to stress the important point concerning the validity of the expansions to be used. The Hamiltonian obtained has actually been derived earlier by Chang, Pélissier and Durand [5] and Heully et al. [6] will be denoted as the zeroth order regular approximated (ZORA) Hamiltonian H^{zora} (we leave aside the further regularisation of the kinetic energy applied by Chang et al.). We will not study higher order terms of the Hamiltonian but we note that Chang et al. have derived and used high order terms in the expansion of H^{esc}. Although our zero order hamiltonian is identical to the one obtained by Chang et al., this does not hold for the higher orders since they did not use the renormalisation operator O and obtained non-hermitian higher orders. Our first order regular approximated H^{fora} is actually identical to the hermitian Des Cloizeaux H^1 [5].

The ZORA effective Hamiltonian may be further developed:

$$H^{zora} = V + \vec{\sigma}\cdot\vec{p}\frac{c^2}{2c^2-V}\vec{\sigma}\cdot\vec{p}$$

$$= V + \vec{p}\frac{c^2}{2c^2-V}\vec{p} + \frac{c^2}{(2c^2-V)^2}\vec{\sigma}\cdot(\vec{\nabla}V\times\vec{p}) \quad (3.1)$$

One can now see that the spin-orbit splitting is already present in the zeroth order Hamiltonian. This spin-orbit term is regular because of the $(2c^2-V)^{-2}$ factor in it. It poses no problems in variational calculations. The eigen-value equation:

$$H^{zora}\Phi^{zora} = (V + \vec{\sigma}\cdot\vec{p}\frac{c^2}{2c^2-V}\vec{\sigma}\cdot\vec{p})\Phi^{zora}$$

$$= E^{zora}\Phi^{zora} \quad (3.2)$$

is only a second order differential equation. The two-component wave function Φ^{zora} will now be referred to as the ZORA wave function. In first order perturbation calculations the FORA-energy E^{fora} is:

$$E^{fora} = E^{zora}\times$$

$$(1 - \langle\Phi^{zora}|\vec{\sigma}\cdot\vec{p}\frac{c^2}{(2c^2-V)^2}\vec{\sigma}\cdot\vec{p}|\Phi^{zora}\rangle) \quad (3.3)$$

and the scaled ZORA energy, which sums certain higher order contributions to infinite order, is:

$$E^{scaled} = \frac{E^{zora}}{1 + \langle\Phi^{zora}|\vec{\sigma}\cdot\vec{p}\frac{c^2}{(2c^2-V)^2}\vec{\sigma}\cdot\vec{p}|\Phi^{zora}\rangle} \quad (3.4)$$

Because the Hamiltonian H^{zora} is energy-independent and Hermitian the eigenfunctions belonging to different eigenvalues E^{zora} are orthogonal. In the ZORA method the electron density is the sum of the squared orbital wave functions (two-component functions), whereas in the ZORA-4 method (4-component functions) the small component is taken into account (see section 2.2.3).
In quantum chemistry there are many situations where the spin-orbit splitting is not important. One can therefore be interested in a scalar relativistic equation, which has the same symmetry as the Schrödinger equation. In refs. [41] and [42] such a scalar relativistic equation (SR) was suggested and applied to some atomic and solid state problems. This equation is given by:

$$(V + \vec{p}\frac{c^2}{2c^2 + E^{SR} - V}\vec{p})\phi^{SR} = E^{SR}\phi^{SR} \quad (3.5)$$

with orbital density:

$$\rho^{SR}(\vec{r}) = \phi^{SR\dagger}(\vec{r})\phi^{SR}(\vec{r}) \quad (3.6)$$

The zeroth order regular approximate (ZORA) scalar relativistic equation is obtained as the zeroth order term in an expansion in $E/(2c^2-V)$ of this equation:

$$H_{SR}^{zora}\Phi_{SR}^{zora} \equiv (V + \vec{p}\frac{c^2}{2c^2-V}\vec{p})\Phi_{SR}^{zora}$$

$$= E_{SR}^{zora}\Phi_{SR}^{zora} \tag{3.7}$$

which is just the ZORA Hamiltonian (see equation 3.1) without spin-orbit coupling. The FORA and scaled ZORA scalar relativistic energies can be derived analoguous to the ones with spinorbit. In the scalar relativistic case they are:

$$E_{SR}^{fora} = E_{SR}^{zora} \times$$

$$(1 - \langle\Phi_{SR}^{zora}|\vec{p}\frac{c^2}{(2c^2-V)^2}\vec{p}|\Phi_{SR}^{zora}\rangle) \tag{3.8}$$

$$E_{SR}^{scaled} = \frac{E_{SR}^{zora}}{1 + \langle\Phi_{SR}^{zora}|\vec{p}\frac{c^2}{(2c^2-V)^2}\vec{p}|\Phi_{SR}^{zora}\rangle} \tag{3.9}$$

3.2 Boundedness from below

An important question is whether the eigenvalue spectrum of the ZORA Hamiltonian is bounded from below. We first briefly investigate this problem along the lines of the analysis of Landau and Lifshitz [43] for the nonrelativistic case, before we give a rigorous proof that the ZORA eigenvalue spectrum is bounded from below. We only consider potentials V for which $2c^2 - V > 0$ everywhere, so that the ZORA kinetic energy operator T^{zora}

$$T^{zora} = \vec{\sigma}\cdot\vec{p}\frac{c^2}{2c^2-V}\vec{\sigma}\cdot\vec{p} \tag{3.10}$$

is a positive operator. If the potential is bounded from below by V_{min}, then all the ZORA eigenvalues $E_n^{zora} \geq V_{min}$, because the mean value of $T^{zora} \geq 0$. Now suppose the potential V is of the form:

$$V = -\frac{Z}{r^s} \tag{3.11}$$

near the origin. Consider a wave function localized in some small region (of radius r_0) around the origin. The uncertainty in the momentum of the particle is then of order $1/r_0$ (uncertainty principle). The sum of the mean values of the potential and kinetic energy then is of the order:

$$-\frac{Z}{r_0^s} + \frac{c^2}{r_0^2(2c^2 + \frac{Z}{r_0^s})} \tag{3.12}$$

For $s < 1$ this energy expression can not take arbitrarily large negative values. However, whereas in the nonrelativistic case the energy is bounded from below for $s < 2$ and conditionally so for $s = 2$ (depending on the strength of the potential, cf. ref. [43], §35), the case $s = 1$ is already a special one for the ZORA eigenvalue spectrum. Equation 3.12 suggests that for $s = 1$, i.e. a Coulomb potential, the ZORA Hamiltonian will only be a bounded operator for $Z < c$. In fact, the condition $Z < c$ for the strength of the Coulomb potential is familiar from the Dirac equation. Analogous conditions for the potential in the Dirac and the ZORA equation may perhaps be expected from the identical asymptotic behaviour for $r \to 0$ for the regular solutions, which is $r^{\gamma-1}$ in both cases (see section 4.5). Here

$$\gamma = \sqrt{\kappa^2 - \frac{Z^2}{c^2}} \tag{3.13}$$

and κ is the usual relativistic quantum number. However, these arguments are qualitative.

Now a more detailed treatment of this important question, that the ZORA eigenvalue spectrum is bounded from below if $Z < c$ s given. In chapter 4 it will be shown, that the solutions of the zeroth order of this two-component regular approximate (ZORA) equation for hydrogen-like atoms are simply scaled solutions of the large component of the Dirac wave function for this problem. The eigenvalues are related in a similar way as (see eq. 4.9):

$$E^{zora} = \frac{2c^2E^D}{2c^2 + E^D} \tag{3.14}$$

For $Z < c$ the Dirac equation has eigenvalues below $-2c^2$ (negative energy continuum), between $-c^2$ and 0 (discrete spectrum) and above zero (positive energy continuum). According to equation 3.14 these parts of the Dirac spectrum are mapped onto the ZORA spectrum as follows (see figure 3.1): the positive energy continuum $(0,\infty)$ onto $(0,2c^2)$; the discrete part $(-c^2,0)$ onto $(-2c^2,0)$; the negative energy continuum $(-\infty,-2c^2)$ onto $(2c^2,\infty)$. So all the eigenvalues of the ZORA equation are larger than $-2c^2$, which means that for this potential the zeroth order regular approximate Hamiltonian is bounded from below.

Now suppose the potential is given by:

$$V = -\frac{Z}{r} + V_1(r) \tag{3.15}$$

where V_1 is larger than zero everywhere. This V_1 will usually be the mean repulsive potential of some electron density. We can divide the ZORA Hamiltonian for this potential in operators, which are all bounded from below:

$$H^{zora} = -\frac{Z}{r} + V_1 + \vec{\sigma}\cdot\vec{p}\frac{c^2}{2c^2 + \frac{Z}{r} - V_1}\vec{\sigma}\cdot\vec{p} =$$

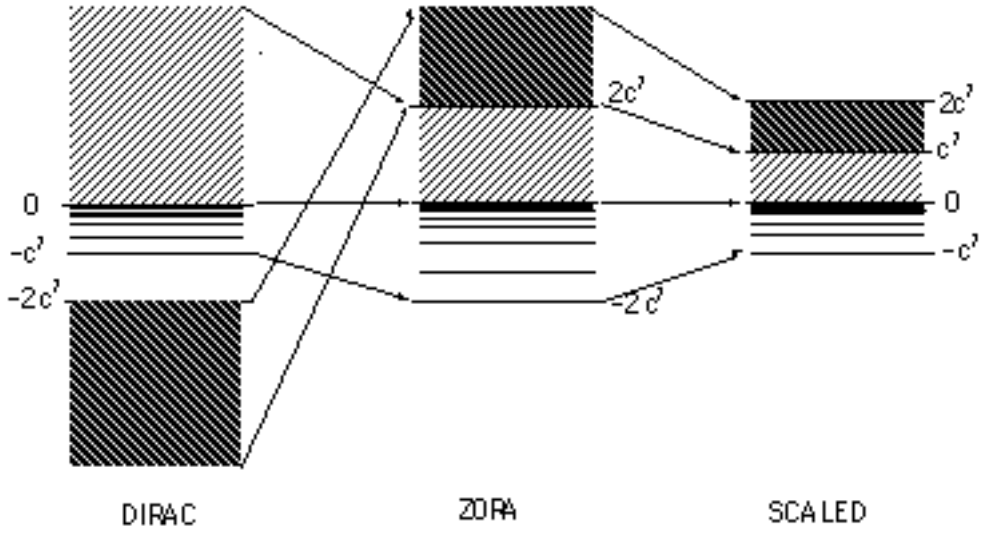

Figure 3.1: Relation between Dirac, ZORA and scaled ZORA eigenvalues for a hydrogen-like atom

$$= -\frac{Z}{r} + \vec{\sigma}\cdot\vec{p}\frac{c^2}{2c^2+\frac{Z}{r}}\vec{\sigma}\cdot\vec{p} + V_1$$

$$+\vec{\sigma}\cdot\vec{p}\frac{c^2 V_1}{(2c^2+\frac{Z}{r})(2c^2+\frac{Z}{r}-V_1)}\vec{\sigma}\cdot\vec{p} \qquad (3.16)$$

From the discussion earlier in this section we know that the first two terms together give an operator that is bounded from below. The last two terms are both positive operators because V_1 is positive and the last operator can be written as the product of an operator with its hermitian adjoint if $(2c^2+\frac{Z}{r}-V_1)>0$. This last condition will always be satisfied in atomic and molecular electronic structure calculations. Again we have because of $V<2c^2$ that the ZORA "kinetic energy" operator T^{zora} is a positive operator.
The former analysis can be extended to molecular systems, by splitting up the space into regions which contain only one nucleus. In each region the contribution to the expectation value of the Hamiltonian for every wavefunction is bounded from below (as long as all nuclear charges are smaller than c), since the contributions to the potential coming from the tails of the nuclear potentials of other regions are finite. Consequently the total Hamiltonian is also bounded from below.
The ZORA Hamiltonian is not bounded from below for a hydrogen-like potential of a point charge with $Z>c$. The Dirac equation then also becomes problematic. To prove that the ZORA Hamiltonian is not bounded from below, we may use the fact that all expectation values of a bounded operator with some normalized wave function should be larger than a minimum. If we can prove that for some trial wave function the expectation value of this operator can be as negative as one likes, than this operator is not bounded from below. Let us try therefore a wavefunction Φ^T, with quantum number $\kappa=-1$ and a radial behaviour as:

$$\Phi^T = r^\alpha e^{-\beta r} \qquad (3.17)$$

Here α should be larger than -1 for the expectation value of the potential to be meaningful. The expectation value $\langle E\rangle$ of the ZORA Hamiltonian is:

$$\langle E\rangle = \frac{\langle\Phi^T|H^{zora}|\Phi^T\rangle}{\langle\Phi^T|\Phi^T\rangle} =$$

$$= \frac{\langle\Phi^T|-\frac{Z}{r}+\vec{\sigma}\cdot\vec{p}\frac{c^2}{2c^2+\frac{Z}{r}}\vec{\sigma}\cdot\vec{p}|\Phi^T\rangle}{\langle\Phi^T|\Phi^T\rangle}$$

$$< \frac{\langle\Phi^T|-\frac{Z}{r}+\vec{\sigma}\cdot\vec{p}\frac{c^2 r}{Z}\vec{\sigma}\cdot\vec{p}|\Phi^T\rangle}{\langle\Phi^T|\Phi^T\rangle} \qquad (3.18)$$

This last term can easily be calculated giving:

$$\langle E\rangle < -\frac{Z\beta}{\alpha+1}+\frac{c^2\beta(\alpha+3)}{2Z(\alpha+1)} \qquad (3.19)$$

Suppose $\alpha=-1+\epsilon$, where ϵ is some small positive number, we can rewrite this as:

$$\langle E\rangle < \frac{\beta}{\epsilon}\left(-Z+\frac{c^2(2+\epsilon)}{2Z}\right) \qquad (3.20)$$

Here it can easily be seen that if $Z > c$ we can choose ϵ sufficiently small, so that the term between brackets is negative. Now we still have the freedom to choose β in such a way as to make the term on the right hand side of the inequality as negative as one likes. This proves that the operator is unbounded from below.
If we take the more physical point of view that the nucleus is finite, then the nuclear potential will not have a singularity. The ZORA Hamiltonian in this case is bounded from below if $V < 2c^2$ everywhere, because the potential is bounded from below and the ZORA kinetic energy operator T^{zora} is a positive operator.

3.3 Total energy

In this section we will derive an expression for the total ZORA energy. We will use the results of section 2.2.2 for the regular expansions in the Foldy-Wouthuysen approach.
We can write the total energy of a many-electron system in a density functional approach (without the interaction energy of the nuclei), using the one-electron orbitals of the Kohn-Sham independent particle formulation of the theory, as:

$$E_{TOT}^{Dirac} =$$

$$\sum_{i=1}^{N} \int (\phi_i^\dagger c\vec{\sigma}\cdot\vec{p}\chi_i + \chi_i^\dagger c\vec{\sigma}\cdot\vec{p}\phi_i - 2c^2\chi_i^\dagger\chi_i)$$

$$+ \int \rho V_N + \frac{1}{2}\int\int \frac{\rho(1)\rho(2)}{r_{12}} + E_{XC}[\rho] \qquad (3.21)$$

where:

$$\rho = \sum_{i=1}^{N} (\phi_i^\dagger\phi_i + \chi_i^\dagger\chi_i) \qquad (3.22)$$

The Kohn-Sham approach assumes that there exists a model system of N non-interacting electrons moving in a local potential $V(\vec{r})$ which has the same density as the exact interacting system. The one-electron Kohn-Sham orbitals yield the non-interacting (Dirac) kinetic energy and the above equation is essentially a definition of $E_{XC}[\rho]$ which evidently, apart from the exchange and correlation energies, also has to incoporate the difference between the true and the non-interacting kinetic energies. For the electron-electron repulsion the non-relativistic operator is used. Optimisation of the total energy yields the following one-electron equations, which are the relativistic equivalents of the Kohn-Sham equations:

$$c\vec{\sigma}\cdot\vec{p}\chi_i + V\phi_i = E_i\phi_i$$

$$c\vec{\sigma}\cdot\vec{p}\phi_i - 2c^2\chi_i + V\chi_i = E_i\chi_i \qquad (3.23)$$

where:

$$V(\vec{r}_1) = V_N(\vec{r}_1) + \int \frac{\rho(2)}{r_{12}} d\vec{r}_2 + \frac{\delta E_{XC}[\rho]}{\delta\rho(\vec{r}_1)} \qquad (3.24)$$

Using these one-electron equations in the expression for the total energy, one obtains

$$E_{TOT} = \sum_{i=1}^{N} E_i - \frac{1}{2}\int\int \frac{\rho(1)\rho(2)}{r_{12}} d1\,d2$$

$$+E_{XC}[\rho] - \int \rho(1)\frac{\delta E_{XC}[\rho]}{\delta\rho(1)} d1 \qquad (3.25)$$

We now wish to transform to a two-component formulation by decoupling the large and small components by way of a Foldy-Wouthuysen transformation. Using a unitary matrix U (see [30] and section 2.2.2):

$$U = \begin{pmatrix} \frac{1}{\sqrt{1+X^\dagger X}} & \frac{1}{\sqrt{1+X^\dagger X}}X^\dagger \\ -\frac{1}{\sqrt{1+XX^\dagger}}X & \frac{1}{\sqrt{1+XX^\dagger}} \end{pmatrix} \qquad (3.26)$$

one can transform the Dirac-Hamiltonian H_D to a block-diagonal form if:

$$-XV - Xc\vec{\sigma}\cdot\vec{p}X + c\vec{\sigma}\cdot\vec{p} + (V - 2c^2)X = 0 \qquad (3.27)$$

We can express the large and small component ϕ and χ of the Dirac wave function in terms of the Foldy-Wouthuysen transformed wave function Φ^{FW} as:

$$\begin{pmatrix} \phi \\ \chi \end{pmatrix} = U^{-1}\begin{pmatrix} \Phi^{FW} \\ 0 \end{pmatrix} =$$

$$\begin{pmatrix} \frac{1}{\sqrt{1+X^\dagger X}}\Phi^{FW} \\ X\frac{1}{\sqrt{1+X^\dagger X}}\Phi^{FW} \end{pmatrix} \qquad (3.28)$$

The same one-electron energies E_i as obtained in eq.3.23 result from the Foldy-Wouthuysen transformed Dirac-Kohn-Sham equation 2.35:

$$\frac{1}{\sqrt{1+X^\dagger X}}\times$$

$$(c\vec{\sigma}\cdot\vec{p}X + X^\dagger c\vec{\sigma}\cdot\vec{p} - 2c^2X^\dagger X + V + X^\dagger VX)\times$$

$$\frac{1}{\sqrt{1+X^\dagger X}}\Phi_i^{FW} = E_i\Phi_i^{FW} \qquad (3.29)$$

The total energy may therefore also be written as:

$$E_{TOT}^{FW} = \sum_{i=1}^{N} \int d1 (\Phi_i^{FW})^\dagger \frac{1}{\sqrt{1+X^\dagger X}}\times$$

$$(c\vec{\sigma}\cdot\vec{p}X + X^\dagger c\vec{\sigma}\cdot\vec{p} - 2c^2X^\dagger X + V + X^\dagger VX)\times$$

$$\frac{1}{\sqrt{1+X^\dagger X}}\Phi_i^{FW} - \frac{1}{2}\int\int\frac{\rho(1)\rho(2)}{r_{12}}d1d2$$
$$+E_{XC}[\rho] - \int\rho(1)\frac{\delta E_{XC}[\rho]}{\delta\rho(1)}d1 \quad (3.30)$$

where:

$$\rho = \sum_{i=1}^{N}[\frac{1}{\sqrt{1+X^\dagger X}}\Phi_i^{FW})^\dagger(\frac{1}{\sqrt{1+X^\dagger X}}\Phi_i^{FW})+$$
$$(X\frac{1}{\sqrt{1+X^\dagger X}}\Phi_i^{FW})^\dagger(X\frac{1}{\sqrt{1+X^\dagger X}}\Phi_i^{FW})] \quad (3.31)$$

We will approximate X in the same way as before (see section 2.2.2). The transformed Dirac Hamiltonian will not be block diagonal, but we will neglect this residual coupling.

$$X \approx \frac{c}{2c^2-V}\vec{\sigma}\cdot\vec{p} \quad (3.32)$$

together with the following approximations that lead to the scaled ZORA energy:

$$\frac{1}{\sqrt{1+X^\dagger X}}\Phi_i \approx \frac{1}{\sqrt{1+\langle\Phi_i|X^\dagger X|\Phi_i\rangle}}\Phi_i$$
$$(X\Phi_i)^\dagger(X\Phi_i) \approx \langle\Phi_i|X^\dagger X|\Phi_i\rangle\Phi_i^\dagger\Phi_i \quad (3.33)$$

The norm of $X\Phi_i$ will be exact in the approximation above. Using these approximations the density can be written as:

$$\rho = \sum_{i=1}^{N}\Phi_i^\dagger\Phi_i \quad (3.34)$$

which is equivalent to a neglect of picture change. A slightly different approach is the ZORA-4 method (see section 2.2.3), where we will use also a small component for the density. The approximate Foldy-Wouthuysen transformed Dirac equation now becomes an equation, which we shall call the scaled ZORA equation:

$$\frac{\vec{\sigma}\cdot\vec{p}\frac{c^2}{2c^2-V}\vec{\sigma}\cdot\vec{p}+V}{1+\langle\Phi_i|\vec{\sigma}\cdot\vec{p}\frac{c^2}{(2c^2-V)^2}\vec{\sigma}\cdot\vec{p}|\Phi_i\rangle}\Phi_i$$
$$= E_i^{scaled}\Phi_i \quad (3.35)$$

which only differs from the ZORA equation:

$$(\vec{\sigma}\cdot\vec{p}\frac{c^2}{2c^2-V}\vec{\sigma}\cdot\vec{p}+V)\Phi_i = E_i^{zora}\Phi_i \quad (3.36)$$

in the scaling factor in the denominator. The total energy is:

$$E_{TOT}^{scaled} = \sum_{i=1}^{N}E_i^{scaled} - \frac{1}{2}\int\int\frac{\rho(1)\rho(2)}{r_{12}}d1d2$$
$$+E_{XC}[\rho] - \int\rho(1)\frac{\delta E_{XC}[\rho]}{\delta\rho(1)}d1 \quad (3.37)$$

Due to the approximations made, the one-electron equations 3.35 are not variationally connected with this total energy. In order to get total energy expressions for the ZORA and FORA method we just have to replace, in zeroth order, in the total energy expression the sum of scaled one-electron energies by the sum of ZORA one-electron energies and in first order by the sum of FORA (first order regular approximate) one-electron energies. The ZORA-4 method (see section 2.2.3) differs only in the way the electron density is obtained.

To solve the scaled ZORA equation 3.35 we simply have to solve the ZORA equation 3.36. The ZORA and scaled ZORA eigenfunctions are the same. To obtain the energy the ZORA energy is scaled (see eq. 3.4):

$$E_i^{scaled} = \frac{E_i^{zora}}{1+\langle\Phi_i|\vec{\sigma}\cdot\vec{p}\frac{c^2}{(2c^2-V)^2}\vec{\sigma}\cdot\vec{p}|\Phi_i\rangle}$$
$$= \frac{E_i^{zora}}{1+\langle\Phi_i|X^\dagger X|\Phi_i\rangle} \quad (3.38)$$

The FORA energy is defined as in equation 3.3:

$$E_i^{fora} = E_i^{zora}\times$$
$$(1-\langle\Phi_i|\vec{\sigma}\cdot\vec{p}\frac{c^2}{(2c^2-V)^2}\vec{\sigma}\cdot\vec{p}|\Phi_i\rangle) \quad (3.39)$$

In chapter 4 we discuss the ZORA eigenvalues of the hydrogen-like atoms, where the nucleus is a point charge. There we found that those were exactly equal to the Dirac energy, thus $E^{scaled} = E^D$. In this case the scaled ZORA energy thus corrects completely for the error in the ZORA one-electron energies. This holds true in particular for the deep core levels, where the error, being of order $(E^{zora})^2/2c^2$, is largest, relatively and in an absolute sense.
In table 3.1 some of the core one-electron energies are shown for the neutral Uranium atom using the $X\alpha$ approximation to the exchange-correlation potential with $\alpha = 0.7$. The scaled ZORA energies are now not exact anymore. Still from the table we can see that the scaled ZORA $1s_{1/2}$ orbital energy is much closer to the Dirac energy than the ZORA or FORA orbital energy. For the other core orbitals the improvement of scaled ZORA over FORA, which is already rather accurate, is smaller. For valence orbitals, which are shown in table 3.2, the ZORA energies are quite close to the Dirac energies and the scaled ZORA values are

Table 3.1: Uranium orbital energies of some deep core levels in a.u.

	$1s_{1/2}$	$2s_{1/2}$	$2p_{1/2}$	$2p_{3/2}$	$3s_{1/2}$
NR	-3690.78	-640.21	-619.59	-619.59	-161.26
ZORA	-4872.99	-818.96	-789.87	-641.99	-202.63
FORA	-4158.88	-793.51	-765.24	-625.15	-200.51
SCALED	-4250.15	-794.28	-765.99	-625.58	-200.54
DIRAC	-4255.55	-795.00	-766.70	-625.96	-200.69

Table 3.2: Uranium orbital energies of some valence levels in a.u.

	$6s_{1/2}$	$6p_{1/2}$	$6p_{3/2}$	$5f_{5/2}$	$6d_{3/2}$	$7s_{1/2}$
NR	-1.2984	-0.7945	-0.7945	-0.3419	-0.1157	-0.1071
ZORA	-1.7190	-1.0687	-0.7409	-0.1040	-0.0711	-0.1339
FORA	-1.7185	-1.0684	-0.7407	-0.1040	-0.0711	-0.1339
SCALED	-1.7185	-1.0684	-0.7407	-0.1040	-0.0711	-0.1339
DIRAC	-1.7198	-1.0694	-0.7410	-0.1033	-0.0710	-0.1340

Table 3.3: X-Alpha total energies of Gold and Uranium in a.u.

METHOD	Gold	Uranium
NR	-18412.52	-25669.49
ZORA	-19719.60	-29516.25
FORA	-18986.33	-27892.70
SCALED	-19046.02	-28080.24
DIRAC	-19046.59	-28081.76

practically identical to the ZORA and FORA ones.

In table 3.3 the total energies of the neutral Gold and Uranium atom are given for the different methods. We can see that the scaled ZORA total energy is in far better agreement with the DIRAC total energy than the ZORA or FORA total energy. For comparison also the non-relativistic (NR) value is given. It is evident from the foregoing that the relatively poor behaviour of ZORA can be ascribed almost entirely to the ZORA error for the one-electron energies of the deep core levels.
One might suppose that this deficiency of the ZORA one-electron energies for the deep core is not relevant when one computes valence properties such as the first ionisation energies and molecular bond energies. Such properties can even be obtained from frozen core calculations to very good accuracy. However, for all-electron calculations this question requires a careful treatment due to the special circumstance that the ZORA one-electron equation is not gauge invariant. The lack of gauge invariance and its consequences both in all-electron and in frozen-core calculations, will be discussed in the next section.

3.4 Gauge invariance

The ZORA equation is not gauge invariant. Let us take for example the hydrogen-like atom, with a point charge for the nucleus, and add a constant Δ to the potential:

$$V_\Delta = -\frac{Z}{r} + \Delta \tag{3.40}$$

The ZORA equation for this potential will not have eigenvalues E_Δ^{zora} which are shifted with the same constant. For a hydrogen-like atom we can calculate exactly the deviation from a shift Δ:

$$E_\Delta^{zora} = E^{zora} + \Delta - \frac{E^{zora}\Delta}{2c^2} \tag{3.41}$$

So the ZORA equation will break gauge invariance with $E^{zora}\Delta/2c^2$. This is small compared to Δ if E^{zora} is small compared to $2c^2$, which is true for valence orbitals. For core levels this lack of gauge invariance can be a problem, as we shall see in an example at the end of this section. The eigenfunction Φ_Δ of the ZORA equation for V_Δ is a scaled eigenfunction Φ of the ZORA equation for the potential without the constant Δ:

$$\Phi_\Delta(\vec{r}) = \Phi(\frac{\vec{r}(2c^2-\Delta)}{2c^2}) \tag{3.42}$$

This scaling differs from one by $\Delta/2c^2$. The FORA energy in a potential V_Δ has a shift:

$$E_\Delta^{fora} = E^{fora} + \Delta - \frac{(E^{zora})^2\Delta}{4c^4} \tag{3.43}$$

So in first order the lack of gauge invariance is reduced with a factor of $E^{zora}/2c^2$ compared to the

zeroth order. Going to higher orders will further improve the gauge invariance, but the scaling introduced in the previous section is particularly effective. The scaled ZORA energy E_Δ^{scaled} in a potential V_Δ has the required shift Δ:

$$E_\Delta^{scaled} = E^{scaled} + \Delta \tag{3.44}$$

This is valid in the case of a hydrogen-like atom, in general this will not be true exactly.

In practical calculations on atoms and molecules we will demand the potential to go to zero at infinity, which defines the "natural gauge". One may wonder if the problem of gauge dependency has any practical relevance, but we will see from a simple example that this is very much the case. Such an example is the calculation of ionisation energies, calculated as differences between total energies. In table 3.4 we compare some of the ionisation energies of gold, which were obtained from all electron numerical calculations. These calculations were done in a spherical averaged potential and using the simple $X\alpha$ method, because the purpose here is not to obtain experimental numbers, but to compare methods. Using the total ZORA energy gives poor results. To understand this, we have to notice that the main effect of ionisation of an outer electron on core electrons is a constant shift Δ of the potential, which effectively means a change of gauge. In the Dirac case this will only lead to a shift of the eigenvalues with the same constant. In the ZORA case an extra shift will occur in the eigenvalues of order $E^{zora}\Delta/2c^2$ for deep core orbitals, which feel the nuclear potential almost unscreened. Since the sum of one-electron energies occurs in the total energy, this erroneous gauge dependence of the one-electron energy causes an error in the total energy difference between ion and neutral atom. The FORA result improves upon the ZORA result considerably, but is still not accurate enough for chemical purposes. The scaled ZORA result is within the required "chemical" accuracy of ca. 0.0005 au. It should be noted that the error in the ZORA calculation of the ionisation energy is not of the order of the ZORA error $(E^{zora})^2/2c^2$ in the one-electron energies, which is as high as 300 au for the $1s$ of Au, but it is due to the (much smaller) *change* in this error of $(E^{zora})\Delta/2c^2$ for hydrogenic ions. For a general potential $V(\vec{r})$ an estimate of the gauge dependence, which is of order c^{-2}, can be obtained from the difference in the first order energies (eq. 3.39) for $V+\Delta$ and V. This yields a gauge dependence of order Δ times $\langle\Phi|X^\dagger X|\Phi\rangle$, which can be used for higher core and valence orbitals. Actual calculations show the shifts Δ to be 0.3, 0.4 and 0.8 a.u. for the 6s, 5d and 6s+5d ionisations resp. From these data, the error in the ZORA ionisation energies in table 3.4 can be estimated. The error proves to be essentially due to the gauge dependence in the deep core levels.

In table 3.4 we also report some calculations with a finite nucleus potential, obtained from a homogeneous nuclear charge distribution. The total energy shifted with some 4 a.u., but the differences in the total energies remain practically the same.

In view of this gauge dependence problem for the deep core levels, valence-only calculations seem to be recommended. In this approach the density is split into a core density, which is kept frozen, and a valence density. In our calculations the core density is taken from an all-electron Dirac calculation on the neutral atom, and we use this core density also for calculations on the ion. The Dirac result for the valence-only calculations of ionisation energies differs therefore from the all-electron calculations. Comparing the Dirac results in table 3.5 with those in table 3.4 shows, however, that the use of the neutral atom core in the ion affects the result by less than 0.001 au. In the valence density we only use the $5d_{3/2}$, $5d_{5/2}$ and $6s_{1/2}$ orbital densities. In table 3.5 we compare the different methods for these valence-only calculations. All results (Dirac, ZORA, scaled ZORA, FORA) are now very close. The scaled ZORA and FORA results are practically identical to the Dirac result. The shift Δ obtained in the calculations for the three ionisations is rather uniform and is 0.3, 0.4 and 0.8 a.u. for the valence levels as well. $\langle\Phi|X^\dagger X|\Phi\rangle$ for these valence orbitals is calculated to be about 0.0002, yielding an estimate of the differences between the ZORA and scaled ZORA or FORA that is in perfect agreement with the numbers of the table. Now the ZORA result is already within "chemical" accuracy. The bad performance of ZORA and FORA in the all-electron case can therefore indeed be attributed to the gauge dependence for the core electrons.

The gauge problem is also relevant for molecular bond energy calculations, since the formation of a bond is also accompanied by shifts of the potential at the core region, as is well known from the ESCA shifts measured in X-ray photoelectron spectroscopy. Bond energies may however be computed, according to the results of this section, by freezing the core or by using the scaled ZORA approach (or both). In the next section we will discuss some technical aspects of the calculation of bond energies and then present a number of calculations on molecules in the last section.

Table 3.4: Gold ionisation energies in a.u. from all-electron calculations

	POINT CHARGE NUCLEUS				FINITE NUCLEUS	
ION	DIRAC	ZORA	FORA	SCALED	DIRAC	SCALED
$(6s_{1/2})^{-1}$	0.3286	0.1650	0.3361	0.3288	0.3284	0.3285
$(5d_{5/2})^{-1}$	0.3992	0.1745	0.4095	0.3996	0.3994	0.3996
$(6s_{1/2})^{-1}(5d_{5/2})^{-1}$	1.0609	0.6443	1.0800	1.0615	1.0607	1.0612

Table 3.5: Gold ionisation energies in a.u. from valence-only calculations.

ION	DIRAC	ZORA	FORA	SCALED
$(6s_{1/2})^{-1}$	0.3285	0.3279	0.3286	0.3286
$(5d_{5/2})^{-1}$	0.3999	0.3991	0.3999	0.3999
$(6s_{1/2})^{-1}(5d_{5/2})^{-1}$	1.0618	1.0603	1.0619	1.0619

3.5 Molecular bond energies

In chemistry one is often not interested in total energies, but only in differences in energies, for instance in the diference between ground state and excited or ionized state, or in the difference between the energies of a molecule and its constituent atoms. In computational schemes that rely on three-dimensional numerical integration of the Hamiltonian matrix elements [44, 45] the calculation of such energy differences can be carried out with sufficient numerical precision. This holds even if it would only be possible to obtain the absolute energies, which may be many orders of magnitude larger, to sufficiently high precision with impractically large numbers of sampling points. Since we wish to apply three-dimensional numerical integration, which is obviously very suitable for the calculation of matrix elements of the (scaled) ZORA Hamiltonian in molecules, we have to use similar techniques as in the non-relativistic calculations of bond energies. After some manipulation the total scaled ZORA energy can be written as:

$$E_{TOT}^{scaled} = \sum_{i=1}^{N} \langle \Phi_i | \vec{\sigma} \cdot \vec{p} \frac{c^2}{2c^2 - V} \vec{\sigma} \cdot \vec{p} | \Phi_i \rangle$$

$$- \sum_{i=1}^{N} E_i^{scaled} \langle \Phi_i | \vec{\sigma} \cdot \vec{p} \frac{c^2}{(2c^2 - V)^2} \vec{\sigma} \cdot \vec{p} | \Phi_i \rangle +$$

$$\int \rho(1) V_N(1) d1 + \frac{1}{2} \int \int \frac{\rho(1)\rho(2)}{r_{12}} + E_{XC}[\rho] \quad (3.45)$$

This expression can be compared to the total non-relativistic energy, which can be written as:

$$E_{TOT}^{NR} = \sum_{i=1}^{N} \langle \Phi_i | \frac{p^2}{2} | \Phi_i \rangle + \int \rho(1) V_N(1) d1$$

$$+ \frac{1}{2} \int \int \frac{\rho(1)\rho(2)}{r_{12}} d1 d2 + E_{XC}[\rho] \quad (3.46)$$

The last three terms in the expressions for the total energy are the same. In a bond energy evaluation the differences in these terms between molecule and constituting atoms (fragments) can be calculated for the ZORA and non-relativistic expression in the same way. We will now consider the remaining parts of the energy expression. For the non-relativistic expression this is the kinetic energy. We can write the kinetic energy using the one-particle density matrix:

$$\rho(1, 1') = \sum_{i=1}^{N} \Phi_i^\dagger(r_{1'}) \Phi_i(r_1) \quad (3.47)$$

We can define $\Delta\rho(1,1') = \rho(1,1') - \rho_\Sigma(1,1')$, where ρ_Σ is the sum of the one-particle density matrices of the atoms or larger fragments from which the molecule is built. We can expand the eigenfunctions Φ_i in a set of basis orbitals $\{\phi_\mu\}$, which allows to express $\Delta\rho$ in terms of the density matrix P:

$$\Delta\rho(1, 1') = \sum_{\mu,\nu} \Delta P_{\mu\nu} \phi_\mu(1) \phi_\nu^\dagger(1') \quad (3.48)$$

The difference in the non-relativistic kinetic energy ΔT^{NR} can now be written as:

$$\Delta T^{NR} = \sum_i \langle \Phi_i | \frac{p^2}{2} | \Phi_i \rangle - \sum_A \sum_i \langle \Phi_i^A | \frac{p^2}{2} | \Phi_i^A \rangle$$

$$= \int_{1 \to 1'} \frac{p^2(1)}{2} \Delta\rho(1, 1') d1 =$$

$$\sum_{\mu,\nu} \Delta P_{\mu\nu} \langle \phi_\nu | \frac{p^2}{2} | \phi_\mu \rangle \quad (3.49)$$

where $\sum_A$ runs over the fragments. Matrix elements of $p^2/2$ obtained by numerical integration can be

used in this expression to obtain ΔT. The proposed scheme amounts to employing identically the same grid of sampling points to evaluate the kinetic energies of the fragments and of the molecule, which leads to cancellation of errors and is essential for obtaining a reliable energy difference [46].
We can proceed in the same way for the first term of the scaled ZORA total energy, which we shall call the scaled ZORA kinetic energy. The difference in this scaled ZORA kinetic energy ΔT^{scaled} for a molecule and its fragments is:

$$\Delta T^{scaled} = \sum_i \langle \Phi_i | \vec{\sigma} \cdot \vec{p} \frac{c^2}{2c^2 - V} \vec{\sigma} \cdot \vec{p} | \Phi_i \rangle$$

$$- \sum_i E_i \langle \Phi_i | \vec{\sigma} \cdot \vec{p} \frac{c^2}{(2c^2 - V)^2} \vec{\sigma} \cdot \vec{p} | \Phi_i \rangle$$

$$- \sum_A \sum_i \langle \Phi_i^A | \vec{\sigma} \cdot \vec{p} \frac{c^2}{2c^2 - V_A} \vec{\sigma} \cdot \vec{p} | \Phi_i^A \rangle +$$

$$\sum_A \sum_i E_i^A \langle \Phi_i^A | \vec{\sigma} \cdot \vec{p} \frac{c^2}{(2c^2 - V_A)^2} \vec{\sigma} \cdot \vec{p} | \Phi_i^A \rangle \qquad (3.50)$$

We can expand V_A around V:

$$\frac{c^2}{2c^2 - V_A} = \frac{c^2}{2c^2 - V} + \frac{c^2 (V_A - V)}{(2c^2 - V)^2} +$$

$$\frac{c^2 (V_A - V)^2}{(2c^2 - V)^3} + \cdots \qquad (3.51)$$

This yields for ΔT^{scaled}:

$$\Delta T^{scaled} = \sum_i \langle \Phi_i | \vec{\sigma} \cdot \vec{p} \frac{c^2}{2c^2 - V} \vec{\sigma} \cdot \vec{p} | \Phi_i \rangle$$

$$- \sum_A \sum_j \langle \Phi_j^A | \vec{\sigma} \cdot \vec{p} \frac{c^2}{2c^2 - V} \vec{\sigma} \cdot \vec{p} | \Phi_j^A \rangle$$

$$- \sum_i E_i \langle \Phi_i | \vec{\sigma} \cdot \vec{p} \frac{c^2}{(2c^2 - V)^2} \vec{\sigma} \cdot \vec{p} | \Phi_i \rangle + \qquad (3.52)$$

$$\sum_A \sum_j \langle \Phi_j^A | \vec{\sigma} \cdot \vec{p} \frac{c^2 (E_j^A + V - V_A)}{(2c^2 - V)^2} \vec{\sigma} \cdot \vec{p} | \Phi_j^A \rangle + \cdots$$

The last two lines can be expected to be a factor $E_i / 2c^2$ smaller than the first two lines. This means that a nonnegligible contribution of the last terms can only be expected if E_i is large, which means deep core states. For deep core states the $\Sigma_A \Sigma_j \Phi_j^A$ in equation 3.52 runs over fragment orbitals Φ_j^A, or with suitable symmetry adaptation, over symmetry combinations of fragment orbitals that each match a corresponding molecular orbital orbital Φ_i which it very closely resembles. For these deep core orbitals we can approximate the difference between the molecular potential and the fragment potential, in the region where the orbital has some value, as a constant (the ESCA shift). The difference of the eigenvalues E_i^A of these orbitals with the molecular eigenvalues E_i can then be approximated as $V_A - V$, thus $E_i^A + V - V_A \approx E_i$. For deep core levels the last two lines of equation 3.52 will then be:

$$- \sum_i E_i \langle \Phi_i | \vec{\sigma} \cdot \vec{p} \frac{c^2}{(2c^2 - V)^2} \vec{\sigma} \cdot \vec{p} | \Phi_i \rangle$$

$$+ \sum_i E_i \langle \Phi_i^A | \vec{\sigma} \cdot \vec{p} \frac{c^2}{(2c^2 - V)^2} \vec{\sigma} \cdot \vec{p} | \Phi_i^A \rangle \qquad (3.53)$$

For deep core states the molecular wavefunction is almost identical to (a symmetry combination of) the fragment orbitals, which means that for those orbitals this term is expected to be very small. We therefore will neglect this term altogether. We can write the first two lines of equation 3.52 with help of $\Delta P_{\mu\nu}$ as:

$$\Delta T^{scaled} \approx \sum_{\mu,\nu} \Delta P_{\mu\nu} \langle \phi_\nu | \vec{\sigma} \cdot \vec{p} \frac{c^2}{2c^2 - V} \vec{\sigma} \cdot \vec{p} | \phi_\mu \rangle$$

$$= \Delta T^{ESA} \qquad (3.54)$$

We will call this the electrostatic shift approximation (ESA) of calculating the ZORA bond energy. It is to be noted that the problem of gauge invariance does not enter in this treatment, since we have used the scaled one-electron energies from the outset.

In table 3.6 we check the assumptions above by carrying out the same ionisations of Au as before, comparing the proposed ZORA ESA method with the difference in scaled ZORA total energies which we have already seen to be very close to the Dirac results (cf. tables 3.5 and 3.4). The ZORA ESA calculations are carried out in a basis set of STO's, as we will use basis set expansions in the molecular calculations to be reported in the next section. To check the accuracy of the basis set, both basis set and numerical calculations are presented for the scaled ZORA ionisation energy. Again these calculations were done in spherical symmetry and using the simple $X\alpha$ method, but now the spin-orbit coupling has been omitted, i.e. the scalar relativistic ZORA equation has been used:

$$(\vec{p} \frac{c^2}{2c^2 - V} \vec{p} + V) \Phi_i = E_i^{zora} \Phi_i \qquad (3.55)$$

Table 3.6: Gold ionisation energies in a.u. from ZORA scalar relativistic calculations

ION	All electron			Frozen core	
	NUM	BASIS SET		NUM	BASIS SET
	SCALED	SCALED	ESA	SCALED	ESA
$(6s)^{-1}$	0.3281	0.3282	0.3278	0.3282	0.3281
$(5d)^{-1}$	0.4230	0.4234	0.4234	0.4231	0.4235
$(6s)^{-1}(5d)^{-1}$	1.0853	1.0856	1.0851	1.0856	1.0854

Table 3.7: Optimized Slater exponents of basis set A for all electron ZORA scalar relativistic calculations

s		p		d		f	
n	ζ	n	ζ	n	ζ	n	ζ
1	2000.0	2	60.0	3	27.0	4	15.5
1	450.0	2	36.0	3	17.5	4	8.5
1	152.0	3	21.0	4	11.9	4	4.65
1	87.2	3	16.0	4	7.5	5	2.5
2	100.0	4	13.0	5	4.9		
2	38.25	4	9.0	5	2.75		
3	47.75	5	5.8	5	1.55		
3	20.38	5	3.6				
4	12.475	6	3.2				
4	8.859	6	1.8				
5	6.795						
5	4.514						
6	3.141						
6	1.965						
6	1.239						

The scaled scalar relativistic ZORA energy is:

$$E_i^{scaled} = \frac{E_i^{zora}}{1 + \langle \Phi_i | \vec{p} \frac{c^2}{(2c^2 - V)^2} \vec{p} | \Phi_i \rangle} \tag{3.56}$$

We will also use the scalar relativistic approach in the molecular calculations. The total scaled scalar relativistic ZORA energy is defined as in equation 3.37. If we compare table 3.4 with table 3.6 we can see that the energy required to remove an electron out of the 6s orbital is almost the same for both the full and the scalar relativistic calculations. The reason for this is that the s-orbital has no spin-orbit splitting. For d-orbitals there is a difference due to this spin-orbit effect.

We now consider first the all electron calculations, which are most sensitive to the gauge problems due to the presence of core orbitals. From table 3.6 we can see that the basis set used (basis set A, shown in table 3.7) is large enough since the basis set scaled ZORA results are within 0.0005 a.u. of the numerical results. Next we observe that the additional approximations introduced in the ESA procedure - expansion of V_A around V, putting $E_i^A + V - V_A \approx E_i$ - are certainly valid, since the ZORA ESA ionisation energies, in the all-electron calculations where the same basis set was used, are within 0.0005 a.u. of the scaled ZORA energies. Note that here the neutral atom is the "fragment" and the ion is the "molecule". This is a good test of the ESA approach since the difference between V_A and V in the core region will be of the same order (actually larger) than it will usually be in molecular calculations.
In table 3.6 also results of valence-only calculations are shown. Again the core density is taken from an all-electron Dirac calculation on the neutral atom. In the numerical calculations both core and valence orbitals are generated and the valence orbitals can easily be identified by the number of nodes. In the basis set calculations only valence orbitals are obtained, which are explicitly orthogonalised on frozen core orbitals, coming from an all-electron scalar relativistic ZORA calculation on the neutral atom. The two types of frozen core calculation - numerical scaled *versus* basis set ESA - are very close, confirming the basis set to be adequate and the ESA approach to be valid. Comparison to the all-electron calculations proves the various approaches to be all within 'chemical accuracy' of each other.
We conclude that the ESA approach is an easy and accurate way to obtain relativistic energy differences such as ionisation energies and bond energies.

3.6 Magnetic field

In this section we will consider the ZORA Hamiltonian if a time-independent magnetic field is present. The two-component ZORA (zeroth order regular approximated) Hamiltonian, can be split in a scalar relativistic and a spin-orbit part:

$$H^{zora} = V + \vec{\sigma} \cdot \vec{p} \frac{c^2}{2c^2 - V} \vec{\sigma} \cdot \vec{p} =$$

$$V + \vec{p} \frac{c^2}{2c^2 - V} \vec{p} + \frac{c^2}{(2c^2 - V)^2} \vec{\sigma} \cdot (\vec{\nabla} V \times \vec{p}) \tag{3.57}$$

If we do the usual minimal substitution:

$$\vec{p} \to \vec{\Pi} = \vec{p} - \vec{A} \tag{3.58}$$

we will get the Hamiltonian including a magnetic field:

$$H^{zora} = V + \vec{\sigma} \cdot \vec{\Pi} \frac{c^2}{2c^2 - V} \vec{\sigma} \cdot \vec{\Pi} =$$

$$V + \vec{\Pi} \frac{c^2}{2c^2 - V} \vec{\Pi}$$

$$- \frac{c^2}{2c^2 - V} \vec{\sigma} \cdot \vec{B} + \frac{c^2}{(2c^2 - V)^2} \vec{\sigma} \cdot (\vec{\nabla} V \times \vec{\Pi}) \tag{3.59}$$

where $\vec{B}$ is the magnetic field and $\vec{A}$ is the usual vector potential, such that $\vec{B} = \vec{\nabla} \times \vec{A}$. The $\vec{\sigma} \cdot \vec{B}$ term is now in a regularised form (compare the Pauli approximation at the end of this section). This term (and a part of the last term in equation 3.59) accounts for the hyperfine splitting due to the coupling between the electron spin and the spin of the nucleus and the Zeeman effect in the case of an external magnetic field.
The ZORA equation:

$$H^{zora} \Phi = E^{zora} \Phi \tag{3.60}$$

is gauge invariant under the combined gauge transformation:

$$\Phi \to \Phi e^{i\chi}$$

$$\vec{A} \to \vec{A} + \vec{\nabla} \chi \tag{3.61}$$

The scaled ZORA energy is then also gauge invariant:

$$E_i^{scaled} = \frac{E_i^{zora}}{1 + \langle \Phi_i | \vec{\sigma} \cdot \vec{\Pi} \frac{c^2}{(2c^2 - V)^2} \vec{\sigma} \cdot \vec{\Pi} | \Phi_i \rangle} \tag{3.62}$$

The ZORA equation is almost gauge invariant under the combined gauge transformation:

$$\Phi \to \Phi e^{i\chi}$$

$$\vec{A} \to \vec{A} + \vec{\nabla} \chi$$

$$V \to V - \partial_t \chi \tag{3.63}$$

The scaled ZORA energy improves upon the gauge invariance of the potential part of the combined gauge transformation. In fact then the same problems arise as in the case of no magnetic field.
Compare the Pauli approximation if a static magnetic field is present:

$$H^{Pauli} = V + \frac{1}{2} \vec{\Pi}^2 - \frac{1}{8c^2} \vec{\Pi}^4 - \frac{1}{2} \vec{\sigma} \cdot \vec{B} +$$

$$\frac{1}{4c^2} \vec{\sigma} \cdot (\vec{\nabla} V \times \vec{\Pi}) + \frac{1}{8c^2} \nabla^2 V \tag{3.64}$$

The $\vec{\sigma} \cdot \vec{B}$ term already appears in the non-relativistic Levy-Leblond equation [47, 48], since:

$$V + \frac{1}{2} (\vec{\sigma} \cdot \vec{\Pi})^2 = V + \frac{1}{2} \vec{\Pi}^2 - \frac{1}{2} \vec{\sigma} \cdot \vec{B} \tag{3.65}$$

Chapter 4

Exact relations between DIRAC and ZORA

4.1 Introduction

One of the most important problems in quantum mechanics, that can be solved exactly, is the problem of an electron moving in a Coulomb field. The bound-state solutions of the Schrödinger and Klein-Gordon equation for hydrogen-like atoms were already obtained in the early days of quantum mechanics [49, 50]. For this system the solutions of the Dirac equation are also known [3, 4], which is very convenient when considering approximations. The Schrödinger equation may be considered to be the zeroth order equation of the expansion in c^{-1} of the exact Foldy Wouthuysen transformed Dirac equation. In this section we will give an exact relation between the Dirac solutions and the solutions of the zeroth order of the regular approximate (ZORA) equation in the case of hydrogen-like atoms. Exact solutions of these one electron systems are very useful as a starting point for the calculations on more complex systems.

4.2 Exact solutions for hydrogen-like atoms

We are looking for hydrogen-like solutions of the zeroth order regular approximate (ZORA) equation in a Coulomb potential of a point charge Z:

$$V = -\frac{Z}{r} \tag{4.1}$$

The ZORA equation 3.2 is in this case:

$$(-\frac{Z}{r} + \vec{\sigma}\cdot\vec{p}\frac{c^2}{2c^2 + \frac{Z}{r}}\vec{\sigma}\cdot\vec{p})\phi^{zora}(\vec{r})$$
$$= E^{zora}\phi^{zora}(\vec{r}) \tag{4.2}$$

We can relate the solutions of the ZORA equation to the well known solutions of the Dirac equation for this problem. After elimination of the small component the equation for the large component ϕ^D of the four-component Dirac spinor is:

$$(-\frac{Z}{r} + \vec{\sigma}\cdot\vec{p}\frac{c^2}{2c^2 + E^D + \frac{Z}{r}}\vec{\sigma}\cdot\vec{p})\phi^D(\vec{r})$$
$$= E^D\phi^D(\vec{r}) \tag{4.3}$$

We can transform this equation to the ZORA equation by means of an energy-dependent scaling with λ of the coordinate $\vec{r}$:

$$\vec{r}\,' = \lambda\vec{r} \tag{4.4}$$

hence:

$$\vec{\sigma}\cdot\vec{p}\,' = \frac{1}{\lambda}\vec{\sigma}\cdot\vec{p} \tag{4.5}$$

After dividing by λ, this transforms equation 4.3 into:

$$(-\frac{Z}{r'} + \vec{\sigma}\cdot\vec{p}\,'\frac{c^2}{\frac{2c^2+E^D}{\lambda} + \frac{Z}{r'}}\vec{\sigma}\cdot\vec{p}\,')\phi^D(\frac{\vec{r}\,'}{\lambda})$$
$$= \frac{E^D}{\lambda}\phi^D(\frac{\vec{r}\,'}{\lambda}) \tag{4.6}$$

Defining the energy-dependent λ by:

$$\lambda = \frac{2c^2 + E^D}{2c^2} \tag{4.7}$$

one obtains:

$$(-\frac{Z}{r'} + \vec{\sigma}\cdot\vec{p}\,'\frac{c^2}{2c^2 + \frac{Z}{r'}}\vec{\sigma}\cdot\vec{p}\,')\phi^D(\frac{\vec{r}\,'}{\lambda})$$
$$= \frac{2c^2E^D}{2c^2 + E^D}\phi^D(\frac{\vec{r}\,'}{\lambda}) \tag{4.8}$$

Here one recognizes the one-particle ZORA equation 4.2. Thus for every solution of the Dirac-equation with energy E^D, we find a solution of the ZORA equation with energy E^{zora}:

$$E^{zora} = \frac{2c^2 E^D}{2c^2 + E^D} \tag{4.9}$$

with corresponding eigenfunction Φ^{zora}:

$$\Phi^{zora}(\vec{r}) = \phi^D(\frac{\vec{r}}{\lambda}) \tag{4.10}$$

Thus the ZORA eigenfunctions are scaled Dirac large components, in which the scaling factor depends on the energy. The number of nodes in the ZORA eigenfunction is the same as in the large component of the Dirac spinor, because only a scaling has been applied. The derivation of the relativistic virial theorem [51] was also done by scaling of coordinates. From this theorem we can conclude, that the norm of the Dirac large component, belonging to the discrete spectrum in the case of a hydrogen-like atom, is related to its eigenvalue as:

$$\langle \phi^D | \phi^D \rangle = \frac{2c^2 + E^D}{2c^2} \tag{4.11}$$

This norm is the same as the energy-dependent λ we used to scale the Dirac equation.

4.2.1 First order perturbation

Having obtained the exact zeroth order result for the case of hydrogen-like atoms, we will now obtain an exact result for the first order. We can invert equation 4.9 to:

$$E^D = \frac{2c^2 E^{zora}}{2c^2 - E^{zora}} \tag{4.12}$$

Expanding this in powers of c^{-2} gives:

$$E^D = E^{zora} + \frac{(E^{zora})^2}{2c^2} + \cdots \tag{4.13}$$

In this section we will show that the scaled ZORA energy is exactly equal to the Dirac energy and that the FORA energy is just the Dirac energy expanded in powers of c^{-2} up to first order:

$$E^{scaled} = E^D$$

$$E^{fora} = E^{zora} + \frac{(E^{zora})^2}{2c^2} \tag{4.14}$$

In order to do this we need to know for the FORA and scaled ZORA energy the expectation value of the ZORA wavefunction with the following operator:

$$\langle \Phi^{zora} | \vec{\sigma} \cdot \vec{p} \frac{c^2}{(2c^2 - V)^2} \vec{\sigma} \cdot \vec{p} | \Phi^{zora} \rangle \tag{4.15}$$

We will prove the following relation for the discrete part of the spectrum of H^{zora} in the case of a hydrogen-like atom:

$$\langle \Phi^{zora} | \vec{\sigma} \cdot \vec{p} \frac{c^2}{(2c^2 + \frac{Z}{r})^2} \vec{\sigma} \cdot \vec{p} | \Phi^{zora} \rangle = -\frac{E^{zora}}{2c^2} \tag{4.16}$$

We define a scaled eigenfunction of the ZORA Hamiltonian by:

$$\Phi_\lambda(\vec{r}) = \lambda^{\frac{3}{2}} \Phi^{zora}(\lambda \vec{r}) \tag{4.17}$$

Because of the prefactor $\lambda^{\frac{3}{2}}$ the scaled wavefunction is also normalized. We define the following energy E_λ:

$$E_\lambda = \langle \Phi_\lambda | H^{zora} | \Phi_\lambda \rangle \tag{4.18}$$

Because Φ^{zora} is an eigenvector of the discrete spectrum of H^{zora}, its eigenvalue E^{zora} is a stationary value of the functional E_λ [52], thus:

$$\frac{dE_\lambda}{d\lambda}|_{\lambda=1} = 0 \tag{4.19}$$

We can write:

$$E_\lambda = \int \lambda^3 \Phi^{zora\dagger}(\lambda \vec{r}) \frac{-Z}{r} \Phi^{zora}(\lambda \vec{r}) d\vec{r} +$$

$$\int \lambda^3 \Phi^{zora\dagger}(\lambda \vec{r}) \vec{\sigma} \cdot \vec{p} \frac{c^2}{2c^2 + \frac{Z}{r}} \vec{\sigma} \cdot \vec{p} \Phi^{zora}(\lambda \vec{r}) d\vec{r} =$$

$$= \lambda \int \Phi^{zora\dagger}(\lambda \vec{r}) \frac{-Z}{\lambda r} \Phi^{zora}(\lambda \vec{r}) d(\lambda \vec{r}) +$$

$$\lambda^2 \int \Phi^{zora\dagger}(\lambda \vec{r}) \vec{\sigma} \cdot \vec{p}_\lambda \frac{c^2}{2c^2 + \frac{Z\lambda}{\lambda r}} \vec{\sigma} \cdot \vec{p}_\lambda \Phi^{zora}(\lambda \vec{r}) d(\lambda \vec{r})$$

$$= \lambda \langle \Phi^{zora} | \frac{-Z}{r} | \Phi^{zora} \rangle +$$

$$\lambda \langle \Phi^{zora} | \vec{\sigma} \cdot \vec{p} \frac{c^2}{\frac{2c^2}{\lambda} + \frac{Z}{r}} \vec{\sigma} \cdot \vec{p} | \Phi^{zora} \rangle \tag{4.20}$$

where $\vec{\sigma} \cdot \vec{p}_\lambda = \frac{1}{\lambda} \vec{\sigma} \cdot \vec{p}$. Now we can use equation 4.19, which gives:

$$0 = \frac{dE_\lambda}{d\lambda}|_{\lambda=1} = \langle \Phi^{zora} | \frac{-Z}{r} | \Phi^{zora} \rangle$$

$$+ \langle \Phi^{zora} | \vec{\sigma} \cdot \vec{p} \frac{c^2}{2c^2 + \frac{Z}{r}} \vec{\sigma} \cdot \vec{p} | \Phi^{zora} \rangle +$$

$$2c^2 \langle \Phi^{zora} | \vec{\sigma} \cdot \vec{p} \frac{c^2}{(2c^2 + \frac{Z}{r})^2} \vec{\sigma} \cdot \vec{p} | \Phi^{zora} \rangle =$$

$$E^{zora} + 2c^2 \langle \Phi^{zora} | \vec{\sigma} \cdot \vec{p} \frac{c^2}{(2c^2 + \frac{Z}{r})^2} \vec{\sigma} \cdot \vec{p} | \Phi^{zora} \rangle \tag{4.21}$$

Thus:

$$\langle\Phi^{zora}|\vec{\sigma}\cdot\vec{p}\frac{c^2}{(2c^2+\frac{Z}{r})^2}\vec{\sigma}\cdot\vec{p}|\Phi^{zora}\rangle = -\frac{E^{zora}}{2c^2} \quad (4.22)$$

Having obtained this result, we can now prove the equations of 4.14 using equation 3.3 and 3.4 for the definition of the FORA and scaled ZORA energy:

$$E^{scaled} = \frac{E^{zora}}{1+\langle\Phi^{zora}|\vec{\sigma}\cdot\vec{p}\frac{c^2}{(2c^2+\frac{Z}{r})^2}\vec{\sigma}\cdot\vec{p}|\Phi^{zora}\rangle}$$

$$= \frac{2c^2E^{zora}}{2c^2-E^{zora}} = E^D \quad (4.23)$$

$$E^{fora} = E^{zora} + \frac{(E^{zora})^2}{2c^2} \quad (4.24)$$

4.2.2 Scalar relativistic equations

In the case of a hydrogen-like atom all scaling arguments of section 4.2 and 4.2.1 can be repeated for the scalar relativistic (SR) equations. The SR equation (see equation 3.5 for a hydrogen-like atom is given by:

$$(V+\vec{p}\frac{c^2}{2c^2+E^{SR}+\frac{Z}{r}}\vec{p})\phi^{SR} = E^{SR}\phi^{SR} \quad (4.25)$$

and the zeroth order regular approximated SR equation is:

$$(V+\vec{p}\frac{c^2}{2c^2+\frac{Z}{r}}\vec{p})\Phi^{zora}_{SR} = E^{zora}_{SR}\Phi^{zora}_{SR} \quad (4.26)$$

For s-orbitals the SR equations are the same as the equations including spin-orbit. Applying the arguments of section 4.2 and 4.2.1 we get the following relations between the eigenvalues and eigenfunctions of the SR and ZORA SR equation in the case of a hydrogen-like potential:

$$\Phi^{zora}_{SR}(\vec{r}) = \Phi^{SR}(\frac{\vec{r}}{\lambda})$$

$$\lambda = \frac{2c^2+E^{SR}}{2c^2}$$

$$E^{zora}_{SR} = \frac{2c^2E^{SR}}{2c^2+E^{SR}}$$

$$E^{scaled}_{SR} = E^{SR}$$

$$E^{fora}_{SR} = E^{zora}_{SR} + \frac{(E^{zora}_{SR})^2}{2c^2} \quad (4.27)$$

4.3 One electron systems

Scaling of one-electron equations can of course also be done for a general potential. In that case the one-electron Dirac equation for the large component in a potential $V(\vec{r})$:

$$(V(\vec{r})+\vec{\sigma}\cdot\vec{p}\frac{c^2}{2c^2+E^D-V(\vec{r})}\vec{\sigma}\cdot\vec{p})\phi^D(\vec{r})$$

$$= E^D\phi^D(\vec{r}) \quad (4.28)$$

becomes after scaling with $\lambda = (2c^2+E^D)/(2c^2)$ a ZORA equation with a potential $V'(\vec{r})$:

$$V'(\vec{r}) = \frac{1}{\lambda}V(\frac{\vec{r}}{\lambda}) \quad (4.29)$$

which is in general different from $V(\vec{r})$. The ZORA eigenfunction is again a scaled Dirac large component, like in the hydrogen-like atom case. An example is the one-electron diatomic molecule. If one finds a solution to the Dirac equation for a certain distance R between the atoms, one also has a solution to the ZORA equation, but now for a distance λR between the atoms. For a bound electron $E^D < 0$, this means a smaller distance. The situation may also be reversed. If one finds a solution to the ZORA equation one also has a solution to the Dirac equation, but for a different potential. The arguments of section 4.2.1 can only be used if $V'(\vec{r}) = V(\vec{r})$. Thus in general the scaled ZORA energy will not be exactly equal to the Dirac energy.

4.4 Two electron systems

For helium-like ions we can derive some exact relations in the case of the Dirac-Fock equations for two electrons which have the same density and one-electron energies, for example the ground state of helium. In that case the exchange potential for these electrons is just minus half the Coulomb potential V_C. Suppose we have solved the Dirac-Fock equations for such a system:

$$(-\frac{Z}{r}+\frac{1}{2}V_C([\rho^D];\vec{r})+$$

$$\vec{\sigma}\cdot\vec{p}\frac{c^2}{2c^2+E^D+\frac{Z}{r}-\frac{1}{2}V_C([\rho^D];\vec{r})}\vec{\sigma}\cdot\vec{p})\phi^D(\vec{r})$$

$$= E^D\phi^D(\vec{r}) \quad (4.30)$$

and we know that the Coulomb-potential fulfils the simple scaling relation:

$$V_C([\rho^D];\vec{r}) = \lambda V_C([\rho^D_{1/\lambda}];\lambda\vec{r}) \quad (4.31)$$

with:

$$\rho^D_{1/\lambda}(\vec{r}) = \lambda^{-3}\rho^D(\frac{\vec{r}}{\lambda}) \tag{4.32}$$

If we scale the equation with $\lambda = (2c^2 + E^D)/(2c^2)$ we get the ZORA equation:

$$(-\frac{Z}{r'} + \frac{1}{2}V_C([\rho^D_{1/\lambda}]; r') +$$

$$\vec{\sigma}\cdot\vec{p}'\frac{c^2}{2c^2 + \frac{Z}{r'} - \frac{1}{2}V_C([\rho^D_{1/\lambda}]; r')}\vec{\sigma}\cdot\vec{p}')\phi^D(\frac{\vec{r}'}{\lambda})$$

$$= \frac{2c^2E^D}{2c^2 + E^D}\phi^D(\frac{\vec{r}'}{\lambda}) \tag{4.33}$$

with a Coulomb potential of a scaled Dirac density, which is exactly equal to the ZORA-4 density of the ZORA equation. The norm of the ZORA-4 large component is in this case namely equal to the norm of the large component:

$$\phi^{zora}_4(\vec{r}') = \lambda^{-3/2}\phi^D(\frac{\vec{r}'}{\lambda}) \tag{4.34}$$

and the small ZORA-4 component is:

$$\chi^{zora}_4(\vec{r}') =$$

$$\frac{c}{2c^2 + \frac{Z}{r'} - \frac{1}{2}V_C([\rho^D_{1/\lambda}]; r')}\vec{\sigma}\cdot\vec{p}\phi^{zora}_4(\vec{r}') =$$

$$\lambda^{-3/2}\frac{c}{2c^2\lambda + \frac{Z}{\vec{r}} - \frac{1}{2}\lambda V_C([\rho^D_{1/\lambda}]; \lambda\vec{r})}\vec{\sigma}\cdot\vec{p}\phi^D(\vec{r}) =$$

$$\lambda^{-3/2}\chi^D(\vec{r}) = \lambda^{-3/2}\chi^D(\frac{\vec{r}'}{\lambda}) \tag{4.35}$$

which leads to:

$$\rho^{zora}_4(\vec{r}') = \phi^{zora\dagger}_4(\vec{r}')\phi^{zora}_4(\vec{r}') +$$

$$\chi^{zora\dagger}_4(\vec{r}')\chi^{zora}_4(\vec{r}') = \lambda^{-3}\rho^D(\frac{\vec{r}'}{\lambda}) =$$

$$\rho^D_{1/\lambda}(\frac{\vec{r}'}{\lambda}) \tag{4.36}$$

So also in this case the ZORA energy is the Dirac energy scaled with λ, if we use the density of the large and small component (ZORA-4). In the ZORA case we will only use the large component for the density, which means that in that case there exists not a simple relation.
The scaled ZORA-4 energy is in this case not equal to the Dirac energy, because in general:

$$V_C([\rho]; \vec{r}) \neq \lambda V_C([\rho]; \lambda\vec{r}) \tag{4.37}$$

which means that not all arguments of section 4.2.1 can be used. In fact we will see in section 4.5 that the scaled ZORA-4 energy is quite close, but not exact. Maybe here is some room for improvement over the already accurate scaled ZORA energy, because we know the exact scaling relation.
For the Dirac-Fock equations for two electrons in a general external potential we can proceed as in the case of one electron in a general potential $V(\vec{r})$ if the two electrons have the same density and one-electron energies. Then again the exchange potential for these electrons is just minus half the Coulomb potential V_C. The Dirac-Fock equations for such a system is:

$$(V(\vec{r}) + \frac{1}{2}V_C([\rho^D]; \vec{r}) +$$

$$\vec{\sigma}\cdot\vec{p}\frac{c^2}{2c^2 + E^D - V(\vec{r}) - \frac{1}{2}V_C([\rho^D]; \vec{r})}\vec{\sigma}\cdot\vec{p})\phi^D(\vec{r})$$

$$= E^D\phi^D(\vec{r}) \tag{4.38}$$

Scaling again with $\lambda = (2c^2 + E^D)/(2c^2)$ gives the ZORA equation, with the density normalised as in ZORA-4:

$$V'(\vec{r}) + \frac{1}{2}V_C([\rho^{zora}_4]; \vec{r}) +$$

$$\vec{\sigma}\cdot\vec{p}\frac{c^2}{2c^2 - V'(\vec{r}) - \frac{1}{2}V_C([\rho^{zora}_4]; \vec{r})}\vec{\sigma}\cdot\vec{p})\phi^{zora}_4(\vec{r})$$

$$= \frac{2c^2E^D}{2c^2 + E^D}\phi^{zora}_4(\vec{r}) \equiv E^{zora}_4\phi^{zora}_4(\vec{r}) \tag{4.39}$$

with:

$$V'(\vec{r}) = \frac{1}{\lambda}V(\frac{\vec{r}}{\lambda}) \tag{4.40}$$

An example is the hydrogen molecule in the ground state. The Dirac-Fock equation can then be transformed in the ZORA-Fock equation, with density normalisation as in ZORA-4, but then at a scaled distance between the hydrogen atoms. Similar relations exist between the scalar relativistic equation and the scalar relativistic regular approximation. The results can also be used in density functional calculations if the used exchange-correlation potential V_{XC} satisfies the same simple scaling relation as the Coulomb-potential:

$$V_{XC}([\rho]; \vec{r}) = \lambda V_{XC}([\rho_{1/\lambda}]; \lambda\vec{r}) \tag{4.41}$$

The well known $X\alpha$ potential satisfies such a relation, and so do most approximate exchange potentials.
For electrons which have different orbital energies we can not use the results of this section, because the λ is energy-dependent and therefore different for different energies, making the arguments in this section not valid.

4.5 Results

In this section we will first use the exact results for hydrogenic systems obtained in this chapter to give an assessment of the performance of the regular approximation. The error of the ZORA eigenvalues can be estimated to be approximately $-E^2/2c^2$ using the result of section 4.2.1 (see eq. 4.14). This implies that the error is quite small for low energy valence electrons. The error may, however, become large for high energies. In order to understand the different ways the regular approximation and the conventional Pauli approximation treat relativistic effects for low and high energy electrons, it is useful to distinguish the following cases:
a) The energy is large, but the potential is small in comparison.
Consequently we have large momentum everywhere. This situation arises for example for a free electron moving at relativistic velocities. In this case the ZORA hamiltonian reduces to the nonrelativistic hamiltonian:

$$H^{zora} = V + \vec{\sigma}\cdot\vec{p}\frac{c^2}{2c^2 - V}\vec{\sigma}\cdot\vec{p} = \frac{p^2}{2} \tag{4.42}$$

Obviously the ZORA hamiltonian does not contain any relativity at all in this case and in particular the mass-velocity correction is entirely absent. In this case the Pauli approximation is clearly superior to the zeroth order regular approximation. The first order regular approximation is needed in this case to introduce the Pauli type corrections:

$$H^{fora} = H^{zora} - \frac{1}{2}H^{zora}\vec{\sigma}\cdot\vec{p}\frac{c^2}{(2c^2 - V)^2}\vec{\sigma}\cdot\vec{p}$$

$$+c.c. \approx V + \frac{p^2}{2} - \frac{p^4}{8c^2} \tag{4.43}$$

Of course, if $V = 0$ the traditional expansion in $(E - V)/2c^2$ is identical to the regular expansion in $E/(2c^2 - V)$ and the NR and Pauli hamiltonians are identical to the ZORA and FORA hamiltonians.
b) The energy is small, but there are regions of high potential.
This is the situation for the valence electrons of heavy elements. Classically speaking the momentum is only large in those regions where the potential is large as well. In this case the ZORA hamiltonian does recover the bulk of the relativistic effects. It in fact does include in this case the mass-velocity corrections as can be seen by reexpanding the ZORA hamiltonian in inverse powers of c:

$$H^{zora} = V + \vec{\sigma}\cdot\vec{p}\frac{c^2}{2c^2 - V}\vec{\sigma}\cdot\vec{p} \approx$$

$$V + \frac{p^2}{2} + \frac{1}{4c^2}\vec{\sigma}\cdot\vec{p}V\vec{\sigma}\cdot\vec{p} \approx$$

$$V + \frac{p^2}{2} + \frac{1}{4c^2}\vec{\sigma}\cdot\vec{p}(V - E)\vec{\sigma}\cdot\vec{p} + E\frac{p^2}{4c^2} \approx$$

$$V + \frac{p^2}{2} - \frac{p^4}{8c^2} + E\frac{p^2}{4c^2} \tag{4.44}$$

However, in the case of the singular Coulomb potential we have seen that this expansion is not really justified and in fact the ZORA hamiltonian sums the increasingly divergent terms in the Pauli expansion to infinite order leading to a final result that is entirely regular. Therefore in this case even the ZORA hamiltonian is far superior to the Pauli hamiltonian.
c) The energy is high and there is a strong (Coulombic) potential.
In this case the last term in eq. 4.44 becomes important. We note in passing that a high and positive E corresponding to an unbound electron would bring about the case a) effects: the last term would cancel the second (mass-velocity) term in $\tilde{H}_0$. We focus on the interesting case of a bound electron with large negative energy. On account of the virial theorem $E \approx -\langle p^2/2\rangle$ and the last term accounts for the $-E^2/2c^2$ error of the ZORA eigenvalues. The c^{-2} term in the first order regular approximation corrects for this error:

$$-\frac{1}{2}H^{zora}\vec{\sigma}\cdot\vec{p}\frac{c^2}{(2c^2 - V)^2}\vec{\sigma}\cdot\vec{p} + c.c. \approx -E\frac{p^2}{4c^2} \tag{4.45}$$

In contrast to the free particle (case a), we expect the ZORA eigenvalues to be more negative in this case than the Dirac eigenvalues and the FORA correction to be positive, i.e. of opposite sign compared to the Pauli type correction.

We present here results for the hydrogenic ion U^{91+} in order to examine the performance of the regular approximation in the case of both high energy and strong Coulombic potential. Table 4.1 compares the exact eigenvalues of the Dirac equation with on the one hand the zeroth and first order and scaled regular approximations and on the other hand the nonrelativistic (NR) and Pauli energies. All of these energies can be obtained analytically. The eigenvalues E^D of the Dirac equation are given by:

$$E^D + c^2 = \tag{4.46}$$

$$c^2\left[1 + \frac{(Z\alpha)^2}{\left(n - j - \frac{1}{2} + \sqrt{(j+\frac{1}{2})^2 - (Z\alpha)^2}\right)^2}\right]^{-\frac{1}{2}}$$

Table 4.1: orbital energies of Uranium 91+

ORBITAL	DIRAC	ZORA	FORA	SCALED	NR	PAULI
$1s_{1/2}(1s)$	-4861.2	-5583.9	-4753.7	-4861.2	-4232.0	-4708.9
$2s_{1/2}, 2p_{1/2}(2s)$	-1257.39	-1300.95	-1255.88	-1257.39	-1058.00	-1207.02
$2p_{3/2}$	-1089.61	-1122.17	-1088.64	-1089.61		-1087.80
$3s_{1/2}, 3p_{1/2}(3s)$	-539.09	-546.94	-538.98	-539.09	-470.22	-523.21
$3p_{3/2}, 3d_{3/2}$	-489.04	-495.49	-488.95	-489.04		-487.88
$3d_{5/2}$	-476.262	-482.378	-476.183	-476.262		-476.109
$4s_{1/2}, 4p_{1/2}(4s)$	-295.257	-297.597	-295.239	-295.257	-264.500	-288.715
$4p_{3/2}, 4d_{3/2}$	-274.408	-276.427	-274.393	-274.408		-273.814
$4d_{5/2}, 4f_{5/2}$	-268.966	-270.906	-268.952	-268.966		-268.846
$4f_{7/2}$	-266.389	-268.292	-266.376	-266.389		-266.363
$5s_{1/2}, 5p_{1/2}(5s)$	-185.485	-186.405	-185.480	-185.485	-169.280	-182.250
$5p_{3/2}, 5d_{3/2}$	-174.945	-175.763	-174.941	-174.945		-174.621
$5d_{5/2}, 5f_{5/2}$	-172.155	-172.948	-172.152	-172.155		-172.078
$5f_{7/2}, 5g_{7/2}$	-170.829	-171.609	-170.825	-170.829		-170.806
$6s_{1/2}, 6p_{1/2}(6s)$	-127.093	-127.525	-127.092	-127.093	-117.556	-125.282
$6p_{3/2}, 6d_{3/2}$	-121.057	-121.449	-121.056	-121.057		-120.867
$6d_{5/2}, 6f_{5/2}$	-119.445	-119.826	-119.444	-119.445		-119.395
$7s_{1/2}, 7p_{1/2}(7s)$	-92.441	-92.669	-92.440	-92.441	-86.367	-91.333

where n and $\kappa = \pm(j + \frac{1}{2})$ are the usual quantum numbers of the particular orbital and $\alpha = 1/c \approx 1/137.037$. Here we only used the positive total energy eigenvalues, from which we subtracted the rest mass energy in order to compare them with non-relativistic eigenvalues. The regular approximated eigenvalues are related to the Dirac ones according to equation 4.9:

$$E^{zora} = \frac{2c^2 E^D}{2c^2 + E^D}$$

$$E^{scaled} = E^D$$

$$E^{fora} = E^{zora} + \frac{(E^{zora})^2}{2c^2} \tag{4.47}$$

The non-relativistic (NR) eigenvalues are well known to be:

$$E^{NR} = -\frac{Z^2}{2n^2} \tag{4.48}$$

If we expand equation 4.5 up to first order in c^{-2} we get the first order energies, which we call Pauli energies E^{Pauli}:

$$E^{Pauli} = E^{NR} - \frac{(E^{NR})^2}{2c^2}\left(\frac{4n}{j+\frac{1}{2}} - 3\right) \tag{4.49}$$

Let us first note that the energies in table 4.1 are very large compared to the typical valence energy of ca. 0.5 a.u.. Given the $-E^2/2c^2$ error in the ZORA energies, this is not a favourable situation for the zeroth order regular approximation. Still, even at the high energies of this example the ZORA energies for the core-penetrating s and p orbitals are usually superior to Pauli energies. This is true down to an energy of 500 a.u. (the $n = 3$ shell). It is only in the very deep core (note in particular the $1s_{1/2}$ with an energy close to 5000 a.u.) that ZORA starts to perform poorly. In that case it becomes important to include the first order corrections. Of course in all cases (including $1s_{1/2}$) the FORA energies are superior to the Pauli energies. Since the scaled ZORA energies are exactly equal to the Dirac energies this is by far the best method.

In connection with the relation between relativistic effects and the singularity of the Coulomb potential [26], it is interesting to consider the differences between the orbitals with different angular momentum belonging to one shell. Orbitals with high angular momentum are much less core penetrating than orbitals with low angular momentum (cf. plots in ref [26]). This implies that for d,f and g orbitals the balance between case a) effects (relatively flat potential, high energy) and case b) effects (Coulombic singularity) may shift more towards a), and we observe in table 4.1 that indeed the Pauli results are better in those cases than the ZORA results. This is in contrast to the superiority of ZORA over Pauli for the core penetrating s levels. The p has hybrid behaviour: since the zeroth order regular approximate Hamiltonian has spin-orbit coupling and has the same

degeneracy in the eigenvalues as the Dirac Hamiltonian, the $p_{1/2}$ levels have the same behaviour as $s_{1/2}$ and the $p_{3/2}$ levels the same as $d_{3/2}$.

We may also relate the different behaviour of the high and low momentum orbitals of a given shell to the differences they exhibit in the magnitude of the relativistic shift (the difference Dirac-NR). All levels have a downward relativistic shift, but the core penetrating low angular momentum orbitals by far the largest, in complete accordance with all previous arguments. This implies that the nonrelativistic energy of the shell, E_n^{NR}, is above all the Dirac energies of the shell, and closest to the high angular momentum levels. On the other hand, the ZORA energies are all below the Dirac energies by roughly the same amount (approximately $-E_n^2/2c^2$, much smaller than the spin-orbit splitting). As a corollary, the ZORA energy improves much over the nonrelativistic energy for the low l orbitals but relatively little for the high l ones. The Pauli corrections are not able to recover the large error in the nonrelativistic energy for the low l orbitals, making the ZORA energies superior to the Pauli energies, but for the high l orbitals the Pauli corrections pick up almost completely the relatively small relativistic shift and lead to better results for those orbitals than ZORA.
We finally note that the Pauli corrections lower the energies, in agreement with the dominant mass-velocity contribution $-p^4/8c^2$ which is negative, i.e. causes a fast moving relativistic particle with momentum p to have a smaller kinetic energy than a nonrelativistic particle with the same momentum. The first order correction in the regular approximation can be identified with the mass-velocity correction in case of a free particle (cf. case a) above) but has the opposite sign for bound particles in a Coulomb potential, (cf. case c above). The dominant contribution to the FORA correction is given by $-Ep^2/4c^2$ which is a positive correction for a bound particle. From table 4.1 it is evident that the FORA corrections are indeed always positive. Evidently, the direction in which the FORA correction works is different for free and bound particles and does not have the same physical interpretation in the two cases.

Let us turn now to the scalar relativistic equations. We were not able to solve equation 4.25 or 4.26 analytically for orbitals with quantum number $l \neq 0$. For $l = 0$ these are just the same equations as the corresponding fully relativistic ones. In table 4.2 we list some numerically calculated eigenvalues in the case of hydrogen-like Uranium ($Z = 92$). One can compare these with the non-relativistic eigenvalues and the scalar relativistic Pauli energies, which are given by (for $l > 0$):

$$E^{Pauli\ SR} = E^{NR} - \frac{(E^{NR})^2}{2c^2}\left(\frac{4n}{l+\frac{1}{2}} - 3\right) \qquad (4.50)$$

We can follow the same arguments, that were used to explain table 4.1, to understand the results of table 4.2
As a last comparison we now look at the radial behaviour of some of the solutions we have found for a particle in a Coulomb potential near the origin:

$$\begin{aligned}
&\phi^D, \chi^D, \Phi^{zora}\ (j = l - 1/2) \sim r^{\sqrt{l^2 - \frac{Z^2}{c^2}} - 1} \\
&\phi^D, \chi^D, \Phi^{zora}\ (j = l + 1/2) \sim r^{\sqrt{(l+1)^2 - \frac{Z^2}{c^2}} - 1} \\
&\phi^{SR}, \Phi^{zora}_{SR} \sim r^{\sqrt{l(l+1)+1 - \frac{Z^2}{c^2}} - 1} \\
&\Psi^{NR} \sim r^l
\end{aligned} \qquad (4.51)$$

Here χ^D is the small component of the Dirac spinor. In all cases the regular approximate form has the right behaviour. Here we can see that the ZORA solution has the same mild singularity at the origin as the Dirac solution. In fact near the nucleus the radial behaviour of the ZORA solution is the same as that of the large component of the Dirac wave function, because only a scaling has been applied. This was to be expected, because the regular expansion parameter $E/(2c^2 - V)$ tends to zero near the origin. The ZORA orbital is slightly more contracted than the Dirac one. A nice feature of the regular approximations is that already in zeroth order they distinguish between expansions of the Dirac and scalar relativistic equation, because of the spin-orbit operator. Of course in these two cases the c^{-1}-expansion of these equations in zeroth order are identical, namely the Schrödinger equation.

In table 4.3 we list some energies and expectation values of r for helium-like Uranium using relativistic equations with Hartree-Fock exchange. The relativistic equations have been solved selfconsistently numerically. Both electrons are in the 1s shell, having the same density and orbital energy, so we can use the scaling relations of section 4.4:

$$\begin{aligned}
E_4^{zora} &= \frac{2c^2 E^D}{2c^2 + E^D} \\
E_{SR}^{zora} &= \frac{2c^2 E^{SR}}{2c^2 + E^{SR}}
\end{aligned} \qquad (4.52)$$

Table 4.2: orbital energies of Uranium 91+

		ZORA	FORA	SCALED		PAULI
	SR	SR	SR	SR	NR	SR
$2p$	-1130.34	-1165.41	-1129.25	-1130.34	-1058.00	-1127.54
$3p$	-501.341	-508.124	-501.250	-501.341	-470.222	-499.658
$3d$	-481.142	-487.386	-481.061	-481.142	-470.222	-480.819
$4p$	-279.581	-281.677	-279.565	-279.581	-264.500	-278.781
$4d$	-271.046	-273.016	-271.031	-271.046	-264.500	-270.833
$4f$	-267.478	-269.396	-267.464	-267.478	-264.500	-267.427
$5p$	-177.576	-178.419	-177.571	-177.576	-169.280	-177.164
$5d$	-173.222	-174.025	-173.219	-173.222	-169.280	-173.095
$5f$	-171.389	-172.174	-171.384	-171.389	-169.280	-171.351
$6p$	-122.571	-122.972	-122.569	-122.571	-117.556	-122.339
$6d$	-120.062	-120.447	-120.061	-120.062	-117.556	-119.984

Table 4.3: orbital energies and expectation values of r for Uranium 90+

			SCALED		ZORA	SCALED	
	DIRAC	ZORA-4	ZORA-4	SR	SR	SR	NR
ϵ	-4790.28	-5490.56	-4785.10	-4790.29	-5490.57	-4785.11	-4174.67
$\langle r \rangle$	.01356	.01183		.01357	.01184		.01637

The expectation values of r are scaled with the same value as the orbital energies. Because we have only s-electrons, spin-orbit has no effect and the ZORA equation is the same as the scalar relativistic ZORA equation. As explained in section 4.4 the scaled energies are not exactly equal to the relativistic ones, but in table 4.3 we can see that they only differ by an amount of approximately 0.1 %, thus recovering most of the relativistic effect. In the expectation value of r we see that the regular approximation gives a too contracted density, whereas the non-relativistic approximation gives a too expanded density. Because the expectation value of r in the ZORA method are scaled with the same value as the orbital energies we have for orbitals with low energy, the same high accuracy as we saw for the orbital energies.

Chapter 5

Numerical atomic calculations

5.1 Introduction

Relativistic effects are important in the study of heavy elements. Instead of the Schrödinger equation one now has to solve the Dirac equation, which involves a four-component Hamiltonian. Fully relativistic calculations are no more complicated than non-relativistic ones, as far as integral evaluation is concerned, but they are very time consuming. The dimension of the secular problem will be very large since there are four components and many basis functions are required. If one wants to use a variational technique then one has to make sure that no spurious solutions appear. This can be done using so-called kinetically balanced basis sets [53, 54, 55], but then one needs in principal different basis functions for the small component than for the large component of the Dirac spinor, which increases integral evaluation time and storage requirements.
An attractive alternative is to transform the Dirac Hamiltonian to a two-component form. Standard approaches are the elimination-of-small-components (esc) and the Foldy-Wouthuysen (FW) transformation. We refer to the recent discussion by Kutzelnigg [30] for a detailed exposition of the various approaches and the difficulties that arise in the form of divergent terms and singularities at $r \to 0$. The difficulties connected with the Foldy-Wouthuysen transformation have for instance been investigated by Moss et al. [56, 57, 58, 59] and Farazdel and Smith [23] have criticized the mass-velocity term, pointing out that for large momenta ($p > \alpha^{-1}$) the mass-velocity term $-(\alpha^2/8)p^4$ is not obtained unless one uses the expansion of the square-root operator for the kinetic energy outside its radius of convergence. The source of the difficulties is that the expansions that are being used implicitly or explicitly rely on an expansion in $(E-V)/2c^2$, which is invalid for particles in a Coulomb potential, where there will always be a region of space (close to the nucleus) where $(E-V)/2c^2 > 1$ and the expansion is not valid. This was already noticed by Gollisch and Fritsche [41] in their work on a scalar relativistic approximation to the atomic Dirac equation, essentially equivalent to the one of Koelling and Harmon [42].
In chapter 2 we considered expansions which are appropriate in the sense that the expansion "parameter" is $\ll 1$ over all space. In section 2.1 we first discussed expansions in the case of classical relativistic mechanics in a Coulomb potential. This revealed the essential error in the standard expansions as well as providing a simple remedy. In section 2.2.1 we demonstrated that exactly the same expansion is made in the standard derivations (both esc and FW) of the Pauli Hamiltonian, leading to a similar error. It is shown that one can avoid this error, leading in both the esc and FW methods to a two-component relativistic Hamiltonian that is, at least in zeroth order, variationally stable and contains similar relativisitic corrections as are present in the Pauli Hamiltonian but in a regularized form. This zeroth order regular approximated (ZORA) Hamiltonian turns out to be identical to the zeroth order Hamiltonian derived earlier by Chang, Pélissier and Durand using the theory of effective Hamiltonians [5] and by Heully, Lindgren, Lindroth, Lundqvist and Mårtensson-Pendrill [6]. The performance of the derived hamiltonians is investigated first in self-consistent atomic calculations in section 5.3. They perform exceedingly well, especially valence orbital energies are in much better agreement than the energies obtained with the standard Pauli Hamiltonian. For deep core levels the error in the energy is of order $E^2/2c^2$ and is still sizable in an absolute sense. The first order Hamiltonian corrects this deficiency in a first order perturbation calculation. The scaled ZORA approach is even more accurate, because it includes some higher orders up to infinity and gives exact energies for the hydrogen-like atoms. This scaled ZORA approach turns out to give deep core orbital energies that are accurate in the order of 0.1% for

such a heavy system as the neutral Uranium atom. The advantages of the present formulation are that, in contrast to the Pauli Hamiltonian, a variationally stable two-component Hamiltonian has been obtained that includes relativistic effects to a high degree of accuracy. It is important that the relativistic effects can be treated self-consistently, since this has been shown to be important in very heavy elements such as actinides, cf. refs. [27] and [28]. This advantage is shared with the most successful two-component relativistic method to date, the no-pair formalism with external field projectors. This method has been developed for atomic and molecular calculations by Hess [38] on the basis of theoretical work by Sucher [14] and Douglas and Kroll [37]. A density-functional implementation has been provided by Knappe and Rösch [40]. These schemes rely on momentum space evaluation of integrals and require the assumption of completeness of the finite basis sets employed in practical calculations. It is an advantage of the present simpler approach that the required matrix elements can easily be evaluated without further aproximations in schemes that rely on 3D numerical integration, see e.g. refs. [60]and [45], making this method very straightforwardly applicable to molecules.

5.2 Selfconsistent calculations

We discuss first the construction of the potential $V(\vec{r})$ in the hamiltonian H^{zora} from the one-electron solutions to eq. 3.2 during the iterations of a selfconsistent calculation. In the present work the simple Xα version [61] of the density functional theory is used. The electron-electron potential V_{ee} is thus split in the classical Coulomb interaction V_C and the exchange-correlation potential V_{xc}. Magnetic effects and retardation were not taken into account for the electron-electron potential. The potentials are calculated from the electron density ρ in the following way:

$$V = V_N + V_{ee} = V_N + V_C + V_{xc} \tag{5.1}$$

where:

$$V_N(\vec{r}) = -\sum_i \frac{Z_i}{|\vec{r} - \vec{r_i}|} \tag{5.2}$$

$$V_C(\vec{r}) = \int \frac{\rho(\vec{r_2})}{|\vec{r} - \vec{r_2}|} d^3 r_2 \tag{5.3}$$

$$V_{xc}(\vec{r}) = V_{xc}(\rho) = -3\alpha[\frac{3}{8\pi}\rho(\vec{r})]^{\frac{1}{3}} \tag{5.4}$$

with $\alpha = 0.7$. The Dirac equation with this approximation for the exchange-correlation potential is called the Dirac-Slater equation. Our two-component calculations are to be considered as approximations to Dirac-Slater calculations. [In such calculations no attempt is made to include relativistic effects to the exchange-correlation potential (see for example [62]).] When carrying the calculations through to self-consistency, the density and the potential are derived from the solutions Φ^{zora} to eq. 3.2.
We note that Chang et al. [5] did not carry through self-consistent calculations on many-electron atoms. From one-electron calculations they obtained relativistic correction potentials that were used in many-electron systems (noble gases). The potentials they use thus do not take screening effects on the relativistic correction potential into account, which will be treated in the present self-consistent approach.

5.2.1 Separation of the radial variable from angular and spin variables

To solve the equations for an atom it is useful to separate variables just like in the non-relativistic case. Here we follow the standard approach, which can be found in for example refs. [63, 64]. Because the potential of an atom is spherically symmetric, the total angular momentum $\vec{j} = \vec{l} + \vec{s}$ of a particle is conserved. $\vec{j}$ commutes with the ZORA Hamiltonian, so we may construct simultaneous eigenfunctions of H, j^2 and j_z. The eigenfunctions can also be classified according to parity. It is convenient to introduce the operator $\hat{\kappa}$:

$$\hat{\kappa} = \vec{\sigma} \cdot \vec{l} + 1 = \vec{\sigma} \cdot (\vec{r} \times \vec{p}) + 1 \tag{5.5}$$

Eigenfunctions of this operator are written as η_κ^m with eigenvalue $-\kappa$:

$$\hat{\kappa}\eta_\kappa^m = -\kappa\eta_\kappa^m \tag{5.6}$$

These are functions of angular and spin variables with a definite parity. The relativistic quantum number κ is given by:

$$\kappa = \begin{cases} -(l+1) = -(j+\frac{1}{2}) & j = l + \frac{1}{2} \\ +l = +(j+\frac{1}{2}) & j = l - \frac{1}{2} \end{cases} \tag{5.7}$$

η_κ^m is explicitely given by:

$$\eta_\kappa^m = \sum_{m', m_s} \langle l m' s m_s | j m \rangle Y_{l m'} \theta_{s m_s} \tag{5.8}$$

In this equation $m = m' + m_s$ holds and $\theta_{s m_s}$ is the eigenfunction of S^2 and S_z. One can now separate variables. Writing

$$\Phi = R(r)\eta_\kappa^m \tag{5.9}$$

it is possible to calculate $\vec{\sigma}\cdot\vec{p}\Phi$:

$$\sigma_r \equiv \frac{\vec{\sigma}\cdot\vec{r}}{r} \quad ; \quad \sigma_r\eta^m_\kappa = -\eta^m_{-\kappa} \quad ; \quad \sigma_r^2 = 1 \qquad (5.10)$$

$$\vec{\sigma}\cdot\vec{p}\Phi = \sigma_r^2\vec{\sigma}\cdot\vec{p}\Phi = \frac{\vec{\sigma}\cdot\vec{r}}{r}(\frac{\vec{\sigma}\cdot\vec{r}}{r}\vec{\sigma}\cdot\vec{p})\,\Phi$$

$$= \sigma_r\left(\frac{1}{r}\vec{r}\cdot\vec{p} + \frac{i}{r}\vec{\sigma}\cdot(\vec{r}\times\vec{p})\right)\Phi =$$

$$= \sigma_r\left(-i\frac{\partial}{\partial r} + \frac{i}{r}\vec{\sigma}\cdot\vec{l}\right)(R(r)\eta^m_\kappa) =$$

$$\sigma_r\left(-i\frac{\partial R}{\partial r} - i\frac{\kappa+1}{r}R\right)\eta^m_\kappa =$$

$$i\left(\frac{\partial R}{\partial r} + \frac{\kappa+1}{r}R\right)\eta^m_{-\kappa} \qquad (5.11)$$

Now it is possible to separate the spin and angular variables from the radial variable in the ZORA-Slater equations, because the $\vec{\sigma}\cdot\vec{p}$ operator appears twice. The first one will give something proportional to $\eta^m_{-\kappa}$, the second one will give back something proportional to η^m_κ.
Due to the separation of radial from angular and spin variables, the Dirac-Slater and the ZORA-Slater equation can be solved numerically. This will be done for the Uranium atom, see next section.

5.2.2 Basis set calculations

To prepare for future applications to molecules, the ZORA-Slater equation is also solved in a basis set expansion. To solve the ZORA-Slater equation 3.2 for atoms in a basis, one needs to calculate the following matrix elements:

$$\langle\Phi_i|\Phi_j\rangle \; ; \quad \langle\Phi_i|V|\Phi_j\rangle \; ; \quad \frac{1}{2}\langle\Phi_i|\vec{\sigma}\cdot\vec{p}f\vec{\sigma}\cdot\vec{p}|\Phi_j\rangle \qquad (5.12)$$

where

$$\Phi_i = R_i(r)\eta^{m_i}_{\kappa_i} \quad ; \quad f = (1 - V/2c^2)^{-1} \qquad (5.13)$$

The first two are the same as in the non-relativistic case. The last one can be written as (with the aid of equation 5.11):

$$\frac{1}{2}\langle\Phi_i|\vec{\sigma}\cdot\vec{p}f\vec{\sigma}\cdot\vec{p}|\Phi_j\rangle =$$

$$\frac{1}{2}\delta_{m_i m_j}\delta_{\kappa_i\kappa_j}\times\int_0^\infty\left(\frac{\partial R_i}{\partial r} + \frac{\kappa+1}{r}R_i\right)\times$$

$$\left(\frac{\partial R_j}{\partial r} + \frac{\kappa+1}{r}R_j\right)fr^2dr \qquad (5.14)$$

Because $f = (1 - V/2c^2)^{-1}$ depends on the potential, it is convenient to do a numerical integration. To solve the ZORA-Slater equations one can now use the same techniques as in the non-relativistic case. The basis set consists of normalized Slater-type functions:

$$[(2n)!]^{-\frac{1}{2}}(2\zeta)^{n+\frac{1}{2}}r^{n-1}e^{-\zeta r} \qquad (5.15)$$

The different n's and ζ's used in the analytical calculation are listed in table 5.1. The exponents were fitted to the numerical orbitals. The reason one needs such high exponents for the $s_{1/2}$-orbitals, is that for $r \to 0$ the wave-function has a weak singularity, just like in the fully relativistic case.

5.3 All-electron calculations on U

Results of all-electron calculations on the U atom are given in table 5.2. The non-relativistic results (NR) are from a numerical solution of the one-electron Hartree-Fock-Slater equations. The results with the Pauli Hamiltonian (PAULI PERT) are from a perturbation theory approach from Snijders and Baerends [65].
The difference between the non-relativistic and relativistic (DIRAC) results is quite large, the non-relativistic one-electron energy of a valence level like the $5f$ deviating by several tenths of an a.u. from the relativistic one. The non-relativistic levels are even in the wrong order. The ZORA energies reproduce the Dirac ones to an accuracy of better than 0.001 a.u. in the valence region. The PAULI PERT results do give the right qualitative picture, but the $6s_{1/2}$ and $6p_{1/2}$ orbital energies still have errors of about 0.1 a.u., compared with the DIRAC values. One reason for this difference between ZORA and PAULI PERT is that if one uses the zero order ZORA Hamiltonian, which includes much of the relativistic effects, one can also fully incorporate indirect effects (from the relativistic orbital contractions and expansions) through the self-consistent calculations. The PAULI PERT results include such effects as a first order perturbation to the potential $V(r)$. It has been noted before [27] that considerable improvement over the PAULI PERT results can be obtained by performing so called quasi-relativistic selfconsistent calculations with the Pauli Hamiltonian, using a diagonalisation in the space of non-relativistic orbitals to avoid collapse to the nucleus and other problems mentioned before (cf. last column of table 5.6). Although this approach has proven quite successful in applications to heavy element compounds, cf. refs. [27], [28] and

Table 5.1: Optimized Slater exponents for all-electron ZORA-Slater calculations on Uranium

$s_{1/2}$		$p_{1/2}$		$p_{3/2}$		$d_{3/2}$		$d_{5/2}$		$f_{5/2}$		$f_{7/2}$	
n	ζ	n	ζ	n	ζ	n	ζ	n	ζn	ζ	n	ζ	
1	27700.0	2	3587.50	2	150.26	3	64.151	3	47.917	4	22.727	4	21.562
1	5409.50	2	958.970	2	58.433	3	30.866	3	28.208	4	13.541	4	12.901
1	440.000	2	337.190	2	41.219	3	21.393	3	20.346	4	8.544	4	8.241
1	454.960	2	138.288	3	25.240	4	15.350	4	14.630	4	4.517	4	3.792
1	180.480	2	66.387	3	19.950	4	10.650	4	10.260	5	3.024	5	4.553
1	106.185	2	45.709	4	16.135	5	7.330	5	7.054	5	1.734	5	2.052
2	223.615	3	28.467	4	11.726	5	4.703	5	4.526	5	0.983	5	1.056
2	47.215	3	22.424	5	8.350	6	2.946	6	2.772				
3	60.110	4	17.715	5	5.775	6	1.644	6	1.520				
3	25.833	4	12.915	6	3.817	6	0.915	6	0.829				
4	15.769	5	9.259	6	2.346								
4	11.075	5	6.464										
5	10.457	6	4.365										
5	7.268	6	2.741										
6	5.008												
6	3.274												
7	2.035												
7	1.199												

[66], it is not devoid of theoretical flaws. The method of the ZORA approach is however well founded and achieves an even better result.

In order to examine the results of table 5.2 more closely it is interesting to compare the zeroth order effective Hamiltonian with the energy-dependent Hamiltonian for the large component ϕ of the Dirac wave function obtained by eliminating the small component χ in the Dirac equation. This Hamiltonian H^{esc} is (equation 2.14):

$$H^{esc} = V + \vec{\sigma} \cdot \vec{p} \frac{c^2}{2c^2 + E - V} \vec{\sigma} \cdot \vec{p} \tag{5.16}$$

Comparing the H^{esc} Hamiltonian with the ZORA Hamiltonian:

$$H^{zora} = V + \vec{\sigma} \cdot \vec{p} \frac{c^2}{2c^2 - V} \vec{\sigma} \cdot \vec{p} \tag{5.17}$$

one notes there are two differences between H^{esc} and the present use of H^{zora}. The H^{esc} is energy-dependent, but if E is small compared to $2c^2$ this is a difference of the order $E^2/2c^2$ (here one assumes that the kinetic energy is about equal to minus the energy). The percentage error is thus expected to increase linearly with E. This is supported by the exact results on the hydrogen-like atom. The second difference arises from our use of $|\Phi(\vec{r})|^2$ to generate the density, which does not yield exactly the Dirac density and potential V, cf. the discussion in section 5.2. This may affect the energies of the higher lying orbitals since those depend strongly on the screening of the nucleus by the densities of all lower lying orbitals. Near the nucleus however the nuclear attraction dominates and the Hamiltonians are practically the same. So one expects the ZORA wave functions to be approximately the same there (apart from normalisation) as the large component of the Dirac wave function. The ZORA wavefunction indeed exhibits the same mild singularity near the nucleus as does the large component of the Dirac spinor.

If one looks at the ZORA-orbital energies in table 5.2 one can see that for the innermost orbitals, which see the nuclear potential almost unscreened, the expectation that the error is about $E^2/2c^2$ is borne out (14.5% error for $1s_{1/2}$, 11.1% expected). If one looks at higher lying orbitals the expected error of $E^2/2c^2$ is very small in an absolute sense. The actual error is in fact larger than $E^2/2c^2$, due to the error in the self-consistent potential used, though still very small (in the upper valence region typically 0.0001 a.u. i.e. 0.1% error, 10^{-4}% expected). Comparing to the non-relativistic energies, in all cases the ZORA energies recover the bulk of the relativistic effect, except for the $1s_{1/2}$. The FORA results are considerably better still, especially for the inner shell orbitals, where the error is reduced to about 10% of the ZORA error. The scaled ZORA approach reduces this further to about 1% of the ZORA error. The largest remain-

Table 5.2: Uranium orbital energies in a.u.

orbital	NR	DIRAC	ZORA	FORA	SCALED ZORA	SCALED BASIS SET	PAULI PERT
$1s_{1/2}$	-3690.78	-4255.56	-4872.99	-4158.88	-4250.15	-4250.02	-4114.71
$2s_{1/2}$	-640.21	-795.01	-818.96	-793.51	-794.28	-794.28	-753.91
$2p_{1/2}$	-619.59	-766.70	-789.88	-765.24	-765.99	-765.81	-728.13
$2p_{3/2}$		-625.96	-642.00	-625.15	-625.58	-625.56	-626.95
$3s_{1/2}$	-161.26	-200.69	-202.63	-200.51	-200.54	-200.53	-190.53
$3p_{1/2}$	-151.14	-187.82	-189.63	-187.65	-187.68	-187.64	-178.43
$3p_{3/2}$		-155.39	-156.71	-155.29	-155.31	-155.31	-155.59
$3d_{3/2}$	-132.14	-134.99	-136.15	-134.93	-134.95	-134.94	-135.29
$3d_{5/2}$		-128.40	-129.47	-128.36	-128.37	-128.37	-128.93
$4s_{1/2}$	-40.57	-51.09	-51.25	-51.05	-51.05	-51.03	-48.28
$4p_{1/2}$	-35.89	-45.30	-45.43	-45.26	-45.26	-45.26	-42.78
$4p_{3/2}$		-36.83	-36.92	-36.80	-36.81	-36.81	-36.90
$4d_{3/2}$	-27.16	-27.59	-27.66	-27.58	-27.58	-27.58	-27.68
$4d_{5/2}$		-26.03	-26.10	-26.02	-26.03	-26.03	-26.19
$5s_{1/2}$	-8.813	-11.33	-11.33	-11.31	-11.32	-11.31	-10.62
$5p_{1/2}$	-7.006	-9.073	-9.077	-9.066	-9.067	-9.067	-8.490
$5p_{3/2}$		-7.058	-7.062	-7.055	-7.055	-7.058	-7.087
$4f_{5/2}$	-15.06	-13.88	-13.91	-13.87	-13.88	-13.88	-14.00
$4f_{7/2}$		-13.47	-13.51	-13.47	-13.47	-13.49	-13.57
$5d_{3/2}$	-3.850	-3.764	-3.767	-3.764	-3.764	-3.766	-3.793
$5d_{5/2}$		-3.466	-3.468	-3.466	-3.466	-3.468	-3.500
$6s_{1/2}$	-1.298	-1.720	-1.719	-1.718	-1.718	-1.718	-1.580
$6p_{1/2}$	-.7945	-1.069	-1.069	-1.068	-1.068	-1.069	-.9725
$6p_{3/2}$		-.7410	-.7409	-.7407	-.7407	-.7416	-.7476
$5f_{5/2}$	-.3419	-.1033	-.1040	-.1040	-.1040	-.1052	-.1047
$5f_{7/2}$		-.0728	-.0735	-.0735	-.0735	-.0750	-.0647
$6d_{3/2}$	-.1157	-.0710	-.0711	-.0711	-.0711	-.0715	-.0728
$6d_{5/2}$		-.0537	-.0538	-.0538	-.0538	-.0542	-.0512
$7s_{1/2}$	-.1071	-.1340	-.1339	-.1339	-.1339	-.1337	-.1231

ing error, is in the $1s_{1/2}$ (2.2% for FORA and 0.1% for scaled ZORA). The ZORA and particularly scaled ZORA results are much superior to the PAULI PERT ones.

If one looks at the spin-orbit splittings the regular Hamiltonians give much better results than the perturbative Pauli result, see table 5.3. The FORA and scaled ZORA orbital splittings all differ less than 0.5% from the DIRAC result, whereas the PAULI PERT results differ up to 40% (PAULI PERT results are much better in frozen core calculations, see ref. [65] and see below). Chang, Pélissier and Durand [5] listed some spin-orbit splitting energies. Especially their valence shells are in poorer agreement with exact relativistic values than the 5p and 6p results listed here. For example the 6p spin-orbit splitting energy for Radon (Z=86) is in their work 0.123 a.u. compared to 0.156 for the exact value. The less accurate results for the valence orbital energies can possibly be understood from the fact that these authors did not take screening effects into account whereas we do. On the other hand, Schwarz et al. [26] have demonstrated that spin-orbit splittings of p AO originate very close to the nucleus (mostly from the spatial region occupied by the K shell electrons). The spin-orbit splitting should therefore not be particularly sensitive to inaccuracy of the (valence) electronic potential.

We now turn to the electron density. In figures 5.1, 5.2, 5.3 and 5.4 some of the orbital electron densities are compared for the Uranium atom. In these pictures the non-relativistic, Dirac-Slater and ZORA-Slater electron densities are presented. It is obvious that the ZORA-Slater electron densities are in much better agreement with the Dirac-Slater ones than are the non-relativistic densities, in particular for the valence levels in the outer region. In contrast with the non-relativistic densities, the Dirac and ZORA densities practically coincide over all shells except the innermost ones. A notable difference is that the ZORA orbital electron densities have nodes, whereas the Dirac ones are always larger than zero, because the large and small component of the Dirac wavefunction do not vanish at the same place. As discussed in section 5.2 this is an expected effect of neglecting to transform also the operator r in the change from Dirac picture to (approximate) Schrödinger picture (also called Foldy-Wouthuysen picture). We may use the results of Baerends et al. [32] concerning the difference of expectation values of the Dirac position r_{charge} and of the average position r_{mass} in order to

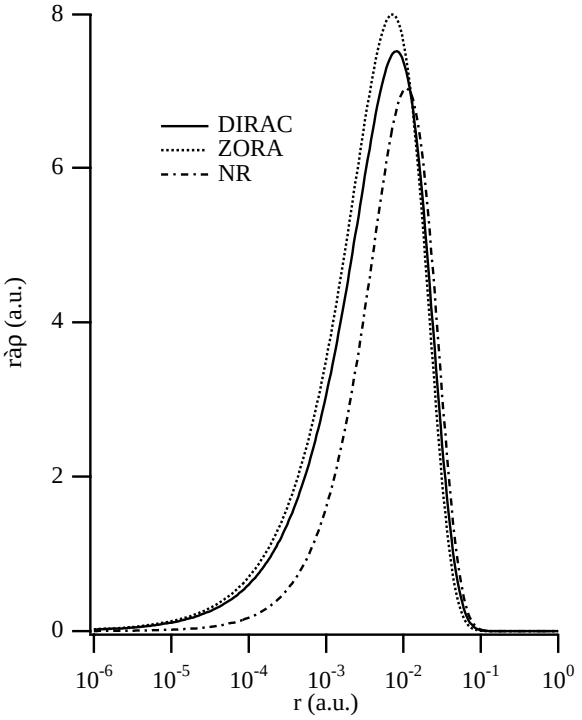

Figure 5.1: r times square root of DIRAC $1s_{1/2}$, ZORA $1s_{1/2}$ and NR $1s$ orbital density of Uranium

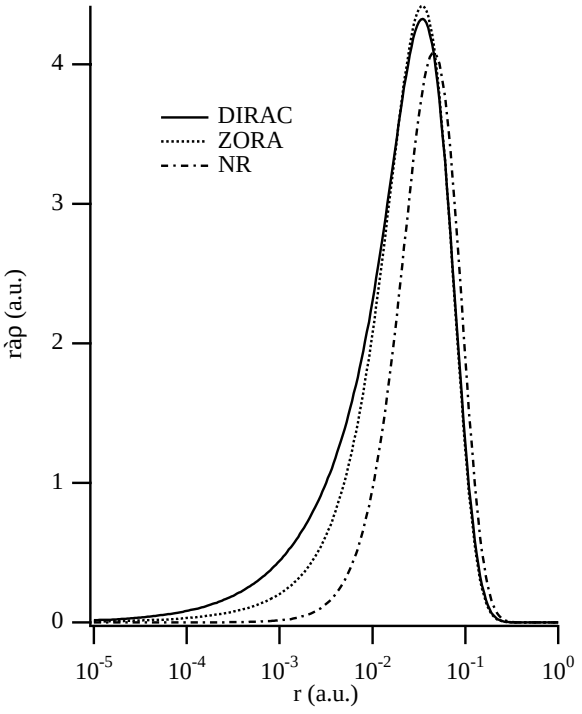

Figure 5.2: r times square root of DIRAC $2p_{1/2}$, ZORA $2p_{1/2}$ and NR $2p$ orbital density of Uranium

Table 5.3: Uranium all-electron spin-orbit splitting

SPIN-ORBIT SPLITTING	DIRAC	ZORA	FORA	SCALED ZORA	PAULI PERT
2p	140.74	147.83	140.09	140.41	101.18
3p	32.44	32.92	32.36	32.37	22.84
4p	8.469	8.503	8.452	8.452	5.88
5p	2.016	2.015	2.011	2.012	1.403
6p	0.3284	0.3278	0.3277	0.3277	0.225
3d	6.584	6.681	6.577	6.578	6.36
4d	1.558	1.565	1.557	1.557	1.49
5d	0.2984	0.2986	0.2982	0.2982	0.293
6d	0.0173	0.0173	0.0173	0.0173	0.0262
4f	0.4064	0.4080	0.4062	0.4062	0.43
5f	0.0305	0.0305	0.0305	0.0305	0.0400

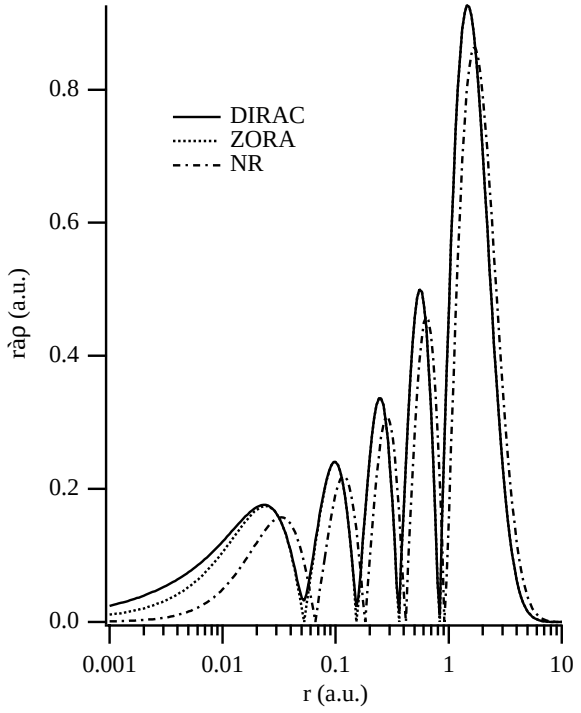

Figure 5.3: r times square root of DIRAC $6p_{1/2}$, ZORA $6p_{1/2}$ and NR $6p$ orbital density of Uranium

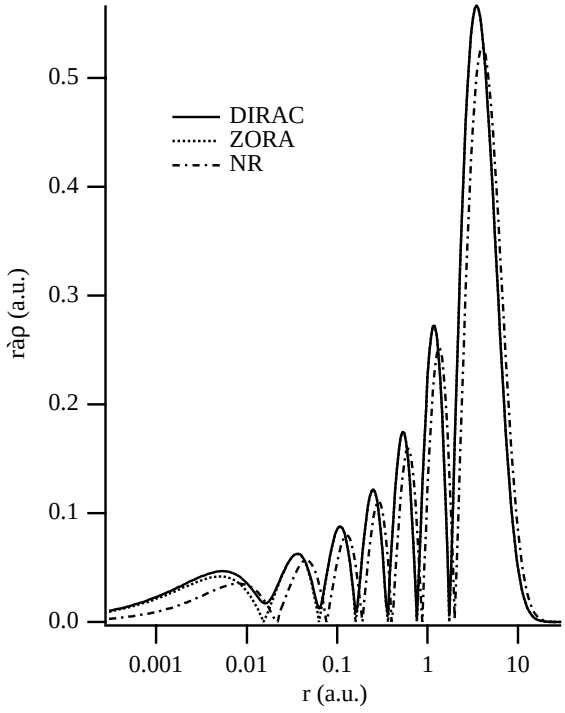

Figure 5.4: r times square root of DIRAC $7s_{1/2}$, ZORA $7s_{1/2}$ and NR $7s$ orbital density of Uranium

infer what consequences we may expect when the orbital density of the ZORA wavefunction Φ is given in terms of the untransformed r rather than the transform $UrU^\dagger$. The ZORA wavefunction Φ is the relativistic wavefunction transformed from Dirac picture to Schrödinger picture:

$$\Phi = U\Psi^D_{rel} \equiv \Psi^S_{rel} \tag{5.18}$$

The superscripts D and S denote Dirac picture and Schrödinger picture respectively. That we are dealing with the relativistic wavefunction is indicated explicitly by the subscript *rel*. The expectation value $\langle\Phi|r|\Phi\rangle = \langle\Psi^S_{rel}|r|\Psi^S_{rel}\rangle$ is just the expectation value of the average position r_{mass}, with operator $R = U^\dagger rU$ in the Dirac picture, for the relativistic wavefunction Ψ^D_{rel}:

$$\langle\Psi^S_{rel}|r|\Psi^S_{rel}\rangle = \langle U\Psi^D_{rel}|r|U\Psi^D_{rel}\rangle$$
$$= \langle\Psi^D_{rel}|R|\Psi^D_{rel}\rangle \tag{5.19}$$

As discussed in detail in ref [32] the expectation value $\langle R\rangle$ is for a $1s_{1/2}$ orbital significantly lower than the expectation value $\langle r\rangle$. This lowering has been calculated for the $1s_{1/2}$ of Uranium to be $1.0.10^{-3}$ a.u., ca. 36% of the nonrelativistic to relativistic contraction of $2.8.10^{-3}$ a.u. (according to the conventional definition, cf. [32]). The shift of the $\rho^{zora}(r)$ curve to lower r with respect to the $\rho^D(r)$ curve observed in fig. 5.1 is perfectly in line with this result. There may of course be other influences, particularly for the outer tail of the $1s_{1/2}$ which already extends sufficiently far out that screening effects by (the core tails of) other orbitals take effect. It is interesting to observe that the $3p_{1/2}$ orbital shows opposite behaviour, the ZORA density being lower than the Dirac density in the inner tail of the wavefunction, which would have an *increasing* effect on $\langle r\rangle$. This is again consistent with the findings about picture change effects. Since according to ref. [32] for a hydrogenic orbital we have

$$\langle R\rangle - \langle r\rangle = -\frac{Z}{4c^2}\left(-\frac{\kappa}{n^2}\right) \tag{5.20}$$

(which shows that for large Z and small n the effect is in the order of the Compton wavelength) one may expect opposite behaviour for $\kappa < 0$ orbitals (the $j = l + 1/2$ upper spin-orbit components such as $1s_{1/2}$) compared to the $\kappa > 0$, $j = l - 1/2$ lower spin-orbit components such as the $3p_{1/2}$ AO. The latter have indeed been found to show *expansion* when going from $\langle r\rangle$ to $\langle R\rangle$ (see table 5.4). The contracting of the wavefunction going from Dirac to ZORA, we found in the hydrogenic case, is for the $2p_{1/2}$ AO, still more important than this changing of picture effect.

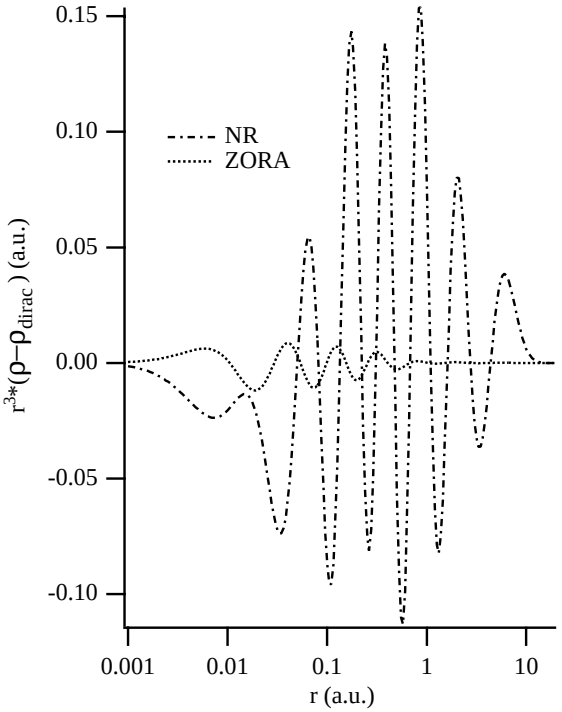

Figure 5.5: r^3 times difference in total density, results are from all-electron calculations on Uranium

These picture change arguments may give some insight in the observed deviations (presence of nodes; contraction or expansion) of the ZORA density from the Dirac density. Keeping in mind that Φ resembles a renormalized large component $N\phi$ of the Dirac wavefunction and using equation 2.50, other details of the differences in figs. 5.1 and 5.2 between ρ^D and ρ^{zora} such as ρ^{zora} being higher than ρ^D close to the maximum, may also be understood. These arguments are however qualitative. There may be other effects, such as the neglect of contributions of residual small components, which may not be completely negligible after transformation with an approximate U. In figure 5.5 we compare the NR and ZORA total densities coming from all-electron calculations with the total DIRAC density. This figure clearly shows how accurate the ZORA density is. Especially in the valence region there is hardly any difference between the ZORA and DIRAC densities, as we also have seen in figure 5.3 and 5.4 for the orbital densities. Only in the 1s-shell region the difference of the ZORA density with DIRAC is comparable to that of NR with DIRAC. Altogether the ZORA density is so close to the Dirac density that the valence orbital energies and outer tail densities of the ZORA wavefunctions are very accurate, well within "chemical accuracy" of

Table 5.4: Comparison of radial expectation values for some core orbitals obtained from all-electron calculations. The Dirac density is given in a.u., the errors Δ are given in percent $\Delta = (\langle r^n\rangle^{Approx} - \langle r^n\rangle^D)/\langle r^n\rangle^D \times 100\%$

orbital	$\langle r\rangle^D$	Δ^{zora}	Δ_4^{zora}	$\langle r^2\rangle^D$	Δ^{zora}	Δ_4^{zora}	$\langle r^{-1}\rangle^D$	Δ^{zora}	Δ_4^{zora}	$\langle r^{-2}\rangle^D$	Δ^{zora}	Δ_4^{zora}
$1s_{1/2}$	.01364	-11.6	-11.6	.000262	-21.8	-21.8	123.0	13.0	13.0	46615	27.7	27.7
$2s_{1/2}$	.05650	-.72	-2.1	.003854	-2.8	-4.2	31.08	-4.8	2.2	7488	-7.7	4.4
$2p_{1/2}$	.04576	-.29	-2.0	.002656	-1.9	-4.1	30.97	-4.7	2.0	2194	-34.5	4.0
$2p_{3/2}$	.05599	-1.8	-1.7	.003821	-3.5	-3.4	22.79	1.8	1.7	713	3.5	3.4
$3s_{1/2}$	.1471	.04	-.48	.02494	-.47	-.97	11.30	-5.1	.49	1771	-12.7	.96
$3p_{1/2}$	.1382	.12	-.42	.02240	-.30	-.85	11.19	-5.0	.41	540	-39.9	.64
$3p_{3/2}$	.1566	-.11	-.36	.02853	-.53	-.73	9.030	-.63	.36	177	-1.5	.70

Table 5.5: same as table 5.4, but now for some valence orbitals.

orbital	$\langle r\rangle^D$	Δ^{zora}	Δ_4^{zora}	$\langle r^2\rangle^D$	Δ^{zora}	Δ_4^{zora}	$\langle r^{-1}\rangle^D$	Δ^{zora}	Δ_4^{zora}	$\langle r^{-2}\rangle^D$	Δ^{zora}	Δ_4^{zora}
$6s_{1/2}$	1.473	.05	.10	2.423	.08	.20	.9059	-1.2	-.10	25.40	-14.4	-.25
$6p_{1/2}$	1.650	.05	.14	3.065	.08	.28	.7997	-1.0	-.15	6.351	-39.0	-.53
$6p_{3/2}$	1.897	.03	.10	4.061	.04	.20	.6814	-.29	-.10	2.063	-2.9	-.23
$5f_{5/2}$	1.486	-.04	-.20	2.814	-.13	-.51	.9181	-.07	.13	1.516	-.56	.19
$5f_{7/2}$	1.547	-.06	-.25	3.094	-.17	-.67	.8885	-.01	.16	1.419	-.12	.25
$6d_{3/2}$	3.237	-.01	-.03	12.69	-.04	.04	.4054	-.11	-.04	.4560	-3.0	-.10
$6d_{5/2}$	3.497	-.03	-.01	14.94	-.06	-.03	.3762	-.04	-.01	.3739	-.65	-.02
$7s_{1/2}$	4.114	.04	.10	19.21	.08	.20	.3059	-.41	-.10	2.645	-14.2	-.26

the Dirac values. We will nevertheless consider in the next section possible further improvement by using more accurate potentials in the hamiltonian H^{zora}.
In the last discussion we have taken the viewpoint for the two-component ZORA wave function, that it is an approximate Foldy-Wouthuysen wave function and we considered the picture change effects (see also section 9.4). We will leave this aside for the moment. Now we will take the viewpoint as is done in ref. [34] and section 2.2.3, that the ZORA wave function is an approximation to the Dirac wave function, by making a 4-component wave function where the large component is the ZORA wave function and the small component is defined in section 2.2.3. In ref. [34] the accuracy of the ZORA wave function was tested by comparing the expectation values of several powers of the radial coordinate (r^2, r, r^{-1} and r^{-2}). There also first order equations were proposed in order to improve upon the ZORA wave function, which we will not discuss here. In ref. [34] the r^{-2} values were not calculated with enough accuracy for the $s_{1/2}$ and $p_{1/2}$-orbitals, which are off by some 2%. On the other hand, the relative errors of the several approximations remain practically the same, which means that the discussion of the results can be left unaltered. In table 5.4 and 5.5 we give the results for some core and some valence levels, comparing Dirac with ZORA and ZORA-4 calculations. The ZORA-4 calculations were done using 4-component densities in a selfconsistent scheme, which is a little different from ref. [34], where the ZORA-4 calculations were done in the converged ZORA potential. For the analysis we will follow ref.[34]. We will first concentrate on the valence orbitals. If we look at the operators weighing the outer parts of the density (r and r^2), we see that the ZORA method already gives excellent results. The deviations from the full Dirac density hardly exceeds the 0.1%. The ZORA-4 accuracy is of the same order, maybe a bit worse. However, if we consider the operators which weigh the inner tail of the density (r^{-1} and r^{-2}), we see that the accuracy of the ZORA density is considerably lower, giving errors up to almost 40% for the subvalence $6p_{1/2}$ and 14% for the valence $7s_{1/2}$ orbital in the r^{-2} expectation value. On the other hand, the ZORA-4 result is still accurate within 0.5%, showing that the main error in the ZORA approach for the valence orbitals in the inner part of the orbital densities is due to a lack of small component.
If we now turn to the core orbitals, the results are quite different. Now the ZORA expectation values are rather inaccurate for every operator, which is not remedied by the ZORA-4 method. We can understand most of this behaviour by considering the

hydrogenic case. From chapter 4 we know that the ZORA-4 wave function is a (contracted) scaled Dirac wave function. This contraction leads to too small expectation values of r^2 and r and too large values for r^{-1} and r^{-2}. The scaling parameter in the hydrogenic case differs from one with $E^{Dirac}/2c^2$. This explains the relative errors for the expectation values of r and r^{-1}. For r^2 and r^{-2} the relative error is approximately two times as large, as can be expected. In the ZORA case only the large component is a (contracted) scaled Dirac large component. For solutions corresponding to the lowest principal quantum number for each total angular momentum j (i.e., $1s_{1/2}$, $2p_{3/2}$, $3d_{5/2}$, $4f_{7/2}$, etc.) the radial Dirac small component densities are in the hydrogenic case proportional to the Dirac large component densities. So for those orbitals the ZORA error will approximately be the same as in the ZORA-4 case. For other orbitals the Dirac small component has a more contracted density than the large component. The lack of small component in the ZORA density then partly compensates for the too contracted large component density. This can be seen in the core expectation values of r and r^2. For r^{-1} and r^{-2} the small component contribution becomes more important and then the ZORA-4 results usually are more accurate. This is especially true for $p_{1/2}$ orbitals, since these have compact small component densities of a $s_{1/2}$-like form. For such orbitals the ZORA-4 method indeed improves considerably upon the expectation values for r^{-1} and r^{-2} compared to the ZORA method, as can be seen in table 5.4. In the next section we will also show the expectation values for valence-only calculations on Uranium using the Dirac core density.

5.4 Valence-only calculations on Uranium using the Dirac core density

In view of its great utility in molecular calculations on large heavy-element compounds we briefly investigate valence-only calculations. In this approach the electron density is split into a core density ρ_{core} and a valence density ρ_{val}. Only the valence orbitals are optimized and the core density is taken from an all electron Dirac-Slater calculation. Although the difference with a ZORA core density would not be large, this procedure does correct for the the deviations from the Dirac density we discussed in the previous section and which should not enter the potential. The core density is frozen during the SCF calculations

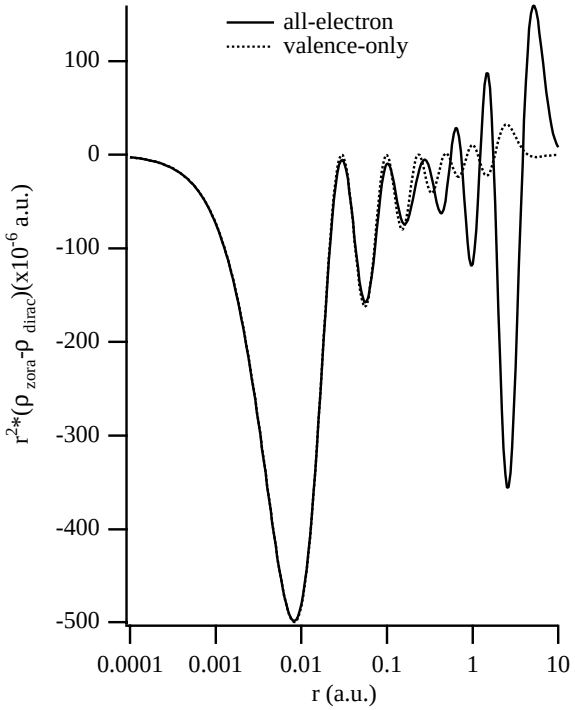

Figure 5.6: r^2 times difference in Uranium $7s_{1/2}$ orbital density, results are from all-electron and valence only calculations

for the valence orbitals. We solved the ZORA-Slater equations numerically. In this particular application the only condition for the valence orbitals was that the number of nodes was correct. This ensures orthogonality on the lower states that are solutions in the same potential.

Results are given in table 5.6 for Uranium. For comparison results are shown from calculations which use the standard Pauli Hamiltonian and the frozen core approximation. First order perturbation theory (FOPT) and quasi relativistic (QR) results are shown (results taken from [28]). We observe a considerable improvement over the results of the previous section. The ZORA results have an accuracy of about 0.0006 a.u., and the FORA and scaled ZORA about 0.00015 a.u. compared with the DIRAC results. The results with the Pauli Hamiltonian have errors more than 0.01 a.u. for the $6s_{1/2}$ and $6p_{1/2}$ orbital energies.

In figure 5.6 we plot r^2 times the ZORA minus Dirac orbital densities for the $7s_{1/2}$ orbital for the all-electron and for the present valence-only calculations. Both ZORA densities are very close to the DIRAC orbital density (note the scale of the plots).

Table 5.6: Uranium valence orbital energies from valence-only calculations

orbital	EL	DIRAC	ZORA	FORA	SCALED ZORA	PAULI FOPT	PAULI QR
$6s_{1/2}$	2	-1.7198	-1.7204	-1.7199	-1.7199	-1.580	-1.749
$6p_{1/2}$	2	-1.0694	-1.0696	-1.0694	-1.0694	-.9718	-1.019
$6p_{3/2}$	4	-.74095	-.74109	-.74096	-.74096	-.7468	-.7456
$5f_{5/2}$	3	-.10330	-.10347	-.10344	-.10334	-.1090	-.0928
$5f_{7/2}$	0	-.07286	-.07300	-.07298	-.07298	-.0690	-.0676
$6d_{3/2}$	1	-.07103	-.07102	-.07102	-.07102	-.0726	-.0722
$6d_{5/2}$	0	-.05373	-.05371	-.05371	-.05371	-.0510	-.0560
$7s_{1/2}$	2	-.13399	-.13399	-.13398	-.13398	-.1231	-.1330

Table 5.7: same as table 5.4, but now for some valence levels using valence only calculations.

orbital	$\langle r\rangle^D$	Δ^{zora}	Δ_4^{zora}	$\langle r^2\rangle^D$	Δ^{zora}	Δ_4^{zora}	$\langle r^{-1}\rangle^D$	Δ^{zora}	Δ_4^{zora}	$\langle r^{-2}\rangle^D$	Δ^{zora}	Δ_4^{zora}
$6s_{1/2}$	1.473	.01	-.01	2.423	-.01	-.02	.9059	-1.2	.01	25.40	-14.3	.02
$6p_{1/2}$	1.650	.01	-.01	3.065	-.01	-.01	.7997	-1.0	.01	6.351	-38.8	.01
$6p_{3/2}$	1.897	.00	-.00	4.061	-.01	-.01	.6814	-.26	.00	2.063	-2.9	.01
$5f_{5/2}$	1.486	-.01	.01	2.814	-.04	.02	.9181	-.09	-.00	1.516	-.59	-.01
$5f_{7/2}$	1.547	-.02	.01	3.094	-.05	.02	.8885	-.03	-.01	1.419	-.15	-.01
$6d_{3/2}$	3.237	.01	.01	12.69	.01	.01	.4054	-.13	-.01	.4560	-3.0	-.01
$6d_{5/2}$	3.497	.01	.01	14.94	.01	.01	.3762	-.06	-.01	.3739	-.71	-.01
$7s_{1/2}$	4.114	.00	.00	19.21	.00	.00	.3059	-.37	-.00	2.645	-14.1	-.00

The maximum differences are about 0.0005 a.u. in both cases. If one would calculate the same maximum difference between the non-relativistic (NR) $7s$ and the DIRAC $7s_{1/2}$ orbital then one would find 0.12 a.u., which is more than two orders of magnitude larger than the present result (see also figure 5.4). The valence-only results are significantly improved compared to the all-electron results, particularly in the valence region. In the most important outer lobe of the $7s$, between 1 and 10 bohr (cf. fig. 5.4), the difference between ZORA and Dirac is now only 3.10^{-5} a.u.!

We make two more observations concerning these curves in fig 5.6. The DIRAC orbital density is always larger than zero whereas the ZORA orbital densities have nodes. The difference curve is therefore expected to show negative minima close to these nodes. When the nodes of the ZORA densities (nearly) coincide with the minima in the Dirac densities, a behaviour that is observed in fig. 5.4 except in the deep core, the minima in the ZORA-Dirac curves will be equal to the Dirac density at those points. This explains the behaviour of the curves at the minima. As for the maxima, we observe that the ZORA results do not deviate much from Dirac in the positive direction and the deviation is even strictly negative in the innermost region. Explanation of this behaviour can be given if one looks for example at the exact results on the hydrogen-like atoms (chapter 4). In the core region the difference is mainly due to picture change effects, which partly can be solved by using the ZORA-4 formalism, where the density also comes from a small component. This can particularly be seen in table tab:ufcvrn, where results are shown for orbital expectation values using the ZORA and ZORA-4 method compared to the Dirac values. The inner and outer tails of the ZORA-4 orbital densities are now extremely accurate (relative errors less than 0.02%). The results further improve on the already accurate all-electron calculations (see table 5.5). This is also true for the outer tails of the ZORA orbitals. However, the inner tails of the ZORA orbitals (r^{-1} and r^{-2}) are described as inaccurately as in the all-electron calculations. The errors are thus almost completely due to a lack of small component. For the errors in the total density the inner tails of valence orbitals are not so important because there the core density dominates.

Chapter 6

Implementation of ZORA

6.1 Implementation of ZORA in ADF

The ADF (Amsterdam Density Functional) program is a program that can perform electronic structure calculations on molecular systems. It performs self consistent field calculations using density functional theory, solving the so called one-electron Kohn-Sham equations. The calculations are done using a Slater type orbital (STO) basis set. To solve the SR ZORA and ZORA Kohn-Sham equations one needs to calculate some matrix elements differently than in non-relativistic theory. In the SR ZORA equations the only difference is the calculation of the kinetic energy matrix. In ADF matrix elements are calculated by numerical integration. Use is made of the point group symmetry of the molecule. In the non-relativistic and scalar relativistic case the basis functions form an orthonormalised set of single group symmetry adapted functions. In the ADF program the derivatives of the basis functions with respect to the Cartesian coordinates $(\partial/\partial x, \partial/\partial y, \partial/\partial z)$ are calculated in the relativistic case, which can be done easily for STO's. The SR ZORA kinetic energy matrix is then calculated numerically, between basisfunction ϕ_i and ϕ_j as:

$$\langle\phi_i|T_{sr}^{zora}|\phi_j\rangle = \langle\phi_i|\vec{p}\frac{c^2}{2c^2-V}\vec{p}|\phi_j\rangle =$$

$$\sum_k \langle\frac{\partial\phi_i}{\partial x_k}|\frac{c^2}{2c^2-V}|\frac{\partial\phi_j}{\partial x_k}\rangle \tag{6.1}$$

where in the last step partial integration is used. For the potential in the ZORA kinetic energy matrix two possibilities are implemented. One can either use the frozen core potential, which means that one only has to calculate this matrix once, or one can use the full potential, which means that in every cycle in the SCF scheme this matrix has to be calculated. In section 6.1.1 we will show the differences between these possibilities in an example.
In the ZORA case, which includes spin-orbit, double group symmetry adapted functions have to be used. In this case one needs apart from the SR ZORA kinetic energy, also the ZORA spin-orbit matrix. In terms of double group symmetry adapted functions ϕ_i^d and ϕ_j^d (two-component functions), the ZORA spin-orbit matrix is:

$$\langle\phi_i^d|H_{so}^{zora}|\phi_j^d\rangle = \langle\phi_i^d|\frac{c^2}{(2c^2-V)^2}\vec{\sigma}\cdot(\vec{\nabla}V\times\vec{p})|\phi_j^d\rangle$$

$$= \langle\phi_i^d|\vec{\sigma}\cdot\vec{\nabla}(\frac{c^2}{2c^2-V})\times\vec{p})|\phi_j^d\rangle =$$

$$\langle\phi_i^d|\vec{\sigma}\cdot\vec{\nabla}(\frac{V}{4c^2-2V})\times\vec{p})|\phi_j^d\rangle =$$

$$i\sum_{lmn}\epsilon_{lmn}\langle\frac{\partial\phi_i^d}{\partial x_m}|\sigma_l\frac{V}{4c^2-2V}|\frac{\partial\phi_j^d}{\partial x_n}\rangle \tag{6.2}$$

where again in the last step partial integration is used. A double group symmetry adapted functions can be written as a spatial function times spin α plus a spatial function times spin β:

$$\phi_i^d(\vec{r},s) = \phi_i^\alpha(\vec{r})\alpha + \phi_i^\beta(\vec{r})\beta \tag{6.3}$$

The spin integration can be done easily using the Pauli spin matrices. The spatial integration one still has to do is then of the form:

$$i\sum_{mn}\epsilon_{lmn}\langle\frac{\partial\phi_i}{\partial x_m}|\frac{V}{4c^2-2V}|\frac{\partial\phi_j}{\partial x_n}\rangle \tag{6.4}$$

Again two possibilities for the potential are implemented. One can either use the frozen core potential, which means that one only has to calculate this spin-orbit matrix once, or one can use the full potential, which means that in every cycle in the SCF scheme this spin-orbit matrix has to be calculated.
The actual implementation of double group symmetry in ADF is done along the lines of Snijders [67]. All

symmetry arguments using the Pauli Hamiltonian, which are used in ref [67] remain valid for the ZORA Hamiltonians, we will not repeat them here. In the Pauli approximation one needs to calculate spin-orbit matrix elements of the form:

$$i\sum_{mn}\epsilon_{lmn}\langle\frac{\partial\phi_i}{\partial x_m}|\frac{V}{4c^2}|\frac{\partial\phi_j}{\partial x_n}\rangle \tag{6.5}$$

Compared to this matrix, the ZORA spin-orbit matrix is regularised by the potential in the numerator, which makes it effectively a $1/r$ potential close to a nuclues, whereas the Pauli spin-orbit behaves like a $1/r^3$ potential.
For the calculation of the scaled SR ZORA orbital energies (see equation 3.9) we need matrix elements of the form:

$$\langle\phi_i|\vec{p}\frac{c^2}{(2c^2-V)^2}\vec{p}|\phi_j\rangle =$$

$$\sum_k\langle\frac{\partial\phi_i}{\partial x_k}|\frac{c^2}{(2c^2-V)^2}|\frac{\partial\phi_j}{\partial x_k}\rangle \tag{6.6}$$

For the calculation of the scaled ZORA orbital energies (see equation 3.4) we need matrix elements of the form:

$$\langle\phi_i^d|\vec{\sigma}\cdot\vec{p}\frac{c^2}{(2c^2-V)^2}\vec{\sigma}\cdot\vec{p}|\phi_j^d\rangle =$$

$$\langle\phi_i^d|\vec{p}\frac{c^2}{(2c^2-V)^2}\vec{p}|\phi_j^d\rangle +$$

$$\langle\phi_i^d|\vec{\sigma}\cdot\vec{\nabla}(\frac{c^2}{(2c^2-V)^2})\times\vec{p})|\phi_j^d\rangle \tag{6.7}$$

The first term we already have in the SR ZORA case. The last term can be written as (the gradient of a constant is zero):

$$\langle\phi_i^d|\vec{\sigma}\cdot\vec{\nabla}(\frac{c^2}{(2c^2-V)^2})\times\vec{p})|\phi_j^d\rangle =$$

$$\langle\phi_i^d|\vec{\sigma}\cdot\vec{\nabla}(\frac{V(4c^2-V)}{4c^2(2c^2-V)^2})\times\vec{p})|\phi_j^d\rangle =$$

$$i\sum_{lmn}\epsilon_{lmn}\langle\frac{\partial\phi_i^d}{\partial x_m}|\sigma_l\frac{V(4c^2-V)}{4c^2(2c^2-V)^2}|\frac{\partial\phi_j^d}{\partial x_n}\rangle \tag{6.8}$$

These matrix elements, needed in the scaled (SR) ZORA case, are not more difficult to calculate than the ones we needed for the (SR) ZORA kinetic energy. The scaled (SR) ZORA orbital energies only have to be calculated once, after selfconsistency is reached, so we also have to calculate these matrix elements only once.
The scaled orbital energies are not used for the calculation of differences in energies. For this we use the (SR) ZORA ESA method described in some detail in section 3.5, because it is an easy and accurate way.

6.1.1 The frozen core approximation

In ADF usually the frozen core approximation is used. In this program the frozen core approximation in the ZORA case (incuding spin-orbit) is not (yet) implemented. One core orthogonalisation function, a Slater-type orbital (STO), per core orbital is used to orhogonalise the basis function on the accurately calculated core orbitals, coming from atomic calculations. In general the NR core orbitals are not the same as scalar relativistic ZORA core orbitals, which are again different to fully relativistic ZORA (including spin-orbit coupling) core orbitals. The most optimal core orthogonalisation functions will also differ whether one uses NR, SR ZORA or ZORA. In the NR case the core wiggles of the valence functions can accurately be described by the core orthogonalisations function, such that one does not need core-like basis functions to get an accuracy of a few milli atomic units. On the other hand, in SR ZORA and ZORA one does need extra core-like basis functions, to get such high accuracy for the heavier systems. This is due to the fact that the core wiggles of especially the s-type valence electrons do not behave like Slater type orbitals near the nucleus, but more like Dirac type orbitals which are of the form:

$$r^{\eta-1}e^{-\zeta r} \tag{6.9}$$

where η does not have to be an integer value. For STO's η is an integer.
In the SR ZORA case the frozen core approximation is similar as in the NR case, because one can use the same single group symmetry. The changes one has to make are in order of importance the following. The description of the core orbitals should come from SR ZORA calculations (one can use for example a SR ZORA version of an atomic basis set program), for heavier systems one needs to optimise the STO's in the atomic calculations. The next step is to optimise the core orthogonalisation functions to the core wiggles of accurately calculated SR ZORA valence orbitals for the given atom. A final step is to optimise the valence basis functions. For the heavier atoms one also should add basisfunctions, which are able to describe the tail of the valence orbitals more accurately. In the SR ZORA case it is often enough to add only one extra 1s-type STO with large exponent ζ to get an accuracy of a few milli atomic units in the atomic orbital energies.

In table 6.1 we will show the effects if one uses NR core functions to orthogonalise on in a SR ZORA calculation. If we use the standard ADF IV basis set (triple-ζ valence basis set) with a 5d frozen core, the

Table 6.1: Uranium scaled SR ZORA valence orbital energies in a.u. using NR core description

BASIS SET	6s	6p	5f	6d	7s
ADF IV	-1.599	-0.826	-0.127	-0.076	-0.124
ADF IV + 1S 115	-3.561	-0.726	0.006	-0.027	-0.231

Table 6.2: Optimized Slater exponents of basis set BASREL for frozen core ZORA scalar relativistic calculations

s		*p*		*d*		*f*	
n	ζ	n	ζ	n	ζ	n	ζ
core orthogonalisation functions							
1	101.70	2	52.40	3	28.74	4	15.7
2	37.83	3	23.50	4	13.00		
3	26.83	4	15.00	5	7.44		
4	15.686	5	8.50				
5	9.545						
basis functions							
6	3.610	6	4.40	6	2.91	5	5.37
6	5.247	6	2.90	6	1.58	5	2.79
7	2.512	6	1.80	6	0.85	5	1.33
7	1.607						
7	1.032						

results still seem not too bad (compared to the numerical all electron SR ZORA results of table 6.3). However, if we add a 1s-type STO with $\zeta = 115$ we see the effect of variational collapse. This collapse is caused by the orthogonalisation on NR core orbitals, whereas one should have orthogonalised on SR ZORA core orbitals. The SR ZORA orbitals are too different from the NR orbitals, see for example the figures in section 5.3.

In table 6.3 we see the results for different basis sets if we use the right orthogonalisation on SR ZORA core orbitals. These results can be compared with the given numerically calculated all electron SR ZORA results. The standard ADF IV result is not very accurate. The result of this basis set with an extra 1s-type STO with $\zeta = 115$ does not lead to variational collapse, as was expected. The accuracy on the other hand is still not high. We therefore have optimised the basis set, core orthogonalisation functions and basis functions, to the valence SR ZORA orbitals. This optimised basis set is called BASREL is given in table 6.2, which is of the same size as the ADF IV basis set. The results using basis set BASREL show a large improvement, especially (see the 6s orbital energy) if one also adds an extra 1s-type STO with $\zeta = 450$. This enlarged basis set is able to give orbital energies with an accuracy better than 0.01 atomic units. We also give results using also an extra 2p-type STO with $\zeta = 150$, which does not change results much, showing that the tail of the SR ZORA valence orbital can already be described with some accuracy without an extra core like basis function.

In table 6.4 we have listed results using the frozen core potential (nuclear potential plus Coulomb potential of the core density) in the SR ZORA kinetic energy matrix, instead of the full potential. Comparing table 6.3 with 6.4, we see that the results are very close, the difference being less than the accuracy of the basis set.

If one wants to use the frozen core approximation in the ZORA case (incuding spin-orbit coupling) one should orthogonalise the basis functions on ZORA core orbitals. In ADF-BAND it is implemented, but not in the present ADF. One might think that using a SR ZORA core description could already be sufficient, since one expects the ZORA orbitals not be too different from SR ZORA orbitals. In the spherical case for light atoms, the spin-orbit splitted (ZORA) eigenfunctions have almost the same radial behaviour as the SR ZORA orbitals, the difference is then only the spin and angular part. For closed shell cores then there is no difference whether one uses a SR ZORA or ZORA orbitals, because they span the same space. For heavier atoms, where spin-orbit coupling is important, this is no longer true, especially not for p-like eigenfunctions. In section 4.5 the radial behaviour is given for the eigenfunctions in a Coulomb potential near the origin. Especially the ZORA $p_{1/2}$-orbital differs from the SR ZORA p-orbital, because it has a mild singularity near the origin. We can do the ZORA calculation with basisfunctions orthogonalised on SR ZORA core orbitals and see how large the error becomes. In table 6.5 the results are given using the BASREL basis set . The accuracy is not so high (again the 6*s*-orbital), we therefore add an extra 1s-type STO with $\zeta = 450$ like before, which improves the results. Now we still don't have problems with variational collapse because *s*-orbitals are not affected by spin-orbit coupling, and the ZORA and SR ZORA *s*-orbitals are very close (the only difference is due to difference in the SCF potential). If we add an extra 2p-type core-like STO with $\zeta = 150$

Table 6.3: Uranium scaled SR ZORA valence orbital energies in a.u. using SR ZORA core description

BASIS SET	6s	6p	5f	6d	7s
NUMERICAL	-1.738	-0.830	-0.105	-0.064	-0.136
ADF IV	-1.537	-0.821	-0.169	-0.084	-0.121
ADF IV + 1S 115	-1.593	-0.812	-0.157	-0.079	-0.125
BASREL	-1.677	-0.831	-0.117	-0.069	-0.131
BASREL + 1S 450	-1.735	-0.823	-0.106	-0.065	-0.135
BASREL + 1S 450 + 2P 150	-1.734	-0.824	-0.105	-0.065	-0.135

Table 6.4: same as table 6.3, but now using the frozen core potential in the SR ZORA kinetic energy

BASIS SET	6s	6p	5f	6d	7s
ADF IV	-1.537	-0.821	-0.169	-0.084	-0.121
ADF IV + 1S 115	-1.593	-0.812	-0.157	-0.079	-0.125
BASREL	-1.675	-0.830	-0.118	-0.069	-0.131
BASREL + 1S 450	-1.732	-0.822	-0.108	-0.065	-0.135
BASREL + 1S 450 + 2P 150	-1.732	-0.823	-0.107	-0.065	-0.135

we do have problems with variational stability, the $6p_{1/2}$ orbital energy is now 0.1 a.u. too low. This result will get worse if we add more core-like p-type STO's.

6.2 Implementation of ZORA in ADF-BAND

The BAND program, originally written by te Velde [68, 69] and further developed by Wiesenekker and Philipsen, is a program that can perform electronic structure calculations on periodic systems. As basis functions Bloch sums of numerical atomic orbitals and STO's centered around the nuclei are used. The only difference between the ZORA and non-relativistic formalism turns out to be the kinetic energy operator, which means that everything else may remain unchanged. In this section we will show how the ZORA kinetic energy was implemented by Philipsen in this program.
The scalar relativistic ZORA kinetic energy operator T_{sr}^{zora} is:

$$T_{sr}^{zora} = \vec{p}\frac{c^2}{2c^2 - V}\vec{p} \tag{6.10}$$

and the full relativistic one:

$$T^{zora} = \vec{\sigma}\cdot\vec{p}\frac{c^2}{2c^2 - V}\vec{\sigma}\cdot\vec{p} \tag{6.11}$$

Like in ADF we use the electrostatic shift approximation (ESA) of calculating the ZORA bond energy (see section 3.5). In the ZORA ESA approximation, the kinetic energy operator uses the same potential in the fragments (atoms) as in the whole system. So the only difference in these calculations, whether one uses NR, SR ZORA or ZORA, is the difference in evaluating the kinetic energy operator. In the calculations first the neutral atoms from which the system is built are calculated numerically. From these atomic calculations the core density and orbitals are used for the frozen core calculations on the whole system hereafter. The numerically calculated valence orbitals (which are orthogonal to the core orbitals of the same atom) are taken as basis functions for calculations on the whole system, together with extra STO's centered around the nuclei. All these basis functions are made orthogonal to the core orbitals. In calculating the ZORA scalar and full relativistic kinetic energy matrix we will make an approximation to use only the numerically calculated atomic potential V_A in the numerator of this operator, if the operator works on a basis function centered around that atom. One can expand the total potential V around V_A:

$$\frac{c^2}{2c^2 - V} = \frac{c^2}{2c^2 - V_A} + \frac{c^2(V - V_A)}{(2c^2 - V_A)(2c^2 - V)} \tag{6.12}$$

The second term is neglected, since in the neighbourhood of atom A, $(V - V_A)$ is small compared to $2c^2$. For the numerical orbitals ϕ_i^A (solutions of calculations on the atom A) the kinetic energy can then be obtained using:

$$T\phi_i^A = (E_i^A - V_A)\phi_i^A \tag{6.13}$$

where V_A is the atomic (central field) potential of atom A. For the Slater orbitals ϕ_i^A centered around

Table 6.5: Uranium scaled ZORA valence orbital energies in a.u. using SR ZORA core description

BASIS SET	$6s_{1/2}$	$6p_{1/2}$	$6p_{3/2}$	$5f_{5/2}$	$5f_{7/2}$	$6d_{3/2}$	$6d_{5/2}$	$7s_{1/2}$
NUMERICAL	-1.718	-1.068	-0.741	-0.104	-0.074	-0.071	-0.054	-0.134
BASREL	-1.668	-1.057	-0.737	-0.121	-0.095	-0.075	-0.061	-0.129
BASREL + 1S 450	-1.726	-1.048	-0.729	-0.110	-0.084	-0.071	-0.057	-0.133
BASREL + 1S 450 + 2P 150	-1.715	-1.164	-0.726	-0.098	-0.073	-0.070	-0.056	-0.133

atom A (V_A is spherical) this becomes in the scalar relativistic case:

$$T_{sr}^{zora}\phi_i^A = \vec{p}\frac{c^2}{2c^2 - V_A}\vec{p}\phi_i^A =$$

$$-\frac{\partial V_A}{\partial r}\frac{c^2}{(2c^2 - V_A)^2}\frac{\partial \phi_i^A}{\partial r} - \frac{c^2}{2c^2 - V_A}\nabla^2\phi_i^A \qquad (6.14)$$

In the spherical case we may choose eigenfunctions of the orbital angular momentum L^2 and L_z and spin S^2 and S_z:

$$\nabla^2\phi_i^A = \frac{1}{r}\frac{\partial^2}{\partial r^2}(r\phi_i^A) - \frac{l(l+1)}{r^2}\phi_i^A \qquad (6.15)$$

For the Slater orbitals in the full relativictic case:

$$T^{zora}\phi_i^A = \vec{\sigma}\cdot\vec{p}\frac{c^2}{2c^2 - V_A}\vec{\sigma}\cdot\vec{p}\phi_i^A =$$

$$\vec{p}\frac{c^2}{2c^2 - V_A}\vec{p}\phi_i^A + \frac{c^2}{(2c^2 - V_A)^2}\frac{\partial V_A}{\partial r}\frac{1}{r}\vec{\sigma}\cdot(\vec{r}\times\vec{p})\phi_i^A$$

$$= -\frac{\partial V_A}{\partial r}\frac{c^2}{(2c^2 - V_A)^2}\frac{\partial \phi_i^A}{\partial r} - \frac{c^2}{2c^2 - V_A}\nabla^2\phi_i^A +$$

$$\frac{c^2}{(2c^2 - V_A)^2}\frac{\partial V_A}{\partial r}\frac{1}{r}\vec{L}\cdot\vec{\sigma}\phi_i^A \qquad (6.16)$$

In the spherical case we may choose eigenfunctions of the total angular momentum J^2 and J_z and of parity (see section 5.2.1):

$$\vec{L}\cdot\vec{\sigma}\phi_i^A = -(\kappa+1)\phi_i^A \qquad (6.17)$$

where κ is the usual relativistic quantum number:

$$\kappa = \begin{cases} -(l+1) = -(j+\frac{1}{2}) & j = l+\frac{1}{2} \\ +l = +(j+\frac{1}{2}) & j = l-\frac{1}{2} \end{cases} \qquad (6.18)$$

If we have a basis function ϕ_i^A centered around atom A and a basis function ϕ_j^B centered around atom B the ZORA scalar relativistic energy matrix element T_{ij} will be calculated as:

$$\frac{1}{2}\langle\phi_i^A|\vec{p}\frac{c^2}{2c^2 - V_A}\vec{p}|\phi_i^B\rangle + \frac{1}{2}\langle\phi_i^A|\vec{p}\frac{c^2}{2c^2 - V_B}\vec{p}|\phi_i^B\rangle \qquad (6.19)$$

and the full relativistic energy matrix element T_{ij} will be calculated as:

$$T_{ij} = \frac{1}{2}\langle\phi_i^A|\vec{\sigma}\cdot\vec{p}\frac{c^2}{2c^2 - V_A}\vec{\sigma}\cdot\vec{p}|\phi_i^B\rangle +$$

$$\frac{1}{2}\langle\phi_i^A|\vec{\sigma}\cdot\vec{p}\frac{c^2}{2c^2 - V_B}\vec{\sigma}\cdot\vec{p}|\phi_i^B\rangle \qquad (6.20)$$

where V_A and V_B are the the atomic (central field) potentials of atom A and B. This is a good approximation for the usually used basis functions. In ADF-BAND one starts with numerically calculated atoms. Orthogonalisation of basis functions is done using the core orbitals as core orthogonalisation functions. This is slightly different than the implementation in the ADF program, where auxialiry STO's are used as core orthogonalisation functions. In the ADF-BAND program for the (SR) ZORA case the orthogonalisation of basis functions is done on (SR) ZORA core orbitals. An advantage of the ADF-BAND program is that in the basis one has the exact (numerically calculated) atomic valence orbitals. In usual basis set programs, like the molecular ADF program, one already needs many basis functions just to get the core wiggles of the valence orbitals right. Since ADF-BAND has the numerically calculated atomic valence orbitals in the basis, which by definition have the right core wiggles near the nucleus, one usually does not need extra core-like basis functions for a high accuracy.

6.3 Some remarks on the Pauli Hamiltonian

The Pauli Hamiltonian in general poses no problems for bound electrons if one uses it in a first order perturbation theory, where the expectation value of the Pauli Hamiltonian with the non-relativistic wave function is used. Snijders and Baerends [65] proposed a method for the calculation of relativistic effects in a perturbative procedure, where also first order effects in the change of the density are taken into account. In the numerical calculations correct boundary conditions were taken into account and no variational

collapse can occur. In an old version of the molecular program ADF a similar procedure was implemented called PAULI FOPT. To take higher orders into account the so called quasi-relativistic (QR) procedure was developed, which is implemented in standard version of ADF. In this method a diagonalisation is performed in the space of non-relativistic solutions. The variational collapse can be avoided by carefully choosing the basisfunctions. We can see this in an example. Suppose we have a trial s-type wave function, with radial behaviour:

$$\Phi^T = N_\lambda e^{-\lambda r} \tag{6.21}$$

where N_λ is chosen such that the trial wave function is normalised to one. The expectation value of this trial wave function with the Pauli Hamiltonian is (the spin-orbit coupling is zero because we have an s-type function) in the case of a hydrogen-like atom:

$$\langle \Phi^T | H^{Pauli} | \Phi^T \rangle = \langle \Phi^T | V + \frac{p^2}{2} - \frac{p^4}{8c^2} + \frac{\Delta V}{8c^2} | \Phi^T \rangle$$

$$= -Z\lambda + \frac{\lambda^2}{2} - \frac{5\lambda^4}{8c^2} + \frac{4Z\lambda^3}{8c^2} \tag{6.22}$$

If we choose λ large enough, the third term (mass-velocity term), will be the dominating one, because it has a fourth power of λ. This term has a minus sign, so the expectation value can be made arbitrarily negative meaning variational collapse. On the other hand, if we use as trial function a non-relativistic bound solution (for example $\lambda = Z$ gives the 1s non-relativistic eigenfunction of a hydrogen-like atom), the expectation value will improve upon the energy compared to the non-relativistic value. For non-bound solutions already Pauli FOPT may cause problems: for example the mass-velocity term is very large negative for a plane wave (free particle) with very high non-relativistic kinetic energy, which may again lead to arbitrary large negative expectation values. So there is some balance between good and bad behaviour, depending on the choice of basisfunctions. In general one can say that if the basis set allows to make a very peaked function (high kinetic energy), the mass-velocity term may cause variational collapse. To avoid variational collapse one has to make sure that this can not happen. If we take again the example of the hydrogen-like atom, suppose the Uranium 91+ ion. The relativistic Dirac $1s$-orbital energy is -4861 a.u., the non-relativistic (NR) is -4232 and for $\lambda = Z = 92$ (PAULI FOPT) equation 6.22 gives -4709 a.u., which is a great improvement over the NR value. However, for example $\lambda = 2Z = 184$ equation 6.22 gives -22889 a.u., showing the effect of variational collapse. This example shows that one can get in problems very easily for all-electron calculations.

In the ADF program usually the frozen core approximation is used. Now the problems connected with variational collapse are reduced. The usual basis sets only have basis functions for the valence electrons. One core orthogonalisation function per core orbital is used to orhogonalise the basis function on the accurately calculated non-relativistic core orbitals. For the core orthogonalisation functions Slater type orbitals (STO's) are used, which are optimised to the core wiggles of the non-relativistic valence orbitals. This means that the core wiggles of the orthogonalised basis functions near the core will look like the core wiggles of the non-relativistic valence orbitals. We know that with basis functions which look like the non-relativistic bound valence orbitals the Pauli approximation will improve the orbital energies. The only problem can arise if a basis function is core-like and (or) has high kinetic energy. The usual basis sets in ADF have optimised basis functions, which are rather flat (low kinetic energy), because the valence electrons move rather slowly. In practical calculations using these basis sets, the QR method will improve upon Pauli FOPT, which is already a large improvement over the NR approximation. An example of this, calculations on the neutral Uranium atom, can be found in ref. [70]. If we do the same calculations, using a standard basis , the so called ADF IV with 5d frozen core, we get -1.30 a.u. for the NR 6s orbital energy, and -1.75 a.u. using the QR method. This can be compared with the relativistic Dirac result of -1.72 a.u., showing that the QR method improves upon the NR result considerably. A general remark was made in ref. [28], where it was said that for elements up to Z=80 Pauli FOPT is accurate enough, while for heavier systems the QR method is needed. This remark is true for the standard ADF basis sets, it is not true anymore for arbitrary basis sets. This can be shown in some examples.

A first example is to change the core orthogonalisation functions. Instead of using the STO's which are optimised to the core wiggles of the valence functions, we could use the STO's optimised to the core orbitals, still one STO core orhogonalisation function per core orbital. In the NR case we now get -1.24 a.u. for the 6s orbital energy, a bit higher than before. This result can be expected for a basis set which cannot describe the core wiggles of the valence orbitals as accurately as before. However, in the QR method we now already have problems related to variational collapse, the 6s orbital energy in this case is namely -3.75 a.u., which is far too low. The success of the QR method

thus quite heavily depend on the choice of core orthogonalisation functions. A second example is to increase the standard ADF IV basis set with an extra STO in the basis which is core-like, for example a 1s-type STO with $\lambda = 40$. In the NR calculation the 6s energy is then still -1.30 a.u., the difference being less than 0.0001 a.u. with respect to the calculation without this core-like function. Again this could be expected since the basis set was already quite optimal and a core-like function is certainly not able to improve much upon this. In the QR calculation the 6s orbital energy now becomes -485 a.u., showing the drastic effect of variational collapse. Choosing a different core-like basis function one can get every orbital energy one likes. A third example is the same 1s-type STO, but now with $\lambda = 200$ and centered around a place where the potential is almost zero (for example far away from the Uranium atom). To calculate the expectation value of this basis function in the Pauli approximation one then only needs to calculate the non-relativistic kinetic energy and the mass-velocity term, which is 20000-53250=-33250 a.u., showing how variational collapse can occur for very peaked functions. In standard basis sets there are usually only very peaked functions centered around atoms, so this is a rare example.
In the QR method implemented in ADF, the variational collapse can thus be avoided by using the right basis set: choose carefully the core orthogonalisation functions and use only valence-like basis functions and make sure that the basis functions are not too peaked. The standard ADF frozen core basis sets fulfil all these requirements. Using these basis sets the QR method can then be a very useful (and cheap) method for estimating relativistic effects.
The ZORA method described in this thesis is like the NR method variationally stable, and one can use any basis set one likes.

Chapter 7

Molecular calculations

Table 7.1: Optimized Slater exponents of basis set B for all electron ZORA scalar relativistic calculations

s		p		d		f	
n	ζ	n	ζ	n	ζ	n	ζ
1	10000.0	2	600.0	3	87.0	4	22.9
1	2300.0	2	200.0	3	34.9	4	13.25
1	730.0	2	83.0	3	22.2	4	7.7
1	285.0	2	45.1	3	16.2	4	4.5
1	130.0	2	34.4	4	14.2	5	2.5
1	85.7	3	21.85	4	9.6		
2	64.1	3	17.1	4	6.8		
2	50.4	4	16.95	5	4.85		
2	37.0	4	11.2	5	3.05		
3	22.0	4	8.32	5	1.90		
3	17.35	5	6.38	5	1.20		
4	18.8	5	4.40				
4	12.5	5	3.08				
4	9.4	6	3.20				
5	7.95	6	1.80				
5	5.72						
5	4.10						
6	3.25						
6	2.20						
6	1.50						
6	1.00						

7.1 Scalar Relativistic calculations

In chapter 6 we have seen how the ZORA method was implemented in the molecular ADF program. In this section we will look at scalar relativistic calculations on some diatomics. We use the ZORA ESA way of calculating the difference in kinetic energy (see section 3.5). We will first look at calculations on gold compounds. In the all-electron calculations we took a double-ζ STO basis plus two extra 1s functions with high exponents and one extra 6s and 5d function for the valence, which were optimised to numerical orbitals. Two 6p and one 5f polarisation functions were added. This basis set A was shown in table 3.7. The reason that one needs s functions with high exponents is that for s orbitals the wave function has a weak singularity if $r \to 0$. In the frozen core calculations the basis functions were orthogonalised on frozen core orbitals coming from an all-electron neutral atom calculation. The 5d and 6s are treated as valence orbitals, which means there are 11 valence electrons. In these frozen core calculations we used a double-ζ STO basis plus one extra 1s function with a high exponent and two extra 6s and 5d functions for the valence and two 6p and one 5f polarisation function. These basis sets are the same as in the ionisation calculations of section 3.5. For hydrogen a triple-ζ STO basis was used with one 2p and one 3d polarisation function.

Table 7.2: First ionisation energy of Au in eV from ZORA ESA scalar relativistic LDA and GGC calculations

		All electron		Frozen core	
	EXP	LDA	GGC	LDA	GGC
IP	9.23	9.92	9.76	9.93	9.78

We start with the first ionisation energy of gold atom in table 7.2. The selfconsistent calculations were done using the LDA potential. After convergence the density-gradient (GGC) corrections were calculated using the LDA density. We will use this procedure for all our calculations. The calculated ionisation energies are still off by some 0.7 eV for LDA and 0.5 eV for GGC. It is well known that the used density functionals are not so accurate for ionisation energies and even poor for electron affinities. For comparison, the Dirac-Fock result is 7.67 eV (from ref. [71]). The best result for the ionisation potential obtained in ab initio calculations, including cor-

Table 7.3: Molecular properties of Au_2

		All electron				Frozen core					
		Basis set A		Basis set B							
		ZORA-ESA		ZORA-ESA		ZORA ESA		NR		PAULI QR	
	EXP	LDA	GGC	LDA	GGC	LDA	GGC	LDA	GGC	LDA	GGC
r_e (Å)	2.472	2.453	2.513	2.457	2.517	2.458	2.517	2.689	2.776	2.503	2.556
D_e(eV)	2.31	2.96	2.29	2.92	2.26	2.92	2.26	2.00	1.47	2.81	2.19
$\omega(cm^{-1})$	191	197	178	196	177	193	174	137	120	193	175

Table 7.4: Molecular properties of AuH

		All electron		Frozen core					
		ZORA-ESA		ZORA-ESA		NR		PAULI QR	
	EXP	LDA	GGC	LDA	GGC	LDA	GGC	LDA	GGC
r_e (Å)	1.524	1.525	1.535	1.530	1.539	1.710	1.737	1.523	1.531
D_e (eV)	3.36	3.80	3.34	3.78	3.33	2.64	2.28	3.87	3.43
$\omega(cm^{-1})$	2305	2320	2260	2340	2290	1710	1630	2390	2350

relation, using the spin-free no-pair Hamiltonian obtained from a second order Douglas-Kroll transformation, is 9.08 eV (see ref [72]), which is very close to experiment. In table 7.3 and 7.4 results are given of molecular calculations on the gold dimer and gold hydride. The calculations were done using the Amsterdam Density Functional (ADF) program package, where the scalar relativistic ZORA was implemented. The bond energy evaluation uses the ZORA ESA way of calculating the difference in the scaled ZORA kinetic energies of molecule and atoms. The remaining parts of the bond energy evaluation are the same as in the non-relativistic case. Matrix elements of the Hamiltonian were calculated numerically. The ADF program uses a fit of the density in STO's to be able to calculate the Coulomb potential accurately. For this fit an extensive basis set was used. These computational approximations lead to errors in the bond energy less than 0.01 eV. Improving the basis set by adding an extra f polarisation function changed the bond energies less than 0.01 eV. In the all-electron calculations on Au_2 we also used the large basis set B to get some feeling for the remaining basis set error. For the bond distance the difference is less than 0.005 Å and for the dissociation energy the difference is less than 0.05 eV. In the all-electron calculations on AuH basis set A was used. From table 7.3 and 7.4 we can see that the ZORA all-electron and frozen core results are in perfect agreement with each other.

The ZORA LDA bond distance is within 0.02 Å of the experimental value in the case of Au_2 and within 0.01 Å in the case of AuH. For the ZORA GGC this is respectively 0.04 and 0.02 Å. Experimental values are from ref. [73]. The ZORA LDA gives a too large dissociation energy, which is a well known feature of this functional. Here the LDA dissociation energies are typically 0.6 eV too large. The ZORA GGC result is within 0.05 eV of the experimental value. This high accuracy compared to experiment is probably somewhat fortuitous, the average accuracy of the used functionals being ca. 0.15 eV for light systems. For Au_2 and AuH we also did some calculations using the scalar relativistic parts of the standard Pauli Hamiltonian, the mass-velocity and the Darwin term. These were included in the quasi relativistic calculations reported in ref [28]. The quasi-relativistic method, consisting of diagonalisation of the Pauli Hamiltonian, gives reasonable results provided that one takes care (by appropriate basis set choice) that no variational collapse occurs. We always take as basis functions in the quasi-relativistic calculations basis sets that are optimized for nonrelativistic calculations. Apparently the restrictions that are imposed in this way on the variational freedom, particularly in the core region, are sufficient to prevent collapse to the nucleus, at the same time allowing a fairly accurate description of the relativistic changes of the wavefunctions in the valence region. In spite of this lack of firm justification, we observe again in tables 7.3 and 7.4 that the quasi-relativistic calculations ("Pauli Quasi Relativistic") yield quite reasonable agreement with the ZORA ESA results, both at the LDA and GGC levels. In the PAULI QR calculations we used the standard ADF IV basis set (triple-ζ valence plus one polarisation function) for

Table 7.5: Molecular properties for some diatomic systems.

		Au_2	Ag_2	Cu_2	$AgAu$	$AuCu$	$AgCu$	AuH	AgH	CuH
r_e (Å)										
EXP		2.472	2.53	2.220		2.330	2.374	1.524	1.618	1.463
ZORA	LDA	2.458	2.486	2.151	2.473	2.285	2.313	1.530	1.594	1.440
ZOR A	GGC	2.517	2.563	2.212	2.541	2.344	2.383	1.539	1.615	1.453
NR	LDA	2.689	2.564	2.182	2.625	2.426	2.370	1.710	1.661	1.460
NR	GGC	2.776	2.653	2.246	2.713	2.503	2.447	1.737	1.688	1.475
D_e (eV)										
EXP		2.31	1.66	2.05	2.08	2.39	1.76	3.36	2.39	2.85
ZORA	LDA	2.92	2.28	2.77	2.76	3.09	2.51	3.78	2.95	3.40
ZORA	GGC	2.26	1.71	2.19	2.15	2.45	1.93	3.33	2.55	3.03
NR	LDA	2.00	2.01	2.60	2.01	2.28	2.29	2.64	2.68	3.26
NR	GGC	1.47	1.48	2.04	1.48	1.74	1.75	2.28	2.32	2.90
$\omega(cm^{-1})$										
EXP		191	192	265		250	232	2305	1760	1941
ZORA	LDA	193	208	298	209	269	255	2340	1890	2070
ZORA	GGC	174	183	272	185	245	229	2290	1810	2010
NR	LDA	137	181	285	162	212	231	1710	1710	1990
NR	GGC	120	160	258	142	189	206	1630	1630	1940

Au and ADF V basis set (triple-ζ valence plus two polarisation function) for H. The non-relativistic results were obtained, using a largere basis set, which is decscribed below. In ref [74] the bond distance for AuH in the PAULI QR case was not given correctly.

We have extended the calculations to isoelectronic compounds containing the lighter congeners Ag and Cu. These calculations were all done using the frozen core approximation. Only the highest s and d electrons were left unfrozen (11 electrons). The basis sets for silver and copper again were optimised to numerical atomic orbitals. The basis set was a double-ζ STO basis plus two extra valence s and d functions and two p and one f polarisation function. For silver also an extra 1s function with a high exponent was added. The results of the calculations are given in table 7.5 and figure 7.1. The experimental numbers are from ref. [73] and from refs. [75] (R_e of Ag_2) and [76, 77] (R_e of $AuCu$ and $AgCu$). The ZORA GGC dissociation energies are all within 0.2 eV of the experiment, with an average deviation of 0.1 eV. The ZORA LDA results are about 0.4-0.6 eV too large. In table 7.5 also non-relativistic calculations are shown. For these calculations we used a double-ζ basis set, where the valence was made quadruple-ζ and two p and one f polarisation function were added. The non-relativistic basis set is then of comparable quality with the ZORA basis set. A basis set free NR LDA result for the bond distance of CuH can be found in ref [78]. The basis set free result was 1.455 Å, which can be compared with our result of 1.460 Å for the frozen core NR LDA calculations. The calculated frequencies were obtained from polynomial fits to nine $E(R)$ points and have a precision of 1%.

Our results are of comparable quality with ab initio calculations, including correlation, using the spin-free no-pair Hamiltonian obtained from a second order Douglas-Kroll transformation for the silver hydride [79] and the gold hydride [80]. For gold hydride Hess and coworkers obtained a bond distance of 1.52 Å and a binding energy of 3.33 eV. The non-relativistic ab initio calculations of these authors, including correlation, give a bond distance of 1.72 Å and a dissociation energy of 2.19 eV. These are very close to our nonrelativistic GGC results. Schwerdtfeger [71] used large basis sets in non-relativistic and relativistic pseudopotential calculations, including correlation, on the gold dimer to predict relativistic changes in spectroscopic parameters. He predicted a relativistic change of -0.25 Å for the bond distance, -0.9 eV for the dissociation energy and -1.0 mdyn/Å for the force constant, which are close to our findings. Bauschlicher et al. [81] used (relativistic) effective core potentials in ab initio calculations, including correlation, on the dimers (and trimers) of copper, silver and gold. Compared to experiment they overestimate bond distances in the order of 0.05 to 0.1 Å and underestimate dissociation energies in the order of 0.2 to 0.4 eV for the dimers. Häberlen

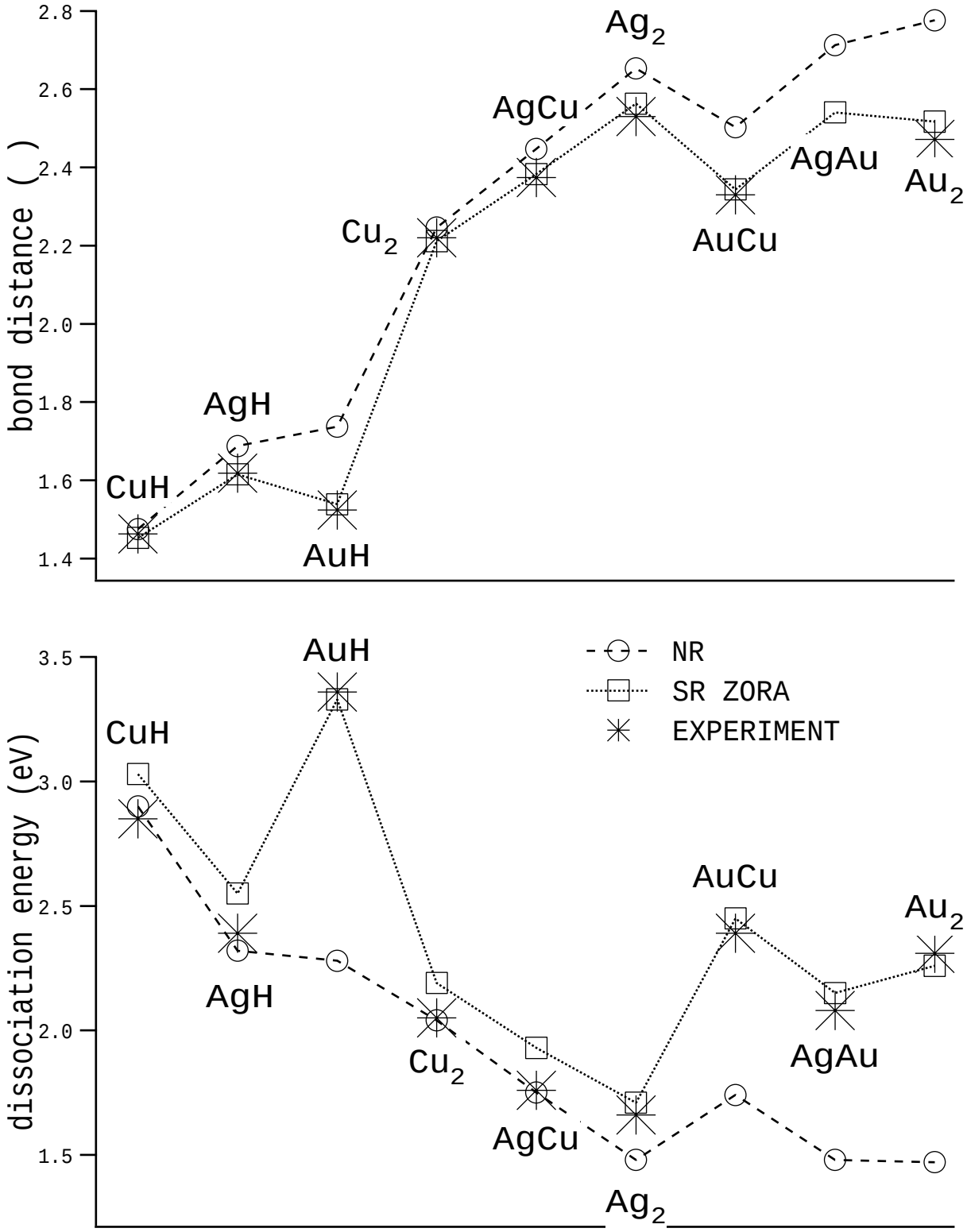

Figure 7.1: Bond distance and dissociation energies for some diatomic systems from frozen core GGC calculations. Results are taken from table 7.5.

and Rösch [82] used the spin-free no-pair Hamiltonian obtained from a second order Douglas-Kroll transformation in local density functional calculations on Au_2, AuH and $AuCl$. Their relativistic and non-relativistic LDA results on the gold dimer are in close agreement with our LDA results. There is more deviation in the results on the gold hydride. We were not able to find an explanation for the discrepancy in the NR LDA calculations on the bond length of this compound. All-electron Dirac-Fock-Slater calculations on Au_2 were carried out by Baştuğ et al. [83]. Our results can not be compared directly, because we use a different density functional, but the calculated relativistic effects are of comparable size.

7.2 Spin-orbit effects

In the last section (see also ref. [74]) the zeroth order regular approximated (ZORA) Dirac equation was successfully applied in scalar relativistic calculations on molecules. In this section we will concentrate on the spin-orbit effects, using non-relativistic local density functionals (LDA) including gradient correction (GGC) terms for the calculation of the exchange-correlation energy. The Becke correction for exchange [84] and the Perdew correction for correlation [85], that have been successfully applied in nonrelativistic calculations [86, 87] and in scalar relativistic ZORA calculations (see last section), have been used.
If spin-orbit coupling is present in closed shell systems we will use a one-determinantal j-j ($\omega - \omega$) coupled state, obtained from one-electron spinorbitals which are eigenfunctions of j^2 and j_z. For open shell atoms j-j coupling is not a good approximation and we use intermediate coupling to ensure the right scalar relativistic limit if the spin-orbit operator goes to zero (see section 7.2.1). In section 7.2.3 results are shown for some atomic multiplets using this method.
In section 7.3 we analyse the spin-orbit effects on some closed shell molecules, namely I_2, Au_2, Bi_2, HI, AuH, TlH, IF, TlF, TlI, PbO and $PbTe$, looking at bond distance, harmonic frequencies, dissociation energies and dipole moments. In order to obtain very accurate results for the dissociation energies it is needed to include gradient correction (GGC) terms in the energy and use the intermediate coupled energy for the atoms. Results are then all within 0.3 eV of the experiment, with an average deviation of 0.1 eV for these compounds.

In spin-orbit calculations we want the energies to converge to the scalar relativistic energies in the limit that the spin-orbit operator goes to zero. In this limit the one-determinantal state obtained using j-j ($\omega - \omega$) coupling is identical to the state obtained using L-S ($\Lambda - \Sigma$) coupling. So for closed shell systems we can use j-j ($\omega - \omega$) coupling without any corrections. For open shell systems this is not true anymore. To let the spin-orbit calculations converge to the scalar relativistic energies, if the spin-orbit operator goes to zero, we have to use intermediate coupling for open shell systems. How we do this in our density functional calculations is shown in the next section.

7.2.1 Open shell systems

An important question in relativistic density functional theory is how to obtain the ground state energy of some open shell system with the present day approximate density functionals. This is also a problem in non-relativistic density functional theory, but the problems become more complicated if the spin-orbit operator is present. In the non-relativistic case one solution is to find the lowest energy, without any symmetry constraints. For an open shell atom this means that the lowest energy can be obtained for a nonspherical density and where the solution is not a pure spin state. In an ab initio scheme these problems can be solved unambiguously, also in the relativistic case.
The relativistic Hamiltonian can be divided in a scalar relativistic (SR) and a spin-orbit (SO) part:

$$H^{REL} = H^{SR} + H^{SO} \tag{7.1}$$

A possibility would be to start with the calculation of the energies of all j-j ($\omega - \omega$) coupled states. Present day density functionals have not been developed to use them in this case. In intermediate coupling, states which have the same total J and J_z can couple, because of the electron-electron interaction.
Another possibility is to solve the whole spectrum of the scalar relativistic Hamiltonian. The energies of the multiplet states can for example be calculated using the diagonal sum-method as suggested in ref [88] or the alternative method of ref. [89] and we have the energies of the L-S coupled states. We then can calculate the spin-orbit interaction between those states. From angular momentum conservation we know that only those states can couple through the spin-orbit operator which have the same total J and J_z. We can diagonalize the resultant matrix and we have the energies of the intermediate coupled states. The problem here is that in principle many states can couple and we have to know the energies of the excited states, which is not straightforward in density functional theory. We therefore have to approximate this

procedure, by using for example only the lowest lying excited states.
The direct effect of the spin-orbit operator on valence orbitals is large if we have an open shell atom with partially occupied p,d or f shells. We can see this in the splitting of states which would be degenerate in the L-S coupled scheme. For light atoms a first order treatment of the spin-orbit coupling is sufficient, whereas for heavier atoms one needs the intermediate coupling scheme. The limit where j-j coupling is much more important than L-S coupling is not reached for the known elements.
There can also be an effect of spin-orbit coupling on fully occupied shells, although if we start with a scalar relativistic solution, the first order effect of the spin-orbit coupling on the energy is zero. The total effect of spin-orbit coupling is not zero anymore for deep core fully occupied shells of heavy atoms. We can see this effect already if we look at the hydrogen-like heavy atom, for example the Uranium 91+ atom. The averaged relativistic 2p orbital energy -1045.54 (1/3 times -1257.39 ($2p_{1/2}$) plus 2/3 times -1089.61 ($2p_{3/2}$)) is approximate 15 a.u. lower than the scalar relativistic orbital energy -1130.34. So even for closed shells spin-orbit interaction can be of importance, due to the second and higher order effects of the spin-orbit coupling. The radial part of the $2p_{1/2}$ orbital is then not so close to the radial part of the $2p_{3/2}$ orbital anymore. If we start with the scalar relativistic states we need very high excited states if we want to take this effect into account. On the other hand, as we have tested in valence only calculations, the effect of the change in density of the core orbitals due to spin-orbit effects has very little effect on valence orbitals.
In practical calculations it is often convenient to express the ground state energy with respect to some average-of-configuration energy. In the scalar relativistic case we will choose this average-of-configuration calculation where the electrons are distributed equally over the subspecies of the open shell irreps. For atoms this will ensure a spherical density and a spin-α density, which is the same as that of spin-β. If spin-orbit coupling is present we will divide the electrons in a spin-orbit averaged way over the different open shell irreps such that if the spin-orbit coupling is zero the occupation would be the same as in the scalar relativistic case. For an atom with a p^1 configuration this will mean that 1/3 of an electron is placed in the $p_{1/2}$ orbital and 2/3 in the $p_{3/2}$ orbital. These reference states are not physical states. The scalar relativistic multiplet states (L-S coupling) can be obtained using the method of ref [88] or ref. [89]. From the difference in energy of the lowest j-j coupled state and the reference state, in which we both use a spherically and spin averaged density, we calculate an effective spin-orbit parameter. Together with the energies of the L-S coupled states we will calculate the energies of the intermediate coupled states, using the results given in section 7.2.2, as if they remain valid in our calculations. In the present approximations we do not take excited states from different configurations into account.

Below we will give an example that may clarify the problems if one uses the spin-orbit operator in present day approximate density functionals, without thinking about their limitations. Suppose we have a hydrogen atom with a p^1 configuration. Many of the present day density functionals will not give the same energy whether the electron is placed in the p_z orbital or in the $(p_x + ip_y)/\sqrt{2}$ orbital. Sometimes a spherically averaged atom is chosen, which will give yet another energy. This problem already occurs if we use density functionals, which do not depend on the spin-polarisation. In general the spin-polarised density functionals will give different results if the electron is placed in the p_z orbital with spin α or with a mixed spin state $(\alpha + \beta)/\sqrt{2}$, although these states are degenerate according to the Schrödinger equation. A solution is then to take only the state which is purely spin α or β. These problems occur when the Schrödinger equation has degenerate solutions, which means that any linear combination of these solutions is also a solution to the Schrödinger equation. In this way one obtains different spin-densities which should have the same energy, but many of the present day density functionals will not give the same energy. In fact similar problems can arise in almost degenerate cases. One of the approximate solutions to these problems is to use a method suggested in ref [88]. Another possibility is to use the method of Becke et al. [89], which uses 'local pair' densities instead of local spin densities in their calculations.
Relativistic Hamiltonians will, besides scalar relativistic corection terms to the non-relativistic Hamiltonian, also have a spin-orbit operator. If we take again the example of the hydrogen atom with p^1 configuration. The $p_{1/2}$ orbitals will have 1/3 of one spin and 2/3 of the other spin. If we use this density in a density functional, which depends on spin-polarisation, we will get a different answer than the scalar relativistic result obtained from a pure spin α or pure spin β density. These results differ even if we let the spin-orbit operator go to zero, in which case the difference is only due to the fact that in the one case we have a pure spin state and in the other some

mixed state.

7.2.2 Intermediate Coupling

In for example ref. [90] it is shown how the atomic energies in intermediate coupling can be calculated using the spin-orbit matrix. Different configuration state functions (CSF) belonging to the same configuration can mix due to the spin-orbit operator. In the simplest approximation, where we only use CSF's belonging to the same configuration and using an effective spin-orbit parameter we will show the results for the p^1, p^2 and p^3 configuration.
For a p^1 configuration we have in the L-S coupled scheme the ^2P state. The energies of the intermediate coupled states are:

$$\begin{array}{rcl} E(^2P_{1/2}) & = & E(^2P) - \zeta_p \\ E(^2P_{3/2}) & = & E(^2P) + \frac{1}{2}\zeta_p \end{array} \tag{7.2}$$

In this case the spin-orbit effect is additive.
Suppose we have a p^2 configuration. In L-S coupling we have the ^3P, ^1D and ^1S state. To obtain intermediate coupling for $J = 0$ and $J = 2$ we have to diagonalize a matrix. For $J = 0$ this is:

$$\begin{pmatrix} E(^3P) - \zeta_p & \sqrt{2}\zeta_p \\ \sqrt{2}\zeta_p & E(^1S) \end{pmatrix} \tag{7.3}$$

and for $J = 2$:

$$\begin{pmatrix} E(^1D) & \frac{1}{\sqrt{2}}\zeta_p \\ \frac{1}{\sqrt{2}}\zeta_p & E(^3P) + \frac{1}{2}\zeta_p \end{pmatrix} \tag{7.4}$$

The diagonal of these matrices shows the first order spin-orbit effect, which is a good approximation if the spin-orbit parameter is small compared to the difference in energy of the energies of the L-S coupled states. The energy of the $^3P_1$ state is:

$$E(^3P_1) = E(^3P) - \frac{1}{2}\zeta_p \tag{7.5}$$

For a p^3 configuration we have in L-S coupling the ^4S, ^2P and ^2D state. In intermediate coupling for $J = 1/2$ and $J = 5/2$ we have:

$$\begin{array}{rcl} E(^2P_{1/2}) & = & E(^2P) \\ E(^2D_{5/2}) & = & E(^2D) \end{array} \tag{7.6}$$

For $J = 3/2$ we have to diagonalise a matrix to obtain the energies of the intermediate coupled states:

$$\begin{pmatrix} E(^2P) & \zeta_p & \frac{\sqrt{5}}{2}\zeta_p \\ \zeta_p & E(^4S) & 0 \\ \frac{\sqrt{5}}{2}\zeta_p & 0 & E(^2D) \end{pmatrix} \tag{7.7}$$

Table 7.6: Energy difference between atomic ground state and average-of-configuration (see text) and the spin-orbit parameter in eV.

	L-S coupling		intermediate coupling		spin-orbit parameter	
	LDA	GGC	LDA	GGC	LDA	GGC
H	-0.90	-0.95	-0.90	-0.95	0.00	0.00
O	-1.58	-1.96	-1.59	-1.97	0.02	0.02
F	-0.41	-0.72	-0.43	-0.74	0.04	0.04
Te	-0.52	-0.71	-0.92	-1.09	0.54	0.53
I	-0.11	-0.19	-0.45	-0.52	0.68	0.66
Au	-0.15	-0.20	-0.15	-0.20	0.00	0.00
Tl	-0.13	-0.23	-0.83	-0.91	0.70	0.68
Pb	-0.48	-0.61	-2.04	-2.11	0.97	0.95
Bi	-1.10	-1.34	-2.14	-2.27	1.27	1.25

Table 7.7: Atomic multiplets in eV. Experimental results are taken from the tables of Moore [91]

	L-S coupling		intermediate coupling			
	LDA	GGC	J	LDA	GGC	EXP
Tellurium						
$^3P_2$	0	0	2	0	0	0
$^3P_0$	0	0	0	0.60	0.63	0.58
$^3P_1$	0	0	1	0.67	0.64	0.59
$^1D_2$	0.70	0.88	2	1.23	1.37	1.31
$^1S_0$	1.93	2.24	0	2.67	2.90	2.88
Iodine						
$^2P_{1/2}$	0	0	1/2	0	0	0
$^2P_{3/2}$	0	0	3/2	1.02	0.99	0.94
Thallium						
$^2P_{1/2}$	0	0	1/2	0	0	0
$^2P_{3/2}$	0	0	3/2	1.05	1.02	0.97
Lead						
$^3P_0$	0	0	0	0	0	0
$^3P_1$	0	0	1	1.08	1.03	0.97
$^3P_2$	0	0	2	1.41	1.40	1.32
$^1D_2$	0.59	0.69	2	2.78	2.76	2.66
$^1S_0$	1.54	1.68	0	3.70	3.74	3.65
Bismuth						
$^4S_{3/2}$	0	0	3/2	0	0	0
$^2D_{3/2}$	0.88	1.03	3/2	1.49	1.48	1.42
$^2D_{5/2}$	0.88	1.03	5/2	1.92	1.96	1.91
$^2P_{1/2}$	1.58	1.73	1/2	2.62	2.66	2.69
$^2P_{3/2}$	1.58	1.73	3/2	4.09	4.07	4.11

7.2.3 Spin-orbit effects in atoms

In section 7.2.2 we have shown how we calculate atomic energies of intermediate coupled states. We will use this in our density functional calculations. Our main objective is to get the energy of the ground state, if spin-orbit coupling is present. We want this energy to converge to the scalar relativistic ground state energy if the spin-orbit operator goes to zero. To obtain the correction term for the energy of the physical ground state compared to the unphysical spin-averaged and spherically averaged atom in the scalar relativistic case, we have done selfconsistent spin-polarised calculations on the atoms in $D_{\infty h}$ symmetry, using every possible way to distribute the electrons. The lowest energy was considered to be the ground state energy. One can also calculate one-determinantal wave-functions using restricted orbitals coming from a spherically averaged and spin-averaged atom and then calculate the energies using spin-polarised density functionals. This may give energies which are higher than the converged results up to 0.15 eV, especially for the lighter open shell systems. For the heavier elements we have used the difference is less than 0.05 eV, between converged and non-converged results. We have used the converged results, which are shown in table 7.6 under the header 'L-S coupling'. For the calculation of the energies of the L-S coupled states using the diagonal sum-method of Ziegler et al. [88] we also used the converged results. Formally this is not justified, but as we have said before the difference between the energies using the restricted or the unrestricted orbitals is small for the heavier atoms, for which we need this diagonal sum-method. In table 7.7 we show the resulting energies for the heavier elements. The diagonal sum-method is only used for Te, Pb and Bi. This method suffers from the cited problems, that two different determinants belonging to the same state yield somewhat different energies, with present day functionals. Due to this arbitrariness the calculated splittings have an accuracy of about 0.2 eV for these systems. For H, F, I, Au and Tl we only have one state in L-S coupling for the lowest configuration, and for O the spin-orbit effect is so small we don't have to consider other L-S coupled states for the calculation of the energy of the intermediate coupled state. In table 7.6 we show the effective spin-orbit parameters we have calculated. For the energies of the intermediate coupled states, we use the method in section 7.2.2. Results for the atomic energies of the intermediate coupled states are shown in 7.7, together with the experimental values [91]. Both LDA and the density gradient corrected (GGC) splittings are in close agreement with experiment, deviations less than 0.1 eV. For Te, Pb and Bi this accuracy is better than the intrinsic accuracy of the diagonal sum-method, so this accuracy has to be considered somewhat fortuitous.

Table 7.8: Optimized Slater exponents for all electron ZORA scalar relativistic calculations for iodine

s		p		d		f	
n	ζ	n	ζ	n	ζ	n	ζ
1	1000.0	2	185.0	3	22.1	4	2.5
1	240.0	2	56.2	3	13.3	4	1.5
1	83.0	2	28.75	3	9.05		
1	53.5	2	21.25	4	7.23		
2	42.0	3	16.25	4	4.89		
2	29.5	3	12.2	4	3.40		
2	22.2	3	9.5	4	2.48		
3	13.25	4	9.55	5	2.00		
3	10.4	4	6.05				
4	8.55	4	4.25				
4	6.00	5	3.90				
4	4.45	5	2.60				
5	3.51	5	1.70				
5	2.44	5	1.12				
5	1.70						
6	1.40						

The total energy of the atoms, using spin-orbit interaction, is for the heavier systems much lower than the scalar relativistic total energies. As explained before this is mainly due to the core electrons. For differences in energy this effect will be almost completely negligible. On the other hand, the valence open shell spin-orbit effects are not negligible. We therefore formally put the SR ZORA spin and spherically averaged atomic total energy at the same level as the ZORA spin, spherically and spin-orbit averaged atomic total energy. We then can combine multiplet splittings and spin-orbit effects together using intermediate coupling. The results are shown in table 7.6 under the header 'intermediate coupling'.

7.3 Spin-orbit effects in closed shell molecules

The selfconsistent calculations were done using the LDA potential. After convergence density-gradient (GGC) corrections were calculated using the LDA potential. For gold we use the large basis set B of section 7.1. The hydrogen basis set is also described there. For thallium, lead and bismuth we use optimised basis sets to numerical scalar relativistic ZORA

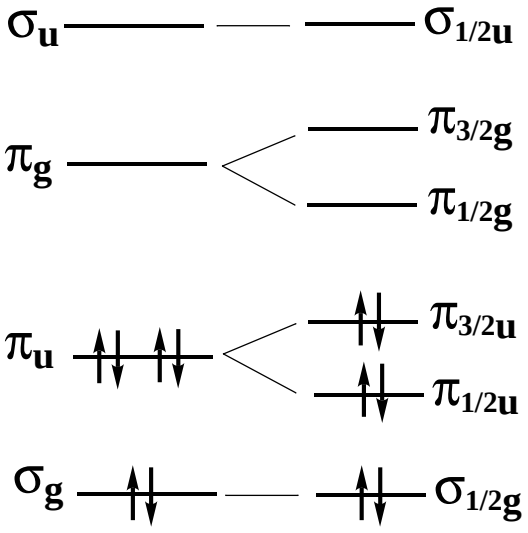

Figure 7.2: Scalare relativistic (left side) and first order spin-orbit split (right side) valence molecular orbital levels for Bi_2

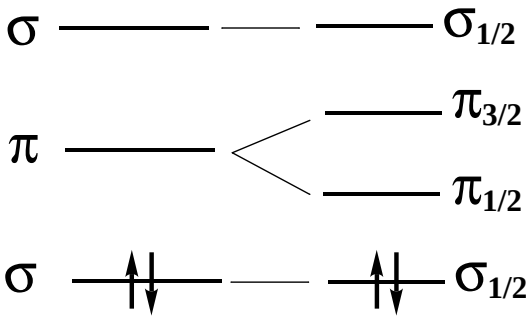

Figure 7.3: Scalare relativistic (left side) and first order spin-orbit split (right side) valence molecular orbital levels for TlH

orbitals, which are as large as the gold basis set, but with two extra $6p$ STO functions. In table 7.8 the basis set for iodine is given. The tellurium basis set is as large as this, but with different optimised exponents. For oxygen and fluorine we use a triple $1s$ and quadruple valence basis set plus two $3d$ and two $4f$ polarisation functions. The large basis sets used give an accuracy of better than 0.02 eV for the atomic valence orbital energies compared to numerical calculations, for both the ZORA and the SR ZORA calculations.

In tables 7.9, 7.10 and 7.11 results are given of all-electron molecular calculations on some diatomic compounds. First we have to note that the spin-orbit effect for most molecular properties is not large for these closed shell systems. The spin-orbit effect on the bond distance never exceeds 0.03 Å, on frequencies it is less than 10%, and the molecular spin-orbit effect on the energies is in most cases less than 0.15 eV, except for Bi_2 and $PbTe$. In table 7.11 these molecular energies are defined with respect to spherically and spin averaged and for ZORA spin-orbit averaged atoms. Explanation of these spin-orbit effects is given below.

For the lighter atoms, hydrogen, oxygen and fluorine, the spin-orbit effect may be neglected, compared to the much larger spin-orbit effect on the heavier atoms. Also the first order effect of spin-orbit coupling for closed shell systems is zero. The effects of spin-orbit coupling for closed shell systems must therefore come from higher orders. For open shell systems one may expect much more effects coming from spin-orbit coupling, especially for the energy as is the case in atoms. Here we will not consider open shell molecules. The spin-orbit effects in tables 7.9, 7.10 and 7.11 can for a large part be understood if we only look at the molecular bonding and antibonding orbitals coming from the valence atomic p-electrons. In figure 7.2 schematically the one-electron molecular orbital levels coming from these orbitals for Bi_2 are shown. At the left side of this figure the scalar relativistic energies are shown and on the right side the first order effect of the spin-orbit interaction is included. The energy of the bonding π_u-orbital will split split due to this first order spin-orbit effect, but since both split levels are fully occupied, there is no net first order spin-orbit effect. The effects should therefore come from off-diagonal spin-orbit interaction, which is only possible for orbitals with the same j and for homonuclear diatomics with the same parity. There is only a net effect of this off-diagonal spin-orbit interaction if it is between an occupied and an unoccupied orbital, in which case it always has a stabilizing effect on the energy. Thus, for the levels shown in figure 7.2, we have off-diagonal spin-orbit interaction between the occupied bonding $\sigma_{1/2g}$-orbital and the unoccupied anti-bonding $\pi_{1/2g}$-orbital and between the occupied bonding $\pi_{1/2u}$-orbital and the unoccupied anti-bonding $\sigma_{1/2u}$-orbital. The effect of the off-diagonal spin-orbit interaction between orbitals will be larger if the difference in energy of

Table 7.9: Bond length r_e and spin-orbit correction to the bond length $\Delta^{so} r_e$ in Ångstroms for some diatomic systems.

		I_2	Au_2	Bi_2	HI	AuH	TlH	IF	TlF	TlI	PbO	$PbTe$
EXP[73]		2.667	2.472	2.661	1.609	1.524	1.870	1.910	2.084	2.814	1.922	2.595
ZORA	GGC	2.719	2.511	2.685	1.628	1.535	1.900	1.951	2.119	2.858	1.937	2.633
SR ZORA	GGC	2.697	2.517	2.655	1.625	1.535	1.931	1.940	2.126	2.872	1.939	2.629
$\Delta^{so} r_e$	GGC	0.022	-0.006	0.030	0.003	0.000	-0.031	0.011	-0.013	-0.014	-0.002	0.004
ZORA	LDA	2.670	2.452	2.637	1.624	1.526	1.868	1.919	2.073	2.783	1.910	2.588
SR ZORA	LDA	2.651	2.457	2.613	1.621	1.525	1.901	1.908	2.081	2.798	1.913	2.586
$\Delta^{so} r_e$	LDA	0.019	-0.005	0.024	0.003	0.001	-0.033	0.011	-0.008	-0.015	-0.003	0.002

Table 7.10: Harmonic frequencies ω_e in cm^{-1} for some diatomic systems.

		I_2	Au_2	Bi_2	HI	AuH	TlH	IF	TlF	TlI	PbO	$PbTe$
EXP[73]		215	191	173	2309	2305	1391	610	477	(150)	721	212
ZORA	GGC	197	178	174	2240	2270	1330	570	455	142	720	204
SR ZORA	GGC	210	177	193	2260	2270	1320	595	450	142	730	212
$\Delta^{so} \omega_e$	GGC	-6%	1%	-10%	-1%	0%	1%	-4%	1%	0%	-1%	-4%
ZORA	LDA	214	198	186	2260	2330	1390	610	490	155	755	216
SR ZORA	LDA	226	196	203	2280	2330	1370	630	485	155	765	223
$\Delta^{so} \omega_e$	LDA	-5%	1%	-8%	-1%	0%	1%	-3%	1%	0%	-1%	-3%

Table 7.11: Molecular dissociation energies in eV with respect to spherically and spin averaged and for ZORA spin-orbit averaged atoms and difference Δ^{so} between the ZORA and SR ZORA result

		I_2	Au_2	Bi_2	HI	AuH	TlH	IF	TlF	TlI	PbO	$PbTe$
ZORA	GGC	2.62	2.71	6.52	4.71	4.52	3.96	4.31	6.37	4.14	8.23	5.74
SR ZORA	GGC	2.51	2.65	5.42	4.68	4.48	3.84	4.21	6.37	4.04	8.08	5.38
Δ^{so}	GGC	0.11	0.06	1.10	0.03	0.04	0.12	0.10	0.00	0.10	0.15	0.36
ZORA	LDA	3.07	3.29	7.11	4.99	4.87	4.12	4.85	6.83	4.53	8.88	6.28
SR ZORA	LDA	2.96	3.22	6.00	4.96	4.83	3.97	4.75	6.83	4.41	8.72	5.91
Δ^{so}	LDA	0.11	0.07	1.11	0.03	0.04	0.15	0.10	0.00	0.12	0.16	0.37

Table 7.12: Molecular dissociation energies D_e in eV for some diatomic systems

		I_2	Au_2	Bi_2	HI	AuH	TlH	IF	TlF	TlI	PbO	$PbTe$
EXP[73]		1.56	2.31	2.03	3.20	3.36	2.06	2.92	4.60	2.77	3.87	2.57
ZORA	GGC	1.58	2.31	1.98	3.24	3.37	2.10	3.05	4.72	2.71	4.15	2.54
SR ZORA	GGC	2.13	2.25	2.74	3.54	3.33	2.66	3.30	5.42	3.62	5.51	4.06
ZORA	LDA	2.17	2.99	2.83	3.64	3.82	2.39	3.97	5.57	3.25	5.25	3.32
SR ZORA	LDA	2.74	2.92	3.80	3.95	3.78	2.94	4.23	6.29	4.17	6.66	4.91

these orbitals is smaller. For Bi_2 the bonding and anti-bonding orbitals will become closer in energy if we increase the distance between the atoms. Thus spin-orbit coupling will in this case have an increasing effect on the bond length and a flattening effect on the bonding curve.
For the iodine molecule I_2 we can use figure 7.2 if we also fully occupy the antibonding π_g-orbital. Now we only have to consider the off-diagonal spin-orbit interaction between the occupied bonding $\pi_{1/2u}$-orbital and the unoccupied anti-bonding $\sigma_{1/2u}$-orbital. Like for Bi_2 the spin-orbit effect will increase, if we enlargen the distance between the atoms, since the bonding and anti-bonding orbitals come closer in energy.
For the gold dimer Au_2 the spin-orbit effect is small, since the bonding effect is mainly due to the atomic $6s$-orbitals, which are not affected by spin-orbit coupling. The remaining small effect comes from the fact that the bonding orbitals have some atomic $6p$ and some extra $6s$ character at the cost of atomic $5d$ character, such that spin-orbit coupling can have some effect. At larger distances between the gold atoms there is less $6p$-mixing, which reduces the spin-orbit effect, and consequently diminishing the spin-orbit stabilisation. Therefore spin-orbit coupling will slightly shorten the bond length of Au_2 and increase its binding energy and harmonic frequency.

We now turn to the hetero-nuclear compounds. Again the net first order effect of spin-orbit coupling for these closed shell compounds is zero. The off-diagonal spin-orbit interaction between two orbitals only can become large if they have atomic character belonging to the same atom with the same l-value ($l \neq 0$) and there is only a net effect if there is off-diagonal spin-orbit interaction between occupied and unoccupied orbitals.
For TlF, TlI, PbO and $PbTe$, we have the same levels and occupation, coming from the valence atomic p-orbitals, as in figure 7.2, except that they are not labelled by g or u anymore. This means that there are now more possibilities for off-diagonal spin-orbit interaction than in the homonuclear case. The relative position of the levels of the occupied bonding π- and σ-orbital may be reversed for some of these compounds compared to position they have in figure 7.2, the unoccupied antibonding π- and σ-orbital are always at the same relative position as in figure 7.2. For TlF, TlI, PbO and $PbTe$, the occupied bonding orbitals have more character of the lighter element, whereas the unoccupied anti-bonding orbitals have more Tl or Pb character. If the distance between the atoms is increased, close to the bond length, the occupied bonding orbitals will even be more biased towards the more electronegative element. Due to this effect the off-diagonal spin-orbit interaction is smaller at longer distances. This first effect of increasing the distance is larger if the difference in electronegativity of the two atoms is larger, like in TlF and TlI. A second effect of increasing the distance between the atoms, close to the bond length, is that the bonding and anti-bonding orbitals will be closer in energy, which will increase the effect of the off-diagonal spin-orbit interaction. For PbO and $PbTe$ there is some competition between these two effects, such that the spin-orbit effect on the bond distance is small. For TlF and TlI the first effect is dominating and spin-orbit coupling shortens the bond distance. The spin-orbit effect on the energy of these four compounds is largest for $PbTe$, since both lead and tellurium have a large effective spin-orbit parameter and the difference in electronegativity is the smallest for these atoms.
Compared to the previous compounds IF also has a fully occupied anti-bonding π-orbital. The off-diagonal spin-orbit interaction will be largest between the occupied anti-bonding $\pi_{1/2}$-orbital and the unoccupied anti-bonding $\sigma_{1/2}$, which both have more iodine than fluorine character. The two spin-orbit effects, which result from an increase in the distance between the atoms, are now in the same direction and will lengthen the bond distance.
In figure 7.3 schematically the one-electron molecular orbital levels of TlH coming from the $1s$-orbital of hydrogen and the $6p$-orbital of thallium are shown. The bonding σ-orbital has more hydrogen character. The energy of the non-bonding thallium π-orbital will not change much if we increase the distance. In this case the first effect is dominating, and spin-orbit coupling will shorten the bond length. For HI we can use figure 7.3 if we also fully occupy the π-orbital. Like in IF the first effect of the spin-orbit interaction will lengthen the bond distance. For AuH the spin-orbit effect is small, since the bonding effect is mainly due to atomic s-orbitals, which are not affected by spin-orbit coupling. The bonding orbital also has almost no gold $6p$ character, which was responsible for a part of the effect in Au_2.

Compared to experiment the ZORA GGC results are too long between 0.011 Å for AuH and 0.044 Å for TlI. The SR ZORA GGC results lie between -0.006 for Bi_2 and +0.061 for TlH. The spin-orbit calculated results seem to give a more consistent deviation from experiment than the scalar relativistic results, especially for the compounds where the spin-orbit ef-

fect has its largest effect, namely Bi_2 and TlH. The theoretical ZORA LDA results deviate from experiment between -0.031 Å for TlI and +0.015 for HI. For the SR ZORA result this is between -0.048 Å for Bi_2 and +0.031 for TlH.
For the harmonic frequencies we can do the same analysis. For most of these diatomics an increase in bond length due to spin-orbit coupling means a flattening effect on the bonding curve and vica versa. The flattening of the curve due to spin-orbit coupling can be quite large, especially for Bi_2, and to a lesser extent for I_2, IF and $PbTe$. Again, the deviation compared to experiment of the scalar relativistic result for Bi_2 is somewhat out of line compared to the other compounds, whereas the spin-orbit calculated result is consistent.
In order to identify the genuinely molecular spin-orbit effect we present in table 7.11 ZORA molecular energies minus spin-orbit averaged, and therefore also spherically and spin averaged, atoms and SR ZORA molecular energies minus spherically and spin averaged atoms. In this table we can see the consequence of the fact that in first order the molecular spin-orbit effect is zero for these closed shell compounds.. In most cases this molecular spin-orbit effect is less than 0.15 eV. However, it can be much larger: for $PbTe$ it is 0.36 eV and for Bi_2 it is even 1.1 eV. From the atomic results one could have expected much more effect for the compounds containing Te, I, Tl, Pb or Bi. As explained before the net off-diagonal spin-orbit effect is zero between fully occupied orbitals. If we take for example TlI in the situation that one electron is completely on the iodine we have Tl^+ and I^-, which are both closed shell systems with almost no spin-orbit effect. The relatively large effect on the energy for Bi_2 can be understood, considering the large effective spin-orbit parameter of of bismuth, and the fact that the diagonal spin-orbit effect on the $\pi_{1/2g}$-orbital pushes its energy towards the $\sigma_{1/2g}$ such that off-diagonal spin-orbit coupling has large effects.
In table 7.12 the molecular dissociation energies are shown where in the SR ZORA case this is done with respect to the L-S coupled atoms, and in the ZORA case with respect to the intermediate coupled atoms. The correction terms were taken from table 7.6. The ZORA GGC calculations gives very accurate dissociation energies compared with experiment, the largest difference is 0.3 eV for PbO. The SR ZORA GGC results for Au_2 and AuH is accurate, since both the molecule and its fragments do not suffer from spin-orbit effects. For the other compounds the difference compared to experiment is larger, between 0.3 (HI) and 1.6 eV (PbO) too deep. The reason for this lies almost entirely in the spin-orbit effect of the atoms. If we would have calculated the atoms in intermediate coupling the results would improve considerably, an accuracy better than 0.2 eV except for $PbTe$ (deviation of 0.4 eV) and Bi_2 (deviation of 1.1 eV), which are exactly the same molecules which have a large molecular spin-orbit correction in the energies (see table 7.11). In figure 7.4 these results are shown in a form that makes it easier to see the atomic and molecular spin-orbit effects on the dissociation energy.
The ZORA LDA results are 0.3-1.4 eV too deep compared to experiment.

Table 7.13: Comparison with results from correlated relativistic calculations using ECP's, where the SO effect is calculated, for I_2 [92], for Bi_2 [93], for HI and TlH [94]

	I_2	Bi_2	HI	TlH
r_e (Å)				
SO	2.77	2.768	1.616	1.925
SR	2.75	2.734	1.614	1.953
ω_e (cm^{-1})				
SO	185	153	2331	1329
SR	199	165	2340	1310
D_e (eV)				
SO	0.76	1.49	2.88	2.32
SR	1.43		3.15	2.41

In table 7.13 we have collected some results from the literature, where calculations, using spin-orbit coupling, are compared with scalar relativistic calculations. The spin-orbit effect for the bond distance and harmonic frequencies are in close agreement to our findings. The spin-orbit effects on the dissociation energy (compared to the results given in table 7.12) are not so close, which we will discuss below. Schwerdtfeger et al. [103] calculated the spin-orbit effects for I_2 and HI. They calculate an increase in bondlength for I_2 of 0.015 and for HI 0.003 Å due to spin-orbit coupling, compared to respectively 0.02 and 0.003 Å from our calculations. The spin-orbit effect in the dissociation energy they calculated for HI 0.06 and for I_2 0.14 eV, which can be compared with respectively 0.03 and 0.11 eV from our calculations. Teichteil and Pélissier [92], who find less than 0.01 eV for the spin-orbit effect on I_2, criticize the results obtained by Schwerdtfeger et al. [103], since Schwerdtfeger et al. use a j-j coupling scheme for the molecule, whereas Teichteil and Pélissier used intermediate coupling. Note that we only use intermediate coupling for open shell systems, since the used

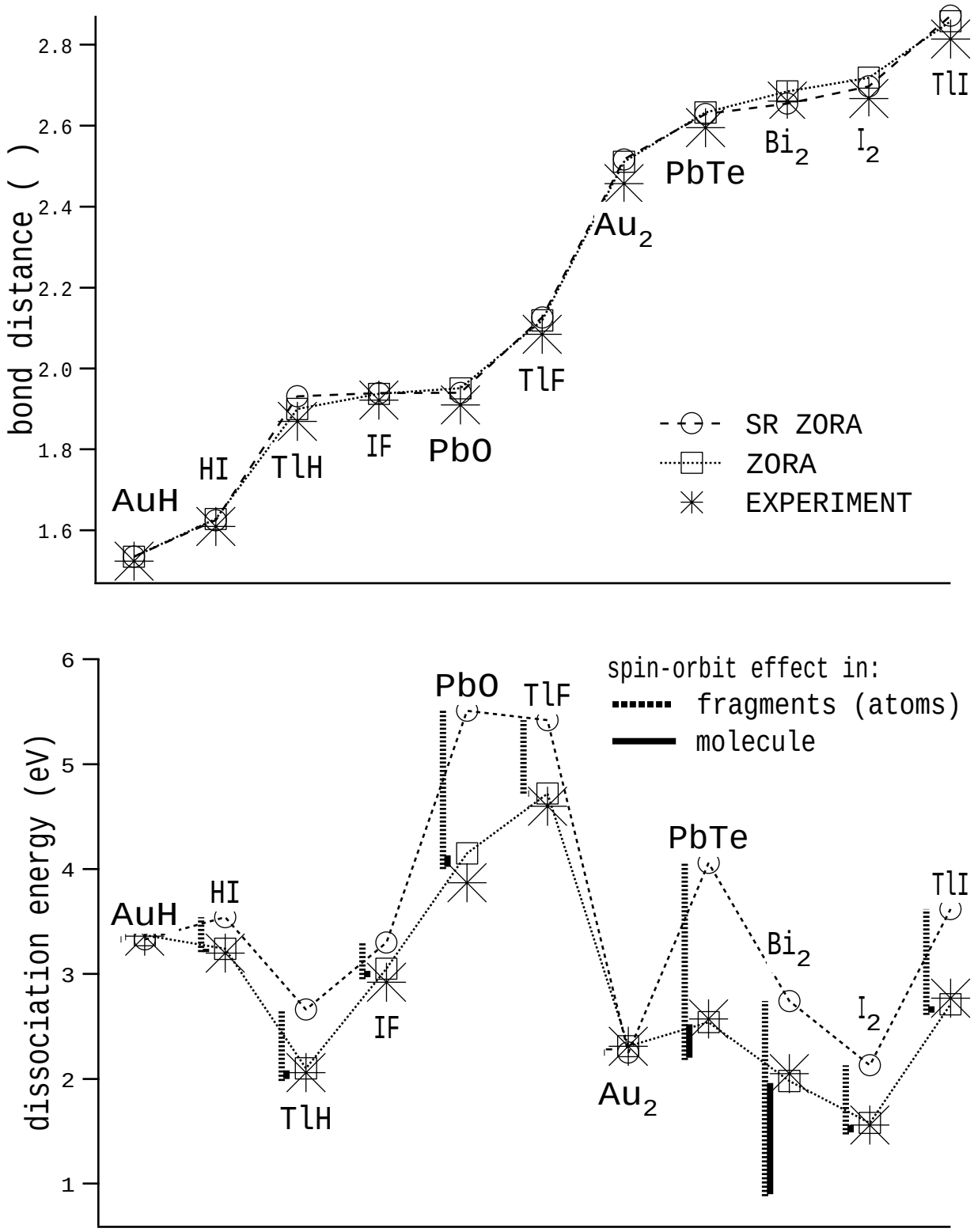

Figure 7.4: Bond distance and dissociation energies for some diatomic systems from all-electron (SR) ZORA GGC calculations.

Table 7.14: Selection of results taken from the literature for the bond length r_e, harmonic frequency ω_e and dissociation energy D_e for some diatomics compared to our ZORA GGC results.

	I_2	Au_2	HI	AuH	IF	TlF	PbO
r_e (Å)							
EXP[73]	2.667	2.472	1.609	1.524	1.910	2.084	1.922
ZORA GGC	2.719	2.511	1.628	1.535	1.951	2.119	1.937
	2.73 [95]	2.537 [71]	1.598 [96]	1.525 [97]	1.916 [98]	2.04 [99]	1.893 [100]
	2.71 [95]	2.466 [82]	1.601 [101]	1.505 [82]	1.944 [98]		1.882 [102]
	2.690 [98]		1.615 [98]				
	2.711 [98]		1.626 [98]				
ω_e (cm^{-1})							
EXP[73]	215	191	2309	2305	610	477	721
ZORA GGC	197	178	2240	2270	570	455	720
	205 [95]	178 [71]	2354 [96]	2288 [97]	621 [98]	592 [99]	785 [100]
	214 [95]	195 [82]	2410 [101]	2619 [82]	624 [98]		800 [102]
			2334 [98]				
			2309 [98]				
D_e (eV)							
EXP[73]	1.56	2.31	3.20	3.36	2.92	4.60	3.87
ZORA GGC	1.58	2.31	3.24	3.37	3.05	4.72	4.15
	1.49 [95]	2.12 [71]	2.03 [101]	2.92 [97]		3.86 [99]	1.3 [102]
	1.69 [95]	2.88 [82]	3.09 [98]	3.75 [82]			3.5-3.8 [102]
	1.43 [98]		2.99 [98]				
	1.42 [98]						

approximate density functionals are not suitable for j-j coupling in the open shell case. We do not have an explanation for the discrepancy in the results on the spin-orbit effect on the dissociation energy of TlH.

In table 7.14 we have selected some results from the literature for some of the compounds. Dirac-Fock calculations were performed by Matsuoka (et al.) [101, 102] on HI and PbO. For PbO they also calculated the dissociation energy using density functionals for correlation. Dyall [100] also reported on Dirac-Fock calculations on PbO. The Douglas-Kroll transformation, in the scalar relativistic approximation, was used in coupled cluster calculations on AuH by Kaldor and Hess [97], and in LDA calculations on Au_2 and AuH by Häberlen and Rösch [82]. Relativistic ECP's including spin-orbit coupling were used by Balasubramanian [99] in correlated calculations on TlF. The other results come from scalar relativistic ECP calculations including correlation. A general conclusion, which most of these references make, is that since relativistic effects and correlation effects are not additive, one should include correlation in relativistic calculations on systems containing heavy elements.

In table 7.15 we compare ZORA and SR ZORA for the dipole moments for the heterogenic diatomics at the experimental geometry. In the GGC results we have used the GGC potential in selfconsistent calculations. Note that for the dissociation energy we find differences in energy less than 0.01 eV compared to the procedure, where the LDA potential is used and afterwards GGC correction terms were calculated. For hydrogen, oxygen, fluorine and gold the spin-orbit effect may be neglected. To remove an electron from thallium and lead will cost more energy in the spin-orbit case than in the scalar relativistic case. In the same way in the spin-orbit case, the gain in energy is less if we add an electron to tellurium or iodine, and it is less expensive to remove an electron from iodine than in the scalar relativistic case. With this in mind we can understand the spin-orbit effects on the dipole moments for these compounds: almost no effect for AuH, a lowering effect for HI, TlH, TlF, TlI, PbO and $PbTe$ and an increasing effect on IF. One can also use look at the one-electron molecular orbital levels coming from the valence atomic orbitals, as we did before. The first order effect of the spin-orbit interaction does not give a different density. For TlF, TlI, PbO and $PbTe$ off-diagonal spin-orbit interaction can only mix

Table 7.15: Dipole moments μ_e in Debye for some diatomic systems at the experimental geometry. Positive values mean A^+B^-.

		HI	AuH	TlH	IF	TlF	TlI	PbO	$PbTe$
EXP[73]		0.45			1.95	4.23	4.61	4.64	2.73
ZORA	GGC	0.41	1.08	1.15	1.77	3.74	3.74	4.28	2.71
SR ZORA	GGC	0.43	1.08	1.40	1.71	3.88	4.17	4.44	3.01
$\Delta^{so}\mu_e$	GGC	-0.02	-0.00	-0.25	0.06	-0.06	-0.43	-0.16	-0.30
ZORA	LDA	0.49	0.95	1.00	1.85	3.78	3.63	4.29	2.61
SR ZORA	LDA	0.51	0.95	1.28	1.78	3.91	4.07	4.46	2.91
$\Delta^{so}\mu_e$	LDA	-0.02	-0.00	-0.28	0.07	-0.07	-0.44	-0.17	-0.30

Table 7.16: Dipole moments μ_e in Debye for some diatomic systems at the (SR) ZORA geometry from table 7.9.

		HI	AuH	TlH	IF	TlF	TlI	PbO	$PbTe$
EXP[73]		0.45			1.95	4.23	4.61	4.64	2.73
ZORA	GGC	0.41	1.08	1.28	1.94	3.97	4.01	4.35	2.85
SR ZORA	GGC	0.43	1.09	1.69	1.83	4.16	4.54	4.53	3.14
$\Delta^{so}\mu_e$	GGC	-0.02	-0.01	-0.41	0.11	-0.19	-0.53	-0.18	-0.29

Table 7.17: Results taken from the literature for dipole moments μ_e in Debye for some diatomic systems. Positive values mean A^+B^-.

	HI	AuH	TlH	TlI	PbO	$PbTe$
EXP[73]	0.45			4.61	4.64	2.73
	0.460 [104]	2.04 [105]	0.77 [105]	4.85 [105]	4.52-4.70 [106]	3.22 [105]
	0.40 [96]	1.58 [107]			3.74 [108]	2.67 [108]
		1.16 [82]			5.389 [100]	

in orbitals, which have more character on Tl or Pb. For IF the main off-diagonal spin-orbit interaction is between an occupied anti-bonding $\pi_{1/2}$-orbital and an unoccupied anti-bonding $\sigma_{1/2}$-orbital. The anti-bonding $\pi_{1/2}$-orbital has more iodine character than the anti-bonding $\sigma_{1/2}$-orbital, thus the spin-orbit effect decreases the charge on iodine. In TlH the unoccupied thallium $\pi_{1/2}$-orbital of fig 7.3 will mix in with the occupied bonding $\sigma_{1/2}$-orbital and in HI the occupied iodine $\pi_{1/2}$-orbital will mix with the unoccupied anti-bonding $\sigma_{1/2}$-orbital, which explains the observed spin-orbit effects.

In ref. [109] the spin-orbit effect on the dipole moment for HI was calculated using correlated relativistic ECP's, At the experimental geometry they find it to be -0.019 Debye, which is the same as we have found. Dolg et al. [106] estimated the spin-orbit correction for PbO to be between -0.07 and -0.23 Debye, our theoretical result -0.16 lies in this range.
Compared to experiment the ZORA GGC and SR ZORA GGC results have an average deviation of about 10%. In table 7.16 we also have calculated the dipole moments for the same systems at the theoretical (SR) ZORA geometry of table 7.9. The deviations from experiment are reduced. Except for IF and $PbTe$ the scalar relativistic results are closer to the (known) experimental values than the spin-orbit results, with an average deviation of approximately 5% for SR ZORA GGC and 7% for ZORA GGC.
In table 7.17 we give some results for the calculation of the dipole moment taken from the literature. Ref. [105] used Dirac-Fock calculations, except for AuH, where correlation effects were included. Dyall [100] also used Dirac-Fock calculations for PbO. The only relativistic LDA results in the table are from Häberlen et al.[82] for AuH. Their result for AuH is much closer to our result than the other two. The remaining results in this table come from calculations using relativistic ECP's.

7.4 Conclusions

In the last sections we have shown what the spin-orbit effects are in closed shell molecules. For the calculated compounds the spin-orbit effect on the bond distance never exceeded 0.03 Å, and on frequencies less than 10%. Also the molecular spin-orbit effect on the energies is often small, except for Bi_2 and $PbTe$. To obtain the spin-orbit effects in the dissociation energy it is also important to look at the effect on the constituent atomic fragments. It is shown that it is necessary to include spin-orbit effects for open shell atoms, since they can be very large. A method is proposed for open shell atoms, which uses present day density functionals in an intermediate coupling scheme. This method is used for the calculation of some atomic multiplet splittings and it is shown to give realistic energy differences. Using these intermediate coupled atomic energies for the calculation of the dissociation energies for the compounds under study, we obtain high accuracy if we include gradient correction (GGC) terms in the energy. The ZORA GGC results are then all within 0.3 eV of the experiment, with an average deviation of 0.1 eV for these compounds. For most compounds this accuracy in energy can be obtained, by only reckoning with spin-orbit effects in the atoms, except for Bi_2 and $PbTe$. For these compounds it is shown that, to obtain high accuracy, it is also necessary to take spin-orbit effects for the molecular energy into account. Except for these energies, in most cases the molecular spin-orbit effects are in the order of the accuracy of the calculations compared to experiment. The theoretical calculated dipole moments at the experimental geometry are still off by approximately 10% compared to the known experimental results in both the spin-orbit and scalar relativistic case.

Chapter 8

Elimination of the small component

In this chapter we will solve the Dirac equation by solving the two-component energy-dependent equation for the large component that results from the elimination of the small component. This requires for every occupied orbital the diagonalisation of a Hamiltonian. Advantages are, however, that these Hamiltonians are all bounded from below, unlike the Dirac Hamiltonian, and that only a basis set for the large component is needed. In this chapter we will use Dirac type Slater orbitals, adapted from solutions to the hydrogen-like atom. This offers the perspective of performing relativistic calculations to the same accuracy as non-relativistic ones, with a comparable number of basis functions.

8.1 Introduction

Traditional relativistic basis set methods (examples can be found in [51, 110, 111, 112, 113] and more recently in [114, 115, 116, 117]) use the four-component Dirac Hamiltonian and need a basis set for the large and the small component. In this chapter we will solve the Dirac equation, using the well known method of elimination of the small component (esc). In our approach the matrix elements of the resulting energy dependent Hamiltonian for the large component are calculated directly, which means we only need a large component basis set and kinetic balance problems never arise. Another possibility is to use an auxiliary basis set for the small component, as done by Wood et al. [118], and to evaluate the matrix elements of the large component Hamiltonian as matrix products. In that case, however, the same kinetic balance problems occur as in four-component methods and much of the advantage of the esc method is lost. It is however easy to calculate the energy-dependent matrix elements directly in a numerical integration scheme [45] when we have a simple local potential. This is the situation in density functional calculations, where numerical integrations are widely employed in nonrelativistic calculations as well. A disadvantage is that the present procedure is already iterative on the one-electron level since the orbital energies are not known beforehand, as was already observed by Aerts [119]. However, this is not a real disadvantage in selfconsistent field procedures, because one can optimise the potential and the orbital energies at the same time. It remains a disadvantage of course that the energy dependent equation has to be solved for every occupied orbital separately.
The Hamiltonians used in this approach are all bounded from below, unlike the Dirac Hamiltonian. For the hydrogen-like atom it was shown [120] that in a finite basis set this procedure gives convergence from above, with increasing number of basis functions, to the exact Dirac eigenvalue. We will show that it is economical to use as basis functions Dirac type Slater functions (DTO's). Working with the large component only and employing the efficient DTO's enables one to performe relativistic calculations to the same accuracy as non-relativistic ones, with a comparable number of basis functions.
The scaled zeroth order regular approximation (scaled ZORA) to the Dirac equation is known to give very accurate deep core and valence orbital energies [121, 74]. For other properties than the energy, the accuracy is high for (sub-) valence orbitals [34] but less so for deep core orbitals. However, if one starts with the converged potential of the ZORA method one obtains after 1 cycle (called FCPD-4 in [34]) already very accurate properties also for the deep core orbitals. If even higher accuracy is required, one may use the method presented in this chapter, which can be thought of as a natural extension of the ZORA approach to all orders. Further (dis-)advantages of this method will be explained in section 8.3. Results using an efficient basis set are presented in section 8.4.

8.2 Solving the large component equation

We can write the total energy of a many-electron system in a relativistic density functional approach (without the interaction energy of the nuclei) as:

$$E_{TOT}^{Dirac} = E_{KIN} + \int d1 \rho V_N + E_C + E_{XC}[\rho] \quad (8.1)$$

where:

$$E_{KIN} =$$

$$\sum_{i=1}^{N} \int d1 (\phi_i^\dagger c\vec{\sigma} \cdot \vec{p} \chi_i + \chi_i^\dagger c\vec{\sigma} \cdot \vec{p} \phi_i - 2c^2 \chi_i^\dagger \chi_i)$$

$$E_C = \frac{1}{2} \int \int d1 d2 \frac{\rho(1)\rho(2)}{r_{12}}$$

$$\rho = \sum_{i=1}^{N} (\phi_i^\dagger \phi_i + \chi_i^\dagger \chi_i) \quad (8.2)$$

and E_{XC} is the exchange-correlation energy density functional, which in this chapter will be approximated with the simple Slater exchange approximation ($\alpha = 0.7$). For the electron-electron repulsion the non-relativistic operator is used. The Kohn-Sham formulation of density functional theory leads to the one-electron Dirac equations:

$$\begin{pmatrix} V & c\vec{\sigma} \cdot \vec{p} \\ c\vec{\sigma} \cdot \vec{p} & -2c^2 + V \end{pmatrix} \begin{pmatrix} \phi_i \\ \chi_i \end{pmatrix} = \epsilon_i \begin{pmatrix} \phi_i \\ \chi_i \end{pmatrix} \quad (8.3)$$

where the Kohn-Sham one-electron potential is given by:

$$V(\vec{r}_1) = V_N(\vec{r}_1) + \int \frac{\rho(2)}{r_{12}} d\vec{r}_2 + \frac{\delta E_{XC}[\rho]}{\delta \rho(\vec{r}_1)} \quad (8.4)$$

In a four-component relativistic basis set calculation one can diagonalise this one-electron full Dirac Hamiltonian. In that case the small component basis set has to be chosen with care in order to avoid kinetic balance failure. The solutions to the one-electron equations can be obtained self-consistently, where the orbitals with the lowest positive energies (eigenvalue $+ c^2$) are occupied. Because of the fact that the Dirac Hamiltonian is not bounded from below, there will also be negative energy solutions, which are not of interest to us but may cause complications.
An alternative procedure is to eliminate the small component χ:

$$\chi_i = \frac{c}{2c^2 + E_i - V} \vec{\sigma} \cdot \vec{p} \phi_i \quad (8.5)$$

to obtain the Hamiltonian H^{esc}, which is energy dependent and works solely on the large component ϕ:

$$H^{esc}\phi_i = (V + \vec{\sigma} \cdot \vec{p} \frac{c^2}{2c^2 + \epsilon_i - V} \vec{\sigma} \cdot \vec{p}) \phi_i = \epsilon_i \phi_i \quad (8.6)$$

We can solve this two-component equation self-consistently in a basis set calculation using only a basis set for the large component, which is a great advantage compared to the four-component calculations. In order to calculate the matrix elements by numerical integration we need in each grid point the density and the Coulomb and exchange-correlation potentials. In order to obtain the density the small component is needed, for which equation 8.5 can be used. In the atomic calculations we performed, the density is calculated in every point of the radial grid. In the essentially one-dimensional atomic problem the potentials can be calculated easily at the grid points from this numerical density. Although we will restrict ourselves to applications to atoms, it should be pointed out that application to molecules is straightforward, at least if numerical integration is used. Once the density has been obtained in all grid points of the molecular integration grid, the Coulomb potential can be calculated in a routine manner, e.g. by using a fit of the density [122] or by solving the Poisson equation numerically [123].
The energy dependent eigenvalue equation is solved iteratively, but apart from the density (or equivalently the potential) also the eigenvalues have to be iterated to self-consistency. This means that on every cycle we have to perform a diagionalisation for every different eigenvalue. Suppose that we have after $N-1$ cycles a potential V^{N-1} and eigenvalues ϵ_j^{N-1}. In the next cycle we have to diagonalise for every j corresponding to an occupied orbital the Hamiltonian H_j^{N-1}:

$$H_j^{N-1} = V^{N-1} + \vec{\sigma} \cdot \vec{p} \frac{c^2}{2c^2 + \epsilon_j^{N-1} - V^{N-1}} \vec{\sigma} \cdot \vec{p} \quad (8.7)$$

If ϵ_j^{N-1} is the j'th energy of a given symmetry, we have to choose the eigenvalue and density of the j'th eigenfunction for the next cycle. In the case of the $s_{1/2}$-symmetry of the neutral Uranium atom it means that one has to diagonalise on every cycle seven times in this symmetry, because there are seven occupied $s_{1/2}$ orbitals. This is a disadvantage of this method compared to four-component calculations, where only one diagonalisation has to be performed on each cycle. In figure 8.1 the procedure is presented in a pictorial way. For each Hamiltonian only the bold eigenvalues and the corresponding orbitals are of interest.

Figure 8.1: Spectra of the Hamiltonians $H_i(E_i)$ corresponding to orbitals i with increasing orbital energies E_i

8.3 (Dis-) advantages of the present method

An advantage of the present method is that the two-component esc Hamiltonian is variational. We will now closely follow the arguments of Hegarty [120]. The expectation value for a normalised arbitrary two-component square-integrable function Ψ, under the usual boundary conditions for physical bound states, was defined in ref [120] as:

$$f(\epsilon) = \langle\Psi|H^{esc}(\epsilon)|\Psi\rangle|_D \tag{8.8}$$

where the ϵ was restricted to domain D:

$$D = \{\epsilon|\epsilon \geq -2c^2\} \tag{8.9}$$

In [120] for the hydrogen-like atom it was proven that:

$$f(\epsilon) \text{ is finite and continuous on D}$$

$$f(\epsilon + \Delta) < f(\epsilon) \qquad (\Delta > 0)$$

$$\lim_{\epsilon\to\infty}[f(\epsilon) - f(\epsilon + \Delta)] = 0 \qquad (\Delta \text{ finite})$$

$$f(\epsilon = -2c^2) > 0 \qquad (Z \leq c) \tag{8.10}$$

and consequently the solution of:

$$\epsilon = f(\epsilon) \tag{8.11}$$

exists and is unique. An additional, but not severe, constraint on Ψ was needed:

$$\lim_{r\to\infty}(r^3\Psi^\dagger(d/dr)\Psi) = 0 \tag{8.12}$$

In figure 8.1 the second condition of equation 8.10 is nicely illustrated. Because of the properties in equation 8.10 it followed that in a finite basis set the procedure gives convergence from above to the exact Dirac eigenvalue, with increasing number of basis functions, which satisfy the same boundary conditions as Ψ, under the usual assumption that the basis set approaches completeness with increasing number of basis functions.
In this chapter we use a relativistic density functional approach, such that the one-particle equations are Dirac equations in a local potential. Now suppose this local potential is given by

$$V = -\frac{Z}{r} + V_1(r) \tag{8.13}$$

where $V_1(r) > 0$ and $V(r) < 0$ everywhere. This V_1 will usually be the mean repulsive potential of some electron density. It is easy to see that the first three properties of equation 8.10 still are satisfied. Now we can use similar arguments as in ref [124] to show that the fourth condition is also satisfied. We can divide H^{esc} in different operators:

$$H^{esc} = -\frac{Z}{r} + V_1 + \vec{\sigma}\cdot\vec{p}\frac{c^2}{2c^2 + \epsilon + \frac{Z}{r} - V_1}\vec{\sigma}\cdot\vec{p} =$$

$$= -\frac{Z}{r} + \vec{\sigma}\cdot\vec{p}\frac{c^2}{2c^2 + \epsilon + \frac{Z}{r}}\vec{\sigma}\cdot\vec{p} + V_1 +$$

$$\vec{\sigma}\cdot\vec{p}\frac{c^2V_1}{(2c^2 + \epsilon + \frac{Z}{r})(2c^2 + \epsilon + \frac{Z}{r} - V_1)}\vec{\sigma}\cdot\vec{p} \tag{8.14}$$

For $f(\epsilon)$ the first two parts are the same as for the hydrogen-like atom and the last two parts are positive because V_1 is positive and the total potential V is negative. Thus for this potential the fourth property of equation 8.10 is also true and the same conclusions as for the hydrogen-like atom may be drawn. Although this is not conclusive proof that this holds during each cycle of a self-consistent field method, in practical calculations on the neutral Uranium atom convergence was reached, without problems of collapsing into the negative energy continuum.

In the present method we only need to calculate matrix elements for the large component. The matrix elements can easily be calculated using numerical integration schemes [45]. In general in four-component basis set methods one needs at least as many, usually more, basis functions for the small component as for the large component, because of the kinetic balance condition [53]. This will lead to a larger diagonalisation problem than in the present method, but here one has to diagonalise for every different eigenvalue of the occupied spectrum. If the number of different occupied orbitals per symmetry is small the present method can be competitive in computational time with respect to four-component methods. Some diagonalisation procedures can make use of the fact that one only needs one eigenfunction and eigenvalue per diagonalisation. One may also think of ways to decrease the number of diagonalisations per cycle. For example one can freeze the core and converge the valence orbitals and then freeze the valence and converge the core orbitals, etcetera.
It is possible to reduce the number of cycles if one starts with an accurate initial potential. For example one can use the solution of the zeroth order regular approximation (ZORA) [121] to the Dirac equation. Matrix elements can be calculated in the present method in practically the same way as in the ZORA method. One of the differences is that in the present method one also has to use the small component density for the calculation of the potential. The small component density can be generated in points of the integration grid using eq. 8.5, without the need of introducing a small component basis set. Implementation of the present method is therefore straightforward, once one has implemented the ZORA method. It is thus perfectly feasible to first converge a ZORA calculation, and subsequently continue with the present method if one wishes to obtain results identical to full Dirac calculations. In the next section we will show some calculations on the Uranium atom which use the converged ZORA result for the start-up potential.
The present method can of course also be used to find solutions of the scalar relativistic equation [41, 42]:

$$H^{SR}\phi_i = (V + \mathbf{p}\frac{c^2}{2c^2 + E_i^{SR} - V}\mathbf{p})\phi_i$$

$$= E_i^{SR}\phi_i \tag{8.15}$$

This equation is analogous to the spin-free modified Dirac equation of ref [125, 33] after eliminating the lower component in that equation.

8.4 Basis set selection and results

Even if the basis set problem is strongly reduced by eliminating the small component, one may still be forced to use more basis functions than in a comparable nonrelativistic calculation because of the weak singularity at the nucleus of the relativistic solutions. An example is provided by the ZORA calculations of ref. [121]. In the STO basis set 6 basis functions were used to describe the $1s_{1/2}$- and $2p_{1/2}$-orbital, yielding an accuracy of about 0.2 a.u. in the deep core eigenvalues. Such a large number of STO's are needed, because the weak singularity at the nucleus is difficult to desribe with Slater type functions.
In order to solve this problem we have employed in the present work Dirac type Slater orbitals (DTO's), which are of the form:

$$r^{\eta-1}e^{-\zeta r} \tag{8.16}$$

where η does not have to be an integer value. The ζ's were optimised by a least squares fit to numerical orbitals. For the lowest DTO in a given symmetry we also optimised η. For the other η's it turned out not to be very critical whether one chooses integer or non-integer values. We chose them in each symmetry by a linear scaling procedure, such that the highest η is equal to the n of the valence level of a given symmetry (see table 8.1). Dirac type Slater orbitals were for example used by Drake and Goldman [126] in four-component Dirac calculations on the hydrogen-like atom. Dirac type Slater orbitals are the natural choice for relativistic calculations on atoms, in the same way as STO's are for nonrelativistic calculations, because the solutions to the hydrogen-like atom with a point charge nucleus have this form. Using DTO's one can easily fulfil the correct boundary conditions at the nucleus. Especially for the $s_{1/2}$- and $p_{1/2}$-symmetry one needs much fewer DTO's to obtain the same accuracy than one needs STO's or Gaussian type orbitals (GTO's). We tested our implementation of DTO basis sets on the problem of one electron in a hydrogen-like potential, using DTO's which could reproduce the exact solution. The exact eigenvalues and eigenfunctions were correctly obtained.

In table 8.1 we give our optimised DTO's in the case of a neutral Uranium atom with a point charge. In table 8.2 the calculated eigenvalues are given for some deep core levels and in table 8.3 for some valence levels using the DTO basis set of table 8.1. In table 8.4 the corresponding radial expectation values

Table 8.1: Optimised Dirac-type Slater exponents for all-electron Dirac-Slater calculations on Uranium

$s_{1/2}$		$p_{1/2}$		$p_{3/2}$		$d_{3/2}$		$d_{5/2}$		$f_{5/2}$		$f_{7/2}$	
η	ζ	η	ζ	η	ζ	η	ζ	η	ζ	η	ζ	η	ζ
0.741	150.00	0.741	62.856	1.369	79.000	2.609	31.164	2.887	37.769	3.627	17.646	3.687	17.797
0.741	92.000	1.728	53.906	1.639	42.806	3.000	25.153	2.939	25.943	3.678	11.233	3.759	11.328
1.845	82.915	1.732	42.712	2.058	38.256	3.000	19.721	2.920	19.483	4.000	7.848	4.000	7.796
1.810	48.535	2.264	25.196	2.551	22.210	3.500	13.480	3.433	12.950	4.333	4.368	4.333	4.221
2.300	43.173	2.797	23.350	3.043	16.700	4.000	10.302	3.947	9.948	4.667	2.430	4.667	2.293
2.665	25.134	3.331	15.693	3.536	15.580	4.500	6.646	4.460	6.410	5.000	1.247	5.000	1.138
3.146	19.745	3.865	12.590	4.029	11.650	5.000	4.581	4.973	4.411				
3.628	17.701	4.399	8.470	4.522	7.738	5.333	2.606	5.333	2.460				
4.110	13.476	4.932	6.324	5.014	5.686	5.667	1.514	5.667	1.405				
4.592	9.099	5.466	4.036	5.507	3.539	6.000	0.887	6.000	0.806				
5.073	6.893	6.000	2.696	6.000	2.307								
5.555	4.582												
6.037	3.188												
6.518	1.872												
7.000	1.171												

Table 8.2: Uranium orbital energies of some deep core levels in a.u., using the scaled ZORA method ("ZORA"), the present method after 1 cycle, starting with the converged ZORA result ("1 CYCLE"), and the present method after convergence ("ESC"), all in the DTO basis set. NUM DIRAC refers to a standard numerical atomic Dirac-Slater calculation.

		$1s_{1/2}$	$2s_{1/2}$	$2p_{1/2}$	$2p_{3/2}$	$3s_{1/2}$
DTO	ZORA	-4250.155	-794.285	-765.991	-625.581	-200.546
DTO	1 CYCLE	-4251.097	-794.324	-766.028	-625.605	-200.549
DTO	ESC	-4255.561	-795.008	-766.702	-625.957	-200.697
NUM	DIRAC	-4255.559	-795.009	-766.703	-625.961	-200.691

Table 8.3: Uranium orbital energies of some valence levels in a.u., for explanation see caption to table 8.2.

		$6s_{1/2}$	$6p_{1/2}$	$6p_{3/2}$	$5f_{5/2}$	$6d_{3/2}$	$7s_{1/2}$
DTO	ZORA	-1.7192	-1.0690	-0.7411	-0.1045	-0.0714	-0.1340
DTO	1 CYCLE	-1.7192	-1.0690	-0.7411	-0.1045	-0.0714	-0.1340
DTO	ESC	-1.7205	-1.0699	-0.7413	-0.1038	-0.0713	-0.1341
NUM	DIRAC	-1.7198	-1.0694	-0.7410	-0.1033	-0.0710	-0.1340

Table 8.4: Uranium radial expectation values $\langle r \rangle$ of some deep core and some valence levels in a.u., for explanation see caption to table 8.2.

	$1s_{1/2}$	$2s_{1/2}$	$2p_{1/2}$	$2p_{3/2}$	$3s_{1/2}$	$6s_{1/2}$	$6p_{1/2}$	$6p_{3/2}$	$5f_{5/2}$	$6d_{3/2}$	$7s_{1/2}$
DTO ZORA	.01206	.05524	.04475	.05498	.1463	1.473	1.651	1.898	1.486	3.237	4.120
DTO 1 CYCLE	.01365	.05653	.04579	.05601	.1472	1.473	1.651	1.898	1.486	3.237	4.120
DTO ESC	.01364	.05650	.04576	.05599	.1471	1.473	1.650	1.897	1.487	3.237	4.118
NUM DIRAC	.01364	.05650	.04576	.05599	.1471	1.473	1.650	1.897	1.486	3.237	4.114

Table 8.5: Uranium energies in a.u., using the esc equation in a STO and a DTO basis set and the numerical Dirac result

		E_{TOT}	$\sum \epsilon_i$	E_{XC}	E_C	$\int \rho V_N$	E_{KIN}
STO	ESC	-28080.51	-17757.57	-477.79	10482.20	-72552.94	34468.02
DTO	ESC	-28081.69	-17759.23	-477.74	10481.71	-72548.38	34462.72
NUM	DIRAC	-28081.76	-17759.07	-477.74	10481.95	-72549.55	34463.58

are given as an example of orbital properties. We may judge the basis set quality by comparing the DTO ESC results with the standard numerical (basis free) four-component Dirac (NUM DIRAC) results, to which they should be identical. The $\langle r \rangle$ expectation values have been obtained in the DTO ESC calculations by including the small component from eq. 8.5. We note that the DTO ESC results are in all cases very close to the numerical Dirac results, which demonstrates the feasibility of the present approach and at the same time shows that a DTO basis set can indeed be very useful in this kind of calculation. Table 8.5 contains various energy terms from both STO and DTO calculations, so one can judge the accuracy of the DTO and STO basis sets for the individual energy terms by comparing to the numerical Dirac reference values. In the DTO basis the accuracy is quite high, although the individual terms (notably the kinetic and nuclear attraction energies) exhibit somewhat stronger deviation than the total energy. The STO basis set is clearly somewhat less accurate, although it is considerably larger.

A similar conclusion can be drawn for the relative performance of DTO's and STO's for one-electron energies. In the current DTO basis set we get an accuracy of better than 0.01 a.u. in the deep core eigenvalues, as can be seen in table 8.2. This compares very favorably to the quoted 0.02 a.u. [121] for the STO basis. This improvement is achieved with only 2 basis functions for the $1s_{1/2}$-orbital and 3 for the $2p_{1/2}$-orbital, which is to be compared to the 6 basis functions for $1s$ and $2p$ in the STO basis. Only replacing in the STO basis set these six $1s$ STO's and six $2p$ STO's for the two resp. three corresponding DTO's already provided the major part of the improvement. [In the present work we also optimised, for consistency, all other DTO basis functions because in ref [121] the STO basis set was optimised to the ZORA orbitals instead of to the large components of the Dirac equation.] We conclude that a DTO basis set, in combination with the present ESC method, offers the perspective of performing relativistic calculations to the same accuracy as non-relativistic ones, with a comparable number of basis functions.

Given the reliability of the DTO basis set, we may compare the performance of the scaled ZORA approach (DTO ZORA [74], cf. CPD-4 in [34]) with the improvement obtained after performing one cycle with the present method using the converged ZORA potential as starting point (DTO 1 CYCLE) and with the fully converged ESC (or, equivalently, full Dirac) result. We observe again [121] that for valence levels the ZORA results are very close to Dirac results. They are so close that even the present accurate basis has errors of the same order of magnitude as the difference between ZORA and Dirac. For deep core orbitals the ZORA error is larger (see also [124]), at least for the $\langle r \rangle$ expection value. If one uses the converged ZORA potential as starting potential for the present method one obtains in the first cycle what is called FCPD-4 in ref [34]. In tables 8.2-8.4 we also show these results (DTO 1 CYCLE) in the same DTO basis set. It is clear that for deep core levels one does still improve upon the scaled ZORA results. For the $\langle r \rangle$ expection value of $1s_{1/2}$ the 1-cycle result is very close to the converged ESC (Dirac) result, see ref [34] for extensive discussion.

8.5 Conclusion

In this chapter we have solved the Dirac equation using only a large component basis set. The method of elimination of the small component has been used, resulting in an energy-dependent equation. In spite of the disadvantage of this method, that on every cycle for every occupied orbital a separate Hamiltonian has to be diagonalised, the method offers the clear advantages of being variationally stable [120], of requiring only modest size basis sets, and of being capable of reproducing the full Dirac result. If Dirac type orbitals (DTO's) are used instead of STO's or GTO's, the basis set size does not have to be any larger than in a nonrelativistic calculation. The DTO's are very efficient due to the fact that they have the right behaviour near the nucleus.

Further it is shown that this method can be very useful if one takes the solution of the scaled ZORA equation [121, 74, 34] as a starting point. If one wants to go beyond this already very accurate scaled ZORA approach, one may use the method of this chapter to calculate the full Dirac result. In fact, most of the time (e.g. for chemical purposes) one is probably already satisfied with the scaled ZORA approach, because it gives very accurate energies and (sub-) valence orbital properties. Only for deep core orbital properties (other than the energy) ZORA may not give enough accuracy, but the error is largely accounted for already after one cycle with the esc Hamiltonian (cf. also [34]). It is with the present method straightforward to converge to the Dirac answer, if desired.

Chapter 9

The exact Foldy-Wouthuysen transformation

In this chapter it is shown how within the framework of a basisset expansion method the exact (i.e. to all orders in the inverse velocity of light) Foldy-Wouthuysen transformation that separates the negative and positive energy spectrum of the Dirac equation, can be constructed for an arbitrary potential once the Dirac equation has been solved. On this basis an iterative procedure to solve the Dirac equation is suggested that involves only the large component. The methods are used to compare the expectation value of the radial distance operator in the Dirac picture and in the Schrödinger picture for the orbitals of the Uranium atom.

9.1 Introduction

As is well known [18] the non-relativistic limit of the Dirac equation for an electron in an external potential is not reached simply by letting the velocity of light go to infinity. Rather this limiting process entails a unitary transformation at the same time, which block diagonalizes the Dirac hamiltonian by separating the positive and negative energy part of its spectrum. This unitary transformation, known as the Foldy-Wouthuysen transformation, is equivalent to a change of picture and consequently in comparing relativistic and non-relativistic expectation values (other than the energy) one has to be aware that the same operator (such as the radial distance operator r in an atom) does not represent the same physical quantity in both pictures [127, 32]. Unfortunately this transformation is only known exactly a priori for a free particle. When an external potential is present, the transformation is usually determined by expanding in the inverse velocity of light to some finite order. In the case the potential is Coulombic in nature, however, this expansion is known to be highly problematic, leading to divergencies except in the lowest order. This does not mean that the transformation as such does not exist, only that it should not be expanded in this way. In this chapter we will show that it is quite possible to obtain this exact unitary transformation within the frame work of a basis set method without resorting to any perturbational expansion once the Dirac equation has been solved for its positive energy solutions.
In section 9.3 it is shown how on the basis of this method, one can in fact obtain the large components of the Dirac orbitals in a finite basis set approximation in an iterative way, without first solving the Dirac equation itself. This iterative procedure, which can also be used in self consistent field calculations, might be an alternative way to solve the Dirac equation that does not involve the small component. The methods are used to compare the expectation value of the radial distance operator in the Dirac picture and in the Schrödinger picture for the orbitals of the Uranium atom.

9.2 The exact Foldy-Wouthuysen transformation

The time-independent Dirac equation for an electron in an external potential V reads (in atomic units):

$$H^D \Psi_i^D \equiv \begin{pmatrix} V & c\vec{\sigma}\cdot\vec{p} \\ c\vec{\sigma}\cdot\vec{p} & V-2c^2 \end{pmatrix} \begin{pmatrix} \phi_i^D \\ \chi_i^D \end{pmatrix} =$$

$$E_i^D \begin{pmatrix} \phi_i^D \\ \chi_i^D \end{pmatrix} = E_i^D \Psi_i^D \tag{9.1}$$

Here Ψ^D is the four-component Dirac wave function and ϕ^D and χ^D are its large and small components.

The Dirac equation has positive and negative total energy solutions, while we are usually only interested in the positive energy part of the spectrum that describes electrons (rather than positrons). The exact Foldy-Wouthuysen transformation [18] decouples this four-component equation in two two-component equations, one of which has only positive energy eigenvalues and the other only negative ones. This transformation can be obtained in a rather simple form [30] by using a unitary matrix U:

$$U = \begin{pmatrix} \frac{1}{\sqrt{1+X^\dagger X}} & \frac{1}{\sqrt{1+X^\dagger X}} X^\dagger \\ -\frac{1}{\sqrt{1+XX^\dagger}} X & \frac{1}{\sqrt{1+XX^\dagger}} \end{pmatrix} \tag{9.2}$$

to transform the Dirac-Hamiltonian H_D. The transformed Hamitonian:

$$H = U H_D U^{-1} \tag{9.3}$$

is block-diagonal provided X satisfies:

$$-XV - Xc\vec{\sigma}\cdot\vec{p}X + c\vec{\sigma}\cdot\vec{p} + (V - 2c^2)X = 0 \tag{9.4}$$

The Foldy-Wouthuysen Hamiltonian H^{FW} is then given by:

$$H^{FW} = \frac{1}{\sqrt{1+X^\dagger X}} \times$$

$$(c\vec{\sigma}\cdot\vec{p}X + X^\dagger c\vec{\sigma}\cdot\vec{p} - 2c^2 X^\dagger X + V + X^\dagger V X) \times$$

$$\frac{1}{\sqrt{1+X^\dagger X}} \tag{9.5}$$

while the relation between the four-component Dirac wave function Ψ^D and the two-component Foldy-Wouthuysen transformed wave function Ψ^{FW} reads:

$$\Psi_i^D = \begin{pmatrix} \phi_i^D \\ \chi_i^D \end{pmatrix} = \begin{pmatrix} \frac{1}{\sqrt{1+X^\dagger X}} \Psi_i^{FW} \\ X \frac{1}{\sqrt{1+X^\dagger X}} \Psi_i^{FW} \end{pmatrix}$$

$$\Psi_i^{FW} = \sqrt{1+X^\dagger X}\,\phi_i^D \tag{9.6}$$

From (6) it immediately follows that the two-component operator X has the special property that when working on the large component ϕ^D of the Dirac wave function it gives the small component [30] χ^D, thus:

$$X\phi_i^D = \frac{c}{2c^2 + E_i - V}\vec{\sigma}\cdot\vec{p}\phi_i^D = \chi_i^D \tag{9.7}$$

This property we can use to calculate the eigenfunctions of the (Hermitian) non-negative operator $X^\dagger X$. Suppose we have solved the Dirac equation for a given external potential V. We can then assume that the large components of the normalised Dirac wave functions which have positive total energy eigenvalues are linearly independent (but not orthogonal) and form a complete basis for the two-component space. In this basis we can easily calculate matrix elements of the operator $X^\dagger X$:

$$\langle\phi_i^D|X^\dagger X|\phi_j^D\rangle =$$

$$\langle\phi_i^D|\vec{\sigma}\cdot\vec{p}\frac{c^2}{(2c^2+E_i-V)(2c^2+E_j-V)}\vec{\sigma}\cdot\vec{p}|\phi_i^D\rangle =$$

$$\langle\chi_i^D|\chi_j^D\rangle = \delta_{ij} - \langle\phi_i^D|\phi_j^D\rangle \tag{9.8}$$

where the last equation follows from the fact that the Dirac wave functions are orthonormal. If we diagonalize the resultant matrix we will find the eigenfunctions θ_i and eigenvalues λ_i^θ of the operator $X^\dagger X$ in this basis. We then know how the orthogonal eigenfunctions θ_i can be expressed in terms of Dirac large components ϕ_j^D and vice versa:

$$\theta_i = \sum_j c_{ij}^{\theta\phi}\phi_j^D \quad ; \quad \phi_i^D = \sum_j c_{ij}^{\phi\theta}\theta_j \tag{9.9}$$

Consequently we can use (6) to write the Foldy-Wouthuysen transformed wave function Ψ^{FW} as:

$$\Psi_i^{FW} = \sum_{j,k}\sqrt{1+\lambda_j^\theta}\; c_{ij}^{\phi\theta} c_{jk}^{\theta\phi}\phi_k^D \tag{9.10}$$

We therefore have an explicit expression for the Foldy-Wouthuysen transformed wave functions that only involves the eigenvalues and eigenfunctions of essentially the overlap matrix of the large components of the Dirac solutions. This transformed wave function can subsequently be used to calculate various properties in the transformed picture (see section 4). Some insight into the nature of the operator $X^\dagger X$ can be obtained by examining its classical form:

$$X^\dagger X = \frac{p^2c^2}{(2c^2+E-V)^2} =$$

$$\frac{p^2c^2}{(\sqrt{c^4+p^2c^2}+c^2)^2} \tag{9.11}$$

Clearly for small momenta it will approximately be equal to $p^2/4c^2$, while for high momenta it will approach 1. Consequently for a free particle, this operator has a continuous spectrum between zero and one, while its eigenfunctions in this case will be plane-waves.

9.3 Iterative solution

We can use the ideas of the last section to formulate an iterative procedure to solve the Dirac equation in an external potential V that avoids using the small component entirely. Using equation 9.5 and 9.6 we can write the Foldy-Wouthuysen transformed Dirac equation:

$$H^{FW}\Psi_i^{FW} = E_i\Psi_i^{FW} \tag{9.12}$$

as an equation for the large component ϕ^D of the Dirac wave function, by multiplying it by $\tilde{S}^{1/2}$:

$$\tilde{H}\phi_i^D = E_i\tilde{S}\phi_i^D \tag{9.13}$$

where:

$$\tilde{H} = c\vec{\sigma}\cdot\vec{p}X + X^\dagger c\vec{\sigma}\cdot\vec{p} - 2c^2X^\dagger X + V + X^\dagger V X \tag{9.14}$$

$$\tilde{S} = 1 + X^\dagger X \tag{9.15}$$

Equation 9.13 is now in the standard form of an eigenvalue equation with a metric $\tilde{S}$. In the basis set of large components we can determine the matrix elements of the operators $\tilde{H}$ and $\tilde{S}$, with the help of equation 9.7.
Equation 9.13 can be solved in an iterative manner. Suppose we have an estimate for the large components and the orbital energies, which will be called ϕ_i^0 and E_i^0 respectively, were i runs over the different approximate (positive energy) solutions of the Dirac equation (the number of which will be equal to the size of the large component basis set) and the superscript will indicate the number of the cycle in the subsequent iterative procedure. We then proceed for the $N-1$th cycle to Nth cycle in the following way. We will first normalise every ϕ_i^{n-1} such that the orbital density is normalised to one:

$$\langle\phi_i^{n-1}|\phi_i^{n-1}\rangle +$$

$$\langle\phi_i^{n-1}|\vec{\sigma}\cdot\vec{p}\frac{c^2}{(2c^2+E_i^{n-1}-V)^2}\vec{\sigma}\cdot\vec{p}|\phi_i^{n-1}\rangle = 1 \tag{9.16}$$

The matrix elements of the operator $\tilde{S}$ are then approximated in the basis of large components ϕ_i^{n-1} according to equation 9.7 as:

$$\langle\phi_i^{n-1}|\tilde{S}|\phi_j^{n-1}\rangle = \langle\phi_i^{n-1}|1 + X^\dagger X|\phi_j^{n-1}\rangle =$$

$$\langle\phi_i^{n-1}|1 + \tag{9.17}$$

$$\vec{\sigma}\cdot\vec{p}\frac{c^2}{(2c^2+E_i^{n-1}-V)(2c^2+E_j^{n-1}-V)}\vec{\sigma}\cdot\vec{p}|\phi_j^{n-1}\rangle$$

while the matrix elements of the Hamiltonian $\tilde{H}$ are determined from:

$$\langle\phi_i^{n-1}|\tilde{H}|\phi_j^{n-1}\rangle =$$

$$\langle\phi_i^{n-1}|V + \vec{\sigma}\cdot\vec{p}\frac{c^2}{(2c^2+E_i^{n-1}-V)}\vec{\sigma}\cdot\vec{p} +$$

$$\vec{\sigma}\cdot\vec{p}\frac{c^2}{(2c^2+E_j^{n-1}-V)}\vec{\sigma}\cdot\vec{p} -$$

$$\vec{\sigma}\cdot\vec{p}\frac{c^2(2c^2-V)}{(2c^2+E_i^{n-1}-V)(2c^2+E_j^{n-1}-V)}\vec{\sigma}\cdot\vec{p}|\phi_j^{n-1}\rangle$$

$$= \langle\phi_i^{n-1}|V + \vec{\sigma}\cdot\vec{p}\frac{c^2}{(2c^2-V)}\vec{\sigma}\cdot\vec{p}|\phi_j^{n-1}\rangle -$$

$$\langle\phi_i^{n-1}|\vec{\sigma}\cdot\vec{p}\frac{E_i^{n-1}E_j^{n-1}}{(2c^2+E_i^{n-1}-V)(2c^2+E_j^{n-1}-V)}\times$$

$$\frac{c^2}{(2c^2-V)}\vec{\sigma}\cdot\vec{p}|\phi_j^{n-1}\rangle \tag{9.18}$$

The first term can be recognized as the zeroth order CPD or ZORA hamiltonian extensively discussed in earlier papers [128] which was shown to already give quite accurate approximations to the full Dirac energies in many cases. The last term, which corrects this ZORA hamiltonian, is small if the orbital energies involved are small compared to c^2.
Diagonalising the generalized eigenfunction equation, one obtains improved eigenvalues E_i^n and eigenfunctions ϕ_i^n. By iterating to selfconsistency we obtain solutions to the Dirac equation without ever having to calculate the small component explicitly. The price to be paid is that the equation has to be solved iteratively. On the other hand this price is not as large as it may seem if one considers the usual case that the potential is not fixed but is also determined iteratively until selfconsistency is reached. In particular in the density functional method the improved potential can be determined from the improved density at the end of each iterative cycle described above and one can converge both the potential and the Dirac large component at the same time. Note however, that the matrix elements of $\tilde{H}$ have to be calculated in a basis set that changes from cycle to cycle. The matrix has only roughly half of the size of the full Dirac Hamiltonian being limited to the positive energy space. Consequently the current scheme might well be competative, especially since it avoids the large bases needed to describe the small components accurately. A very good starting point for the iterative procedure is formed by the zeroth order CPD

or ZORA equation which we studied before [121] and which appears explicitly as the first term in equation 9.18. We know from the results of ref [124], that the ZORA Hamiltonian is bounded from below. Since the second term in equation 9.18 is small if the orbital energies are small compared to c^2, we expect that this term does not destroy the boundedness from below. This expectation is borne out in section 9.4. Crucial is the fact that we start with positive total energies $E_i > -c^2$. When we could have started with for example positron-like energies $E_i < -2c^2$, we might have ended up with converged positron-like solutions of the Dirac equation, because the iterative procedure is also valid for those states. The reason for the fact that we always converge in section 9.4 to positive total energies, should be ascribed to the fact that we start with positive total energies and that our starting wave function is already quite accurate.

9.4 Numerical Test Results

In order to test the above procedures we have applied them to the uranium ion with only one electron where we can compare with exact results and to the neutral uranium atom where we can test the selfconsistent procedure within the density functional framework (here we used the simple $X\alpha$ potential). As a basis set we used the Dirac type Slater orbitals (DTO's) with fractional exponents we discussed in an earlier paper [129] and which were shown to give accurate representations of the Dirac orbitals in this case. In both the ion and the neutral atom the method described above quickly converged and the orbital energies of the full Dirac calculations were reproduced to within numerical accuracy. The basis sets used contain sufficient flexibility to also represent the Foldy-Wouthuysen transformed orbitals, which resemble the renormalised large components, quite accurately.

An interesting question that can now be answered, concerns the difference between the two distinct observables that are represented by the operator $\mathbf{r}$ in the Dirac picture and in the Schrödinger (Foldy-Wouthuysen) picture respectively. An earlier paper [32] we studied this question using the Foldy-Wouthuysen transformation to first order only, but now we are now in a position to investigate the influence of higher orders on this picture change. The expectation value of the "Dirac position" is given by:

$$\langle r \rangle = \langle \Psi^D | \vec{r} | \Psi^D \rangle =$$

$$\langle \Psi^{FW} | U^{FW} \vec{r} (U^{FW})^\dagger | \Psi^{FW} \rangle \tag{9.19}$$

while on the other hand the expectation value of the "Schrödinger position" reads:

$$\langle R \rangle = \langle \Psi^{FW} | \vec{r} | \Psi^{FW} \rangle =$$

$$\langle \Psi^D | (U^{FW})^\dagger \vec{r} U^{FW} | \Psi^D \rangle \tag{9.20}$$

In table 9.1 we show differences between these two observables for some orbitals of the hydrogen-like Uranium 91+ ion. The expectation value of the Dirac position can be calculated analytically [130]:

$$\langle r \rangle = \frac{(\gamma + n - |\kappa|)(3N^2 - \kappa^2) - \kappa N}{2ZN} \tag{9.21}$$

with:

$$\gamma = \sqrt{\kappa^2 - \frac{Z^2}{c^2}}$$

$$N = \sqrt{(n - |\kappa| + \gamma)^2 + \frac{Z^2}{c^2}} \tag{9.22}$$

In first order [32] the difference between the Schrödinger and Dirac position for a hydrogenic orbital with quantum number n and κ is given by:

$$\langle R \rangle - \langle r \rangle = \frac{Z\kappa}{4c^2 n^2} \tag{9.23}$$

where Z is the nuclear charges. The table shows that the influence of higher order terms in the Foldy-Wouthuysen transformation is generally quite small, except in the case of the $1s1/2$ orbital where more then 25% of the effect is seen to arise from these higher order contributions. As an example of the self consistent method we solved the equations for a neutral Uranium atom using the simple $X\alpha$ version of the density functional method. The same DTO basis set was used as in ref [129], where the Dirac equation was solved using a basis set for the large component only. The results are in perfect agreement with each other. In table 9.2 we again compare the difference of the two position observables. Although the basis set results for the valence orbitals of the neutral Uranium atom have an accuracy of about 0.1% for the expectation value of r, the picture change effects are expected in absolute value to be more accurate, because the same basis set was used for both orbitals. For the deep core the picture change effects are roughly the same as for the hydrogenic Uranium. For valence orbitals the absolute value in the picture change is about 4 to 7 times smaller than in the hydrogenic case, which is much smaller than the accuracy of the used basis set. Also in the neutral atom there is opposite behaviour for $\kappa < 0$ orbitals and $\kappa > 0$ orbitals.

Table 9.1: Uranium 91+ orbital expectation values in a.u.

ORBITAL	$\langle r\rangle$	$\langle R\rangle-\langle r\rangle$ exact	$\langle R\rangle-\langle r\rangle$ first order	ORBITAL	$\langle r\rangle$	$\langle R\rangle-\langle r\rangle$ exact	$\langle R\rangle-\langle r\rangle$ first order
$1s_{1/2}$	.01349	-.00097	-.00122	$5s_{1/2}$	.3702	-.00005	-.00005
$2s_{1/2}$	.05334	-.00032	-.00031	$5p_{1/2}$	.3593	.00005	.00005
$2p_{1/2}$	.04247	.00033	.00031	$5p_{3/2}$	.3819	-.00010	-.00010
$2p_{3/2}$	.05183	-.00058	-.00061	$5d_{3/2}$	.3602	.00010	.00010
$3s_{1/2}$	.1263	-.00014	.00014	$5d_{5/2}$	.3668	-.00015	-.00015
$3p_{1/2}$	.1154	.00015	.00014	$5f_{5/2}$	.3342	.00015	.00015
$3p_{3/2}$	.1289	-.00027	-.00027	$5f_{7/2}$	.3376	-.00020	-.00020
$3d_{3/2}$	.1072	.00028	.00027	$6s_{1/2}$	.5411	-.00004	-.00003
$3d_{5/2}$	.1116	-.00040	-.00041	$6p_{1/2}$	.5302	.00004	.00003
$4s_{1/2}$	.2319	-.00008	-.00008	$6p_{3/2}$	.5574	-.00007	-.00007
$4p_{1/2}$	.2211	.00008	.00008	$6d_{3/2}$	.5357	.00007	.00007
$4p_{3/2}$	.2390	-.00015	-.00015	$6d_{5/2}$	.5435	-.00010	-.00010
$4d_{3/2}$	.2173	.00016	.00015	$7s_{1/2}$	.7446	-.00003	-.00002
$4d_{5/2}$	.2228	-.00023	-.00023				
$4f_{5/2}$	.1902	.00023	.00023				
$4f_{7/2}$	.1932	-.00030	-.00031				

Table 9.2: neutral Uranium orbital expectation values in a.u.

ORBITAL	$\langle r\rangle$	$\langle R\rangle-\langle r\rangle$	ORBITAL	$\langle r\rangle$	$\langle R\rangle-\langle r\rangle$
$1s_{1/2}$	.01364	-.00095	$5s_{1/2}$	.6668	-.000027
$2s_{1/2}$	.05650	-.00030	$5p_{1/2}$	.6938	.000025
$2p_{1/2}$	.04576	.00032	$5p_{3/2}$	.7735	-.000046
$2p_{3/2}$	.05599	-.00054	$5d_{3/2}$	.8673	.000040
$3s_{1/2}$	.1471	-.00012	$5d_{5/2}$	.8957	-.000059
$3p_{1/2}$	.1382	.00012	$5f_{5/2}$	1.487	.000038
$3p_{3/2}$	.1566	-.00022	$5f_{7/2}$	1.550	-.000046
$3d_{3/2}$	.1350	.00023	$6s_{1/2}$	1.473	-.000011
$3d_{5/2}$	.1405	-.00033	$6p_{1/2}$	1.650	.000011
$4s_{1/2}$	.3199	-.00006	$6p_{3/2}$	1.897	-.000018
$4p_{1/2}$	.3182	.00006	$6d_{3/2}$	3.237	.000011
$4p_{3/2}$	.3549	-.00010	$6d_{5/2}$	3.499	-.000015
$4d_{3/2}$	.3515	.00010	$7s_{1/2}$	4.118	-.000004
$4d_{5/2}$	.3625	-.00014			
$4f_{5/2}$	.3517	.00014			
$4f_{7/2}$	.3571	-.00017			

9.5 Conclusions

In this chapter the exact Foldy-Wouthuysen transformation is constructed for an arbitrary potential. On the basis of this construction an iterative procedure is formulated that constitutes an alternative way for solving the Dirac equation, obviating the need for a small component basis. The procedure seems especially attractive when used in a self-consistent field scheme, since then the iterative procedure can be run concurrently with the SCF iterations. The method has been applied to the calculation of the picture change effects in the expectation value of the position operators with the uranium atom as an example. Higher then first order effects of this picture change turn out the be only important for the deep core orbitals, where they can be as large as 25% in the case of hydrogen-like uranium.

Samenvatting

De meeste materie om ons heen bestaat uit moleculen of kristallen, die op hun beurt weer te ontleden zijn in atomen. Een atoom bestaat uit een positief geladen kern, die een aantrekkende kracht uitoefent op elektronen die zich rondom die kern bewegen. De atoomkernen bewegen zich veel langzamer dan de relatief lichte elektronen. Zware elementen, zoals bijvoorbeeld goud, kwik en lood, hebben een grote positieve kernlading. Hoe groter deze positieve lading van de atoomkern is, hoe sterker de aantrekkingskracht is op de elektronen. Deze elektrische kracht is ook sterker, naarmate de elektronen dichter bij de kern komen. De binnenste elektronen, die het meest gebonden zijn en ook wel core-elektronen worden genoemd, bewegen daardoor met grote snelheid die in de buurt kan komen van de lichtsnelheid. Voor een juiste beschrijving van de beweging van deze snelle elektronen moet men daarom de speciale relativiteitstheorie van Einstein gebruiken. De buitenste elektronen, de valentie-elektronen, bewegen gemiddeld een stuk langzamer. Deze elektronen zijn chemisch het meest interessant, omdat zij in grote mate bepalen of een binding tussen atomen tot stand komt, en hoe sterk die binding is. Langzame elektronen kunnen zeer goed beschreven worden met niet-relativistische bewegingsvergelijkingen. Echter zelfs valentie-elektronen hebben een kans dat ze vlak in de buurt van de atoomkern komen, en zullen dan door de enorme krachten van de kern erg snel bewegen. De niet-relativistische bewegingsvergelijking is in dit gebied daarom niet nauwkeurig genoeg meer. Men kan zelfs zeggen, klassiek mechanisch gezien, dat voor elke plek in het atoom geldt, dat een valentie-elektron zich harder voortbeweegt dan een core-elektron. Dat een valentie-elektron gemiddeld langzamer beweegt, komt omdat het veel minder kans heeft om vlak bij de atoomkern te komen dan een core-elektron. Hoewel deze kans vrij klein is, is het relativistische effect toch niet te verwaarlozen voor valentie-elektronen van de zwaardere atomen.

In dit proefschrift zullen we een benaderde bewegingsvergelijking gebruiken die nauwkeurig is voor valentie-elektronen, zelfs als ze dicht in de buurt van een atoomkern bewegen. Deze regulier benaderde relativistische vergelijking, genaamd ZORA, is de simpelste vergelijking die men krijgt als men de relativistische vergelijking expandeert in $E/(2mc^2 - V)$. In deze expansie-parameter is E de bindingsenergie van de elektronen, die voor valentie-elektronen van de orde van enkele eV's is. De rustmassa-energie van het elektron mc^2 is ongeveer gelijk aan een half miljoen eV. De potentiaal V, die gerelateerd is aan de elektrische kracht, is in het algemeen klein ten opzichte van de rustmassa-energie van het elektron, behalve in de buurt van een atoomkern. In deze buurt kan de potentaal V erg groot worden, zeker als men kijkt naar de zwaardere elementen. Aangezien de potentiaal V attractief is, dus negatief, is de expansieparameter $E/(2mc^2 - V)$ overal veel kleiner dan 1 voor valentie-elektronen. De ZORA-vergelijking is daarom erg nauwkeurig voor valentie-elektronen. Voor core-elektronen is de bindingsenergie E veel groter, wat tot gevolg heeft dat ook de expansieparameter veel

groter wordt. Voor deze elektronen is de ZORA-vergelijking dan een stuk minder nauwkeurig. De niet-relativistische vergelijking kan men opvatten als de simpelste vergelijking die men krijgt als men de relativistische vergelijking expandeert in $(E-V)/(2mc^2)$. Deze expansieparameter is voor valentie-elektronen niet meer klein in de buurt van een atoomkern, omdat de potentiaal V daar grote waarden kan bereiken. Voor valentie-elektronen is de ZORA-vergelijking dus een betere benadering dan de niet-relativistische vergelijking. Berekeningen laten zien dat dit ook geldt voor de meeste andere elektronen. De expansies die hier gebruikt zijn, kunnen zowel in de klassieke mechanica, als in de quantummechanica gebruikt worden.

Het standaardmodel voor de beschrijving van de electromagnetische wisselwerking en beweging van electronen is tegenwoordig de QuantumElectroDynamica (QED). Nauwkeurige QED berekeningen zijn nog vrijwel alleen gedaan aan kleine systemen, zoals het waterstof- en heliumatoom, maar geven dan ook zeer goede overeenstemming met zeer nauwkeurige experimenten. Voor grotere systemen zijn nauwkeurige QED berekeningen meestal veel te duur (veel computertijd).
Een benadering op deze methode is de Dirac-vergelijking. Dit is een relativistische quantummechanische bewegingsvergelijking voor bijvoorbeeld elektronen. Net als in de klassieke mechanica, kan men in de quatummechanica de relativistische vergelijking benaderen met behulp van expansies. De niet-relativistische quantummechanische vergelijking wordt ook wel de Schrödinger-vergelijking genoemd. In de quatummechanica is het niet meer juist om het (tegelijkertijd) over de plaats en de snelheid van een deeltje te hebben. Deeltjes worden in deze theorie beschreven met behulp van een golffunctie, die de kans aangeeft om een deeltje ergens aan te treffen. De oplossing van de Dirac-vergelijking is een 4-componentige golffunctie, die bestaat uit twee grote en twee kleine componenten. Een van de standaardmethodes om moleculaire quantummechanische vergelijkingen op te lossen gebruikt een ontwikkeling van de golffunctie in basisfuncties. Voor het oplossen van de Dirac-vergelijking worden meestal basisfuncties gebruikt, die de grote en de kleine componenten goed moeten kunnen beschrijven. In hoofdstuk 8 and 9 worden methodes gebruikt om de Dirac-vergelijking op te lossen, die alleen basisfuncties voor de twee grote componenten nodig hebben en waarin de twee kleine componenten alleen impliciet worden gebruikt.
Het hoofdbestanddeel van dit proefschrift gaat over een benadering op de Dirac-vergelijking, de ZORA-vergelijking. In hoodstuk 2 wordt deze deze vergelijking afgeleid met behulp van verschillende methodes en in hoodstuk 3 wordt een aantal eigenschappen van deze vergelijking bekeken. Exacte oplossingen van het het waterstof-achtige atoom worden gegeven in hoofdstuk 4. In dit geval zijn de zogenaamde geschaalde ZORA energieën exact gelijk aan de Dirac energieën. In hoofdstuk 5 worden numerieke atomaire berekeningen gedaan. Het verschil tussen de oplossingen van de Dirac en de ZORA-vergelijking is erg klein, zeker als men kijkt naar valentie-elektronen, die zo belangrijk zijn voor chemische eigenschappen. Het verschil met de niet-relativistische oplossingen is veel groter. Hoofdstuk 6 laat zien hoe de ZORA methode is geimplementeerd in een moleculair rekenprogramma en in een programma dat geschikt is om systemen met periodiciteit (bijvoorbeeld kristallen) uit te rekenen. Hoofdstuk 7 bevat resultaten van berekeningen aan twee-atomige moleculen. De ZORA berekeningen leveren dan een grote mate van overeenstemming op met experimentele gegevens.

Summary

Most matter around us consists of molecules or crystals. These can be further divided into atoms. An atom consists of a postively charged nucleus, which attracts the surrounding electrons. The atomic nuclei move much slower than the relatively light electrons. Heavy elements, like for example gold, mercury and lead, have a large positive nuclear charge. The larger this charge is, the stronger the nucleus attracts the electrons. This electric force is also stronger if the electrons are closer to the nucleus. The inner electrons, or core electrons, move with a speed that might approach closely the velocity of light. For a good decription of the motion of these fast electrons it is necessary to use Einsteins special theory of relativity. The outer electrons, or valence electrons, have a lower average velocity. These electrons are chemically the most interesting ones, since they are for a large part responsible for the bonding and strength of bonding between atoms. Slow electrons can be described satisfactory with non-relativistic equations of motion. However, even valence electrons will move very fast once they come close to an atomic nucleus. In that case the non-relativistic equations of motion are not accurate enough anymore. One can even say, from a classic mechanical point of view, that at every place in an atom a valence electron will move faster than a core electron. On the average a valence electron will move slower, because it has much less chance to come close to an atomic nucleus. Although this chance is relatively small, the relativistic effect can not be neglected for valence electrons of heavy atoms.
In this thesis an approximate equation of motion is used, called the ZORA (zeroth order relativistic approximated) equation, which is the simplest equation one gets if one expands the relativistic equation in $E/(2mc^2 - V)$. This expansion can be used in classical mechanics as well as in quantum mechanics. In this expansion E is the binding energy of the electron, which is in the order of a few eV's for valence electrons and mc^2 is the rest mass energy of the electron, which is approximately half a million eV. The potential V, related to the electric force, is usually small compared to the rest mass energy of the electron, except in the neighbourhood of the atomic nucleus. In this region the potential can be very large, especially for the heavier elements. Since the potential V is attractive, and therefore negative, the expansion parameter $E/(2mc^2 - V)$ is everywhere much smaller than 1 for valence electrons. For for valence electrons the ZORA equation is thus very accurate. For core electrons the binding energy E is much larger, and consequently the expansion parameter is also much larger. For these electrons the ZORA equation is less accurate.
One can consider the non-relativistic equation as the simplest equation one gets if one expands the relativistic equation in $(E - V)/(2mc^2)$. For valence electrons this exansion parameter is not small anymore in the neighbourhood of an atomic nucleus, because the potential V is very large there. For valence electrons the ZORA equation is therefore a better approximation than the non-relativistic equation. Calculations show that this is also true

for most other electrons.
In this thesis the ZORA equation is used in atomic and molecular calculations. The potential-dependent expansion, earlier derived by Chang et al. [5] and Heully et al. [6], is rederived in chapter 2. In the chapters 3 to 7 the ZORA Hamiltonian is further investigated. In chapter 3 it is shown that this Hamiltonian is bounded from below. There it is also shown that the ZORA equation is not gauge invariant, but that the scaled ZORA method almost completely solves this problem. This method again can be approximated using the so called electrostatic shift approximation (ESA), which is an easy and accurate way to obtain energy differences. In chapter 4 the exact solutions of the ZORA equation are given in the case of a hydrogen-like atom. This is done by scaling of coordinates in the Dirac equation. The same scaling arguments are used to obtain exact relations for one and two electron systems in more general systems. For the discrete part of the spectrum of the hydrogen-like atom it is shown there that the scaled ZORA energies are exactly equal to the Dirac energies. Numerical atomic calculations are done in chapter 5, showing the high accuracy of the ZORA method for valence orbitals. The implementation of this method in molecular and in band structure calculations is given in chapter 6. The results of molecular calculations on a number of diatomics is given in chapter 7, with an explicit treatment of the spinorbit operator. In this chapter a method is proposed for the calculation of the total energy of open shell systems using density functionals if spinorbit is present.
Chapter 8 and 9 show methods for solving the Dirac equation, using basis sets for the large components only. In chapter 8 this is done using the standard method of eliminating the small component and requires a diagonalisation of a Hamiltonian for every occupied orbital. In chapter 9 the Dirac equation is solved by a new method. In the iterative procedure used, it requires the evaluation of matrix elements of the Hamiltonian between the large component solutions of the previous cycle. In this chapter also a method was given for construction of the exact Foldy-Wouthuysen transformation, once one has the (large component) solution to the Dirac equation.

Dankwoord

In de eerste plaats wil ik mijn promotoren Evert-Jan Baerends en Jaap Snijders bedanken voor de ruimte die ze me geboden hebben om zelf dingen uit te zoeken en voor de kritiek en stimulans die ze me gegeven hebben. Robert van Leeuwen, ik wil jou bedanken voor de vele aangename discussies, vaak ook samen met Oleg. Voor dit proefschrift zijn jouw schalingsbewijzen van groot belang geweest, resulterend in een aantal artikelen met jou samen. Pier Philipsen, ik bedank jou voor je nuchterheid. Jouw speurtocht naar goud heeft nog niet het gewenste effect gehad, maar het heeft onder andere wel de spin-baan koppeling opgeleverd. Oleg Gritsenko, I thank you for the pleasant time we had sharing the same room and for the many lively discussions we had together with Robert.
Voor vele vragen op computer-gebied kon ik terecht bij Pieter V., Gijsbert, Bert, Walter en Olivier. Ik dank ook de (ex-) collega's, waaronder Eric en Margot, Célia en Matthias, Stan, Simon en Pieter S. en andere leden van de sectie theoretisch chemie, waaronder Ad, Geert-Jan en Andreas voor vele gezellige koffie-uurtjes.
I thank the foreign visitors, among them Paola, Angela, Tony and Roar, for the extra sphere they have created in our group.

Bibliography

[1] P.A.M. Dirac. *Proc. Roy. Soc. (London)*, **A117**:610, 1928.

[2] P.A.M. Dirac. *Proc. Roy. Soc. (London)*, **A118**:351, 1928.

[3] C.G. Darwin. *Proc. Roy. Soc. (London)*, **A118**:654, 1928.

[4] W. Gordon. *Z. Physik*, **48**:11, 1928.

[5] Ch. Chang, M. Pélissier, and Ph. Durand. *Phys. Scr.*, **34**:394, 1986.

[6] J-L. Heully, I. Lindgren, E. Lindroth, S. Lundqvist, and A-M. Mårtensson-Pendrill. *J. Phys. B*, **19**:2799, 1986.

[7] G. Breit. *Phys. Rev.*, **34**:553, 1929.

[8] J.A. Gaunt. *Proc. Roy. Soc. (London)*, **A122**:513, 1929.

[9] P.Hohenberg and W.Kohn. *Phys. Rev.*, **136B**:864, 1964.

[10] A.K. Rajagopal and J. Callaway. *Phys. Rev. B*, **7**:1912, 1973.

[11] A.K. Rajagopal. *J. Phys. C*, **11**:L943, 1978.

[12] A.H. MacDonald and S.H. Vosko. *J. Phys. C*, **12**:2977, 1979.

[13] E. Engel, H. Müller, C. Speicher, and R.M. Dreizler. *in Density Functional Theory, (eds.) E.K.U. Gross and R.M. Dreizler, Plenum Press, New York*, page 65, 1995.

[14] J. Sucher. *Phys. Rev. A*, **22**:348, 1980.

[15] J-L. Heully, I. Lindgren, E. Lindroth, and A-M. Mårtensson-Pendrill. *Phys. Rev. A*, **33**:4426, 1985.

[16] G. Hardekopf and J. Sucher. *Phys. Rev. A*, **30**:703, 1984.

[17] J.J. Sakurai. *Advanced Quantum Mechanics.* Addison Wesley, Reading Massachusetts, 1967.

[18] L.L. Foldy and S.A. Wouthuysen. *Phys. Rev.*, **78**:29, 1950.

[19] G.E. Brown and D.G. Ravenhall. *Proc. Roy. Soc. (London)*, **A208**:55, 1951.

[20] J. Sucher. *Int. J. Quantum Chem.*, **25**:3, 1984.

[21] E. Lindroth, J-L. Heully, I. Lindgren, and A-M. Mårtensson-Pendrill. *J. Phys. B*, **20**:1679, 1987.

[22] W.Kohn and L.J.Sham. *Phys. Rev.*, **140A**:1133, 1965.

[23] A. Farazdel and Jr V.H. Smith. *Int. J. Quantum Chem.*, **29**:311, 1986.

[24] Berestetskiĭ, Lifshitz, and Pitaevskiĭ. *Relativistic Quantum Theory.* Clarendon Press, Oxford, 1971.

[25] R. McWeeny and B.T. Suthcliffe. *Methods of Molecular Quantum Mechanics.* Academic Press, London, 1976.

[26] W.H.E. Schwarz, E.M. van Wezenbeek, E.J. Baerends, and J.G. Snijders. *J. Phys. B*, **22**:1515, 1989.

[27] P.M.Boerrigter. *Spectroscopy and Bonding of heavy element compounds.* PhD thesis, Vrije Universiteit, Amsterdam, The Netherlands, 1987.

[28] T. Ziegler, V. Tschinke, E.J. Baerends, J.G. Snijders, and W. Ravenek. *J. Phys. Chem.*, **93**:3050, 1989.

[29] J. des Cloizeaux. *Nucl. Phys.*, **20**:321, 1960.

[30] W. Kutzelnigg. *Z. Physik D*, **15**:27, 1990.

[31] R.E. Moss. *Advanced Molecular Quantum Mechanics.* Chapman and Hall, London, 1973.

[32] E.J. Baerends, W.H.E. Schwarz, P. Schwerdtfeger, and J.G. Snijders. *J. Phys. B*, **23**:3225, 1990.

[33] A.J. Sadlej and J.G. Snijders. *Chem. Phys. Lett.*, **229**:435, 1994.

[34] A.J. Sadlej, J.G. Snijders, E. van Lenthe, and E.J. Baerends. *J. Chem. Phys.*, **102**:1758, 1995.

[35] A. Rutkowski. *J. Phys. B*, **19**:149, 1986.

[36] W. Kutzelnigg. *Z. Physik D*, **11**:15, 1989.

[37] M. Douglas and N.M. Kroll. *Acta Physica*, **82**:89, 1974.

[38] B.A. Hess. *Phys. Rev. A*, **33**:3742, 1986.

[39] R. Samzow and B.A. Hess. *J. Chem. Phys.*, **96**:1227, 1992.

[40] P. Knappe and N. Rösch. *J. Chem. Phys.*, **92**:1153, 1990.

[41] H. Gollisch and L. Fritsche. *Phys. Stat. Sol.*, **86**:145, 1978.

[42] D.D. Koelling and B.N. Harmon. *J. Phys. C*, **10**:3107, 1977.

[43] L.D. Landau and E.M. Lifshitz. *Quantum Mechanics.* Pergamon Press, Oxford, 1977.

[44] P.M. Boerrigter, G. te Velde, and E.J. Baerends. *Int. J. Quantum Chem.*, **33**:87, 1988.

[45] G. te Velde and E.J. Baerends. *J. Comp. Phys.*, **99**:84, 1992.

[46] E.J.Baerends. Bond energy evaluation. Technical report, Vrije Universiteit, Amsterdam, The Netherlands, 1988.

[47] J.M. Levy-Leblond. *Comm. Math. Phys.*, **6**:286, 1967.

[48] J.M. Levy-Leblond. *Ann. Phys.*, **57**:481, 1970.

[49] E. Schrödinger. *Ann. d. Phys.*, **79**:361, 1926.

[50] V.A. Fock. *Z. Physik*, **40**:632, 1926.

[51] Y-K. Kim. *Phys. Rev.*, **154**:1, 1967.

[52] A. Messiah. *Quantum Mechanics II.* North Holland Publishing Company, Amsterdam, 1965.

[53] R.E. Stanton and S. Havriliak. *J. Chem. Phys.*, **81**:1910, 1984.

[54] W. Kutzelnigg. *Int. J. Quantum Chem.*, **25**:107, 1984.

[55] P.J.C. Aerts and W.C. Nieuwpoort. *Chem. Phys. Lett.*, **125**:83, 1986.

[56] J.D Morrison and R.E. Moss. *Molec. Phys.*, **41**:491, 1980.

[57] I.J. Ketley and R.E. Moss. *Molec. Phys.*, **48**:1131, 1983.

[58] I.J. Ketley and R.E. Moss. *Molec. Phys.*, **49**:1289, 1983.

[59] R.E. Moss. *Molec. Phys.*, **53**:269, 1984.

[60] J. G. Snijders, E. J. Baerends, and P. Ros. *Molec. Phys.*, **38**:1909, 1979.

[61] J.C.Slater. *Phys. Rev.*, **81**:385, 1951.

[62] M.V. Ramana M.P. Das and A.K. Rajagopal. *Phys. Rev. A*, **22**:9, 1980.

[63] M.E. Rose. *Relativistic Electron Theory.* John Wiley and Sons, Inc., New York, 1961.

[64] J.D. Bjorken and S.D. Drell. *Relativistic Quantum Mechanics.* McGraw-Hill, Inc., New York, 1964.

[65] J.G. Snijders and E.J. Baerends. *Molec. Phys.*, **36**:1789, 1978.

[66] P. M. Boerrigter, E. J. Baerends, and J.G. Snijders. *Chem. Phys.*, **122**:357, 1988.

[67] J.G. Snijders. *Relativity and pseudopotentials in the HFS method.* PhD thesis, Vrije Universiteit, Amsterdam, The Netherlands, 1979.

[68] G. te Velde and E.J. Baerends. *Phys. Rev. B*, **44**:7888, 1991.

[69] G. te Velde. *Numerical integration and other methodological aspects of Bandstructure Calculations.* PhD thesis, Vrije Universiteit, Amsterdam, The Netherlands, 1990.

[70] E.M.Wezenbeek. *Relativistic effects in Atoms and in Uranium compounds.* PhD thesis, Vrije Universiteit, Amsterdam, The Netherlands, 1992.

[71] P. Schwerdtfeger. *Chem. Phys. Lett.*, **183**:457, 1991.

[72] A. Pizlo, G. Jansen, B.A. Hess, and W. von Niessen. *J. Chem. Phys.*, **98**:3945, 1993.

[73] K.P. Huber and G.Herzberg. *Molecular spectra and molecular structure, Vol. 4, Constants of diatomic molecules.* Van Nostrand Reinhold, New York, 1979.

[74] E. van Lenthe, E.J. Baerends, and J.G. Snijders. *J. Chem. Phys.*, **101**:9783, 1994.

[75] V. Beutel, H.-G. Krämer, G.L. Bhale, M. Kuhn, K. Weyers, and W. Demtröder. *J. Chem. Phys.*, **98**:2699, 1993.

[76] G.A. Bishea, N. Marak, and M.D. Morse. *J. Chem. Phys.*, **95**:5618, 1991.

[77] G.A. Bishea, J.C. Pinegar, and M.D. Morse. *J. Chem. Phys.*, **95**:5630, 1991.

[78] R.M. Dickson and A.D. Becke. *J. Chem. Phys.*, **99**:3898, 1993.

[79] B.A. Hess and P. Chandra. *Phys. Scr.*, **36**:412, 1987.

[80] G. Jansen and B.A. Hess. *Z. Physik D*, **13**:363, 1989.

[81] Jr. C.W. Bauschlicher, S.R. Langhoff, and H. Partridge. *J. Chem. Phys.*, **91**:2412, 1989.

[82] O.D. Häberlen and N. Rösch. *Chem. Phys. Lett.*, **199**:491, 1992.

[83] T. Baştuğ, D. Heinemann, W.-D. Sepp, D. Kolb, and B. Fricke. *Chem. Phys. Lett.*, **211**:119, 1993.

[84] A.D.Becke. *Phys. Rev. A*, **38**:3098, 1988.

[85] J.P.Perdew. *Phys. Rev. B*, **33**:8822, 1986.

[86] A.D.Becke. *J. Chem. Phys.*, **96**:2155, 1992.

[87] L.Fan and T.Ziegler. *J. Chem. Phys.*, **94**:6057, 1991.

[88] T.Ziegler, A.Rauk, and E.J. Baerends. *Theoret. Chim. Acta*, **43**:261, 1977.

[89] A.D. Becke, A. Savin, and H. Stoll. *Theoret. Chim. Acta*, **91**:147, 1995.

[90] E.U. Condon and G.H. Shortley. *The Theory of Atomic Spectra.* Cambridge University Press, 1951.

[91] C.E. Moore. *Atomic Energy Levels: as derived from the analysis of optical spectra / reissued.* National Bureau of Standard, Washington, 1971.

[92] C. Teichteil and M. Pélissier. *Chem. Phys.*, **180**:1, 1994.

[93] K.K. Das, H.-P. Liebermann, and R.J. Buenker. *J. Chem. Phys.*, **102**:4518, 1995.

[94] L. Seijo. *J. Chem. Phys.*, **102**:8078, 1995.

[95] D. Danovich, J. Hrusak, and S. Shaik. *Chem. Phys. Lett.*, **233**:249, 1995.

[96] V. Kello and A.J. Sadlej. *J. Chem. Phys.*, **93**:8122, 1990.

[97] U. Kaldor and B.A. Hess. *Chem. Phys. Lett.*, **230**:1, 1994.

[98] M.N. Glukhovtsev, A. Pross, M.P. McGrath, and L. Radom. *J. Chem. Phys.*, **103**:1878, 1995.

[99] K. Balasubramanian. *J. Chem. Phys.*, **82**:3741, 1985.

[100] K.G. Dyall. *J. Chem. Phys.*, **98**:2191, 1993.

[101] O. Matsuoka. *J. Chem. Phys.*, **97**:2271, 1992.

[102] O. Matsuoka, L. Pisani, and E. Clementi. *Chem. Phys. Lett.*, **202**:13, 1992.

[103] P. Schwerdtfeger, L. v. Szentpaly, K. Vogel, H. Silberbach, H. Stoll, and H. Preuss. *J. Chem. Phys.*, **84**:1606, 1986.

[104] D.A. Chapman, K. Balasubramanian, and S.H. Lin. *Phys. Rev. A*, **38**:6098, 1988.

[105] A.F. Ramos, N.C. Pyper, and G.L. Malli. *Phys. Rev. A*, **38**:2729, 1988.

[106] M. Dolg, A. Nicklass, and H. Stoll. *J. Chem. Phys.*, **99**:3614, 1993.

[107] A.J. Sadlej. *J. Chem. Phys.*, **95**:2614, 1991.

[108] V. Kello and A.J. Sadlej. *J. Chem. Phys.*, **98**:1345, 1993.

[109] D.A. Chapman, K. Balasubramanian, and S.H. Lin. *J. Chem. Phys.*, **87**:5325, 1987.

[110] T. Kagawa. *Phys. Rev. A*, **22**:2340, 1980.

[111] F. Mark and F. Rosicky. *Chem. Phys. Lett.*, **74**:562, 1980.

[112] O. Matsuoka, N. Suzuki, T. Aoyama, and G. Malli. *J. Chem. Phys.*, **73**:1320, 1980.

[113] Y.S. Lee and A.D. McLean. *J. Chem. Phys.*, **76**:735, 1982.

[114] K.G. Dyall, P.R. Taylor, K. Faegri Jr., and H. Partridge. *J. Chem. Phys.*, **95**:2583, 1991.

[115] O. Visser, L. Visscher, P.J.C. Aerts, and W.C. Nieuwpoort. *J. Chem. Phys.*, **96**:2910, 1992.

[116] O. Matsuoka. *in METECC-94,Vol. A, Chap. 7, (ed.) E. Clementi, STEF, Cagliari, Italy*, 1993.

[117] L. Pisani and E. Clementi. *in METECC-94,Vol. A, Chap. 8, (ed.) E. Clementi, STEF, Cagliari, Italy*, 1993.

[118] J.Wood, I.P. Grant, and S. Wilson. *J. Phys. B*, **18**:3027, 1985.

[119] P.J.C. Aerts. *Towards Relativistic Quantum Chemistry.* PhD thesis, University of Groningen, Groningen, The Netherlands, 1986.

[120] D. Hegarty. *Theoret. Chim. Acta*, **70**:351, 1986.

[121] E. van Lenthe, E.J. Baerends, and J.G. Snijders. *J. Chem. Phys.*, **99**:4597, 1993.

[122] E.J. Baerends, D.E. Ellis, and P. Ros. *Chem. Phys.*, **2**:42, 1973.

[123] A.D. Becke and R.M. Dickson. *J. Chem. Phys.*, **92**:3610, 1990.

[124] R. van Leeuwen, E. van Lenthe, E.J. Baerends, and J.G. Snijders. *J. Chem. Phys.*, **101**:1272, 1994.

[125] K.G. Dyall. *J. Chem. Phys.*, **100**:435, 1994.

[126] G.W.F. Drake and S.P. Goldman. *Phys. Rev. A*, **23**:2093, 1981.

[127] J.G. Snijders and P. Pyykkö. *Chem. Phys. Lett.*, **75**:5, 1980.

[128] E. van Lenthe, R. van Leeuwen, E.J. Baerends, and J.G. Snijders. *in New Challenges in Computational Chemistry, Proceedings of the Symposium in honour of W.C. Nieuwpoort (eds.) R. Broer, P.J.C. Aerts, and P.S. Bagus, Groningen U. P., Groningen*, page 93, 1994.

[129] E. van Lenthe, E.J. Baerends, and J.G. Snijders. *Chem. Phys. Lett.*, **236**:235, 1995.

[130] R.H. Garstang and D.F. Mayers. *Proc. Cambridge Phil. Soc.*, **62**:777, 1966.